Bacterial Exopolysaccharides: A Potential Candidate for Biomedical applications and Green Electronics

VIVEKANANDAN PALANINATHAN

4R10111002

Doctor Course

Bio-Nano Science Fusion

Graduate School of Interdisciplinary New Science

Toyo University

July 2014

Preface

Polysaccharides are relatively complex carbohydrates composed of monosaccharide units bound together by glycosidic linkages. The abundance, tailorable properties and biocompatibility are the key factors that have propelled the use of polysaccharides in biomedical applications. These biomolecules can be categorized based on their source, function, structure, chemical composition and charge. Based on source they can be grouped into plant, animal and microbial polysaccharides. From these available natural resources, microbial polysaccharides have gained a lot of attention in recent years. Microbial polysaccharides have found applications in food, pharmaceutical and medical fields, which could be attributed to their diverse functional and structural properties. Microbial polysaccharides or biopolymers are used as gelling agents and to alter the flow characteristics of liquids. Bacterial polysaccharides have drawn a lot of interest recently and a thorough study on their composition, structure, function and biosynthesis have been reported. Bacterial polysaccharides can be Lipopolysaccharide (LPS), which is confined to the outer membrane of the bacterial cell or capsular polysaccharides (CPS), which forms a capsule (discrete surface layer) or exopolysaccharides (EPS), which is loosely bound to the cell surface. CPS has functions related to the pathogenicity and adherence of bacterial cell, whereas EPS extends support in multiple functions like adhesion, biofilm formation, cell-cell interaction and protection from extreme environment. The function of CPS as virulence factors has encouraged research on these polymers, though commercial applications have not been reported yet. On the contrary EPS have tremendous commercial interest due their material properties.

Among all the bacterial polysaccharides that have been extensively studied, bacterial cellulose is most promising candidate that has been utilized in various fields that includes biomedical sciences, electronics and optoelectronics, food and packaging etc. Based on the availability

and properties, it is evident that bacterial cellulose hold tremendous potential for a sustainable future. The heightened awareness about environment friendly materials now demands a replacement for non-biodegradable films and other films produced through the use of toxic chemicals. Luckily plants and bacteria produce cellulose, which makes it an inexhaustible organic material available at our disposal.

We have achieved large-scale production of bacterial cellulose (BC) through fermentation using *Komagataeibacter sucrofermentans* under controlled conditions. BC was functionalized with sulfate groups and was used to prepare a highly biocompatible transparent film. This novel film has good mechanical properties and is biodegradable. We evaluated the antioxidant properties and hemocompatibility of the film to demonstrate the non-toxic nature of the material. BCS was found to be blood compatible since no significant changes in cells or tissue homogenate antioxidant levels were observed. The film was also used with silver nanoparticles as a versatile nanocomposite material for food packaging and biomedical applications owing to its antimicrobial activities.

The thesis covers 7 chapters that explore the applications of bacterial cellulose in various fields like medicine, tissue engineering, and bionanoelectronics. Following sections summarizes the highlights of each chapter of the thesis entitled “Bacterial Exopolysaccharides: A Potential Candidate For Biomedical Applications And Green Electronics”.

Chapter 1

Polysaccharides, otherwise known as ‘Glycans’ are an integral part of any living system, as a structural unit or as an energy storage unit. All the living organisms contain several forms of polysaccharides and based on their source they can be grouped into plant, animal or microbial polysaccharides. Polysaccharides are one of the indispensible biomolecules on earth. Researchers have minutely observed and utilized several sources of natural polysaccharides for human welfare. This chapter will provide an insight on microbial polysaccharides for various

biomedical and nanotechnological applications. As an introduction to this research thesis, the first chapter discusses various types of polysaccharides available in nature and importance of bacterial polysaccharides among them. Further more, it emphasizes the important applications of BC in biomedical science and bionanotechnology.

Chapter 2

Second chapter covers the bioinstrumentation employed for this work. It includes the list of all sophisticated instruments exploited for the characterization and analysis of bacteria, their polysaccharides and BCS film. It also elaborates the principles and procedures of different colorimetric assays used for the chemical characterization polysaccharides and *in vitro* cell studies.

Chapter 3

This chapter is focused mainly on the cultivation, harvest and purification of BC through fermentation of *Komagataeibacter sucrofermentans*. BC has been used in food industries for making a very famous desert, *nata de coco* that originated from Philippines. The biocompatibility and biodegradability of BC has invited a lot of attention from researchers for wide array of applications in biomedicine and bio-nanoelectronics. Being a nanocellulose it has several advantages over the conventional plant based cellulose. The entire process starts with the microbial cultivation, where a pre-culture is prepared and is transferred to the jar fermenter, through which controlled agitated conditions are provided for bacterial growth and BC production. Thereafter, BC pellicles are harvested and purified through alkali treatment. Post purification, BC is subjected to various physical and chemical characterizations.

Chapter 4

Exceptional properties of bacterial cellulose (BC) have captivated the interests of researchers all over the globe. BC has been chemically modified in several ways corresponding to the application it is considered for. Present study was attempted to evaluate the *in vitro* cytotoxicity, hemocompatibility and antioxidant property of bacterial cellulose sulfate (BCS), which has received lesser attention with respect to the other chemically modified cellulose. BC was produced by *Komagataeibacter sucrofermentans* by controlled agitated method and purified by alkali treatment. Acetosulfation of BC was carried out to functionalize it with sulfate groups. Confirmation of successful sulfation was obtained through FT raman spectroscopy. The cytotoxicity results infer that, BCS is non-toxic and biocompatible. Hemolysis and anticoagulant activity of human blood was also studied using different concentrations of BCS and the results showed that BCS was blood compatible. Also, tested BCS concentrations did not interfere with the blood coagulation activity. No significant difference in the antioxidant levels was observed for the tested BCS concentrations in L929 cells or liver homogenate. Thus, the *in vitro* studies infer that BCS concentrations in the study did not initiate any lethal activity in cells or tissue homogenate and is deemed safe for biomedical applications.

Chapter 5

The increasing awareness about environmental friendly materials and their use now demands a replacement for non-degradable films and the others produced using toxic chemicals. Bacterial cellulose (BC) has found tremendous applications in the optoelectronics and electronics, food and packaging, biomedicine etc., due to good mechanical strength, biocompatibility, relative thermostabilization, high sorption capacity and alterable optical appearance. Though BC has potential merits, they have

some serious drawbacks; insolubility in most solvents, the roughness of cellulose paper is high and transparency is attained from the use of toxic resins. To address this issue, we adopted acetosulfation of BC, produced via batch fermentation process to form bacterial cellulose sulfate (BCS) that was overlooked so far. Here, we demonstrate the synthesis of a highly transparent film with 90 – 92% optical transmittance without the use of any toxic resins that poses serious threat to humans and environment. So produced BCS film was characterized using SEM, AFM, TGA, XRD, FTIR and UV- vis Spectroscopy. It was observed that BCS film had a smooth surface of 1.366 ± 0.348 nm with superior mechanical properties, which is a pivotal factor for optoelectronics substrates. Apart from that, BCS was highly soluble in water but insoluble in oil and alcohol. Thus, this incipient film holds great prospects for electronic devices, biomedical sciences (wound healing, facial packs etc.), food and packaging industries (edible films) in near future.

Chapter 6

Nanotechnology, since its emergence has revolutionized the world of science with wide scope of its applications. The ability to manipulate a material at nanoscale has a huge merit, which directly affects the properties of the material of choice. Nanotechnology has already made tremendous impact on human health through, drug delivery, medicine and tissue engineering applications. Present work is based on the application of functionalized bacterial nanocellulose in food packaging and biomedical applications. Through acetosulfation, BC has been functionalized to BCS and the functionalized BCS was drop cast onto a glass substrate to synthesize a highly transparent film. Thereafter, BCS film was incorporated with AgNPs to get the broad-spectrum antimicrobial properties. Various characterizations to analyze the physical and chemical properties have been performed using FTIR, Zeta potential, UV-vis spectroscopy, TEM and SEM analysis. This film has tremendous potential in food packaging and wound healing applications.

Chapter 7

Chapter 7 summarizes of the entire research work in the previous chapters. It highlights the relevance of BC in bionanotechnology and the introduction of BCS as a novel biomaterial for future biomedical and nanotechnological applications, including therapy, diagnostics, material research, pharmaceutical research, green electronics.

Contents

Chapter 7 Conclusions and Future Prospects

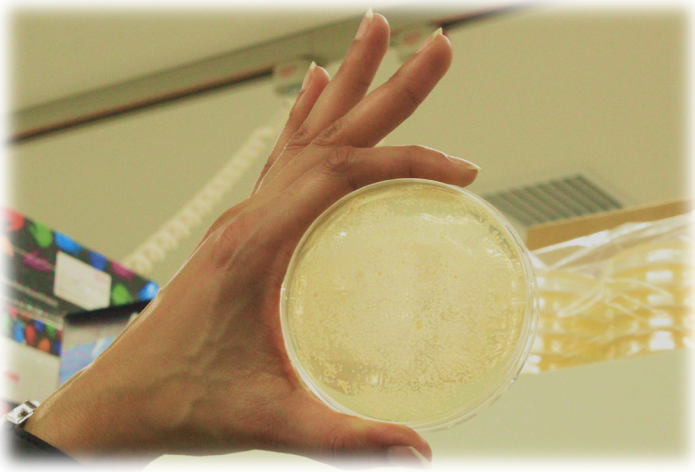

1

Bacterial exopolysaccharides: An overview of diverse applications and prospects

"Necessity is the mother of all inventions"

- *Anonymous*

Polysaccharides, otherwise known as 'Glycans' are an integral part of any living system, as a structural unit or as an energy storage unit. Polysaccharides are fairly complex carbohydrates composed of monosaccharide units bound together by glycosidic linkages. The abundance, tailorable properties and biocompatibility are the key factors that have propelled the use of polysaccharides in biomedical applications. Based on the source of they can be grouped into plant, animal and microbial polysaccharides and all living organisms contain several forms of polysaccharides. Polysaccharides are one of the indispensible biomolecules on earth. Researchers have minutely observed and utilized several sources of natural polysaccharides for human welfare. Here, we have studied and presented a comprehensive review on Microbial polysaccharides for various biomedical and nanotechnological applications. As an introduction to this research thesis, the first chapter discusses various types of polysaccharides available in nature and importance of bacterial polysaccharides among them. Further more, it emphasizes the important applications of BC in biomedical science and bionanotechnology.

Introduction

Microorganisms are ubiquitous in nature. They are known to exist in a wide range of environments from mountaintop to ocean floor. They have adapted themselves to survive in high or low pressure, pH and temperature that are almost unthinkable from human beings point of view. Everyday we are constantly in contact with countless number of diverse microorganisms that are largely beneficial and some are pathogens. The beneficial microorganisms are indispensible, as they have a key role in the processes that provide energy and protect us from diseases. These microorganisms can be grouped into bacteria, algae, fungi, protozoa archaea and viruses. Among these microorganisms, bacteria probably have been studied profoundly and are known to exist in spherical, rod, spiral or filamentous forms. [1] Some bacteria are photosynthetic, while others absorb nutrients from their surroundings. Some of them are motile and others are non-motile. Bacteria can contribute much in scientific research for apparent reasons like, simplicity in structure, can use numerous bacterial cells to obtain reliable results and rapid doubling time that allows us to study several generations. Apart from these factors, they also produce primary and secondary metabolites that have tremendous importance in medicine, food and beverage industries. Primary metabolites are essential for normal growth, development and reproduction of the organism, whereas secondary metabolites are not directly involved in these processes and are synthesized after cell growth. Polysaccharides secreted by bacteria are grouped into the primary metabolites as they have significant role in their cell wall growth and development. [2] The secretion of exopolysaccharides (EPS) by selected microbes was reported in 1880. Now, it is quite evident that several bacteria produce these polymers in a diverse range of chemical structures. [3]

Polysaccharides are relatively complex carbohydrates composed of monosaccharide units bound together by glycosidic linkages. The abundance, tailorable properties and biocompatibility are the key factors that have propelled the use of polysaccharides in biomedical

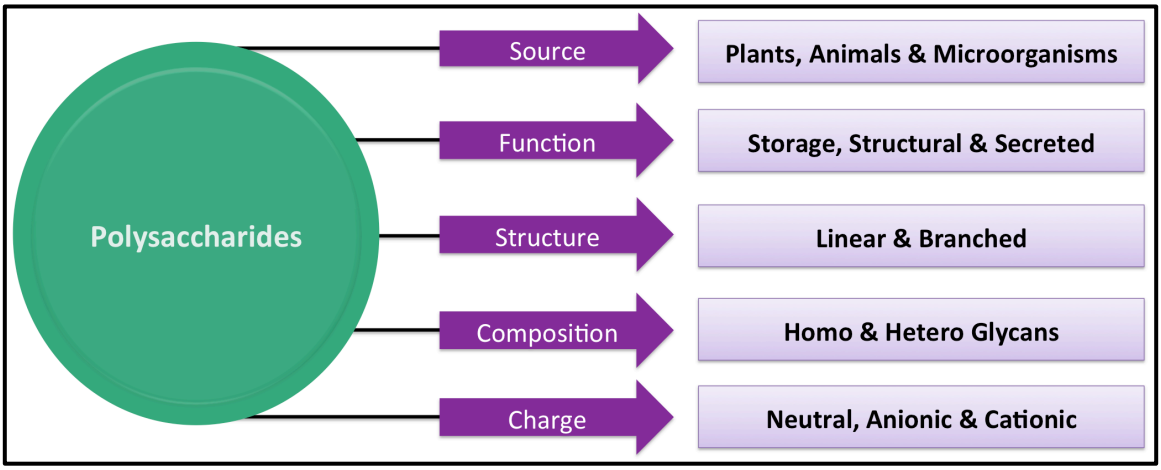

Fig 1: Grouping of polysaccharides

These biomolecules can be categorized based on their source, function, structure, chemical composition and charge. [4] As illustrated in figure 1, based on source they can be grouped into plant, animal and microbial polysaccharides. From these available natural resources, microbial polysaccharides have gained a lot of attention in recent years. Microbial polysaccharides have found applications in food, pharmaceutical and medical fields, which could be attributed to their diverse functional and structural properties. Microbial polysaccharides or biopolymers are used as gelling agents and to alter the flow characteristics of liquids. [2] Bacterial polysaccharides have drawn a lot of interest recently and a thorough study on their composition, structure, function and biosynthesis have been reported. [5] Bacterial polysaccharides can be Lipopolysaccharide (LPS), which is confined to the outer membrane of the bacterial cell or capsular polysaccharides (CPS), which forms a capsule (discrete surface layer) or EPS, which is loosely bound to the cell surface as illustrated in figure 2 (a & b). [6] CPS has functions related to the pathogenicity and adherence of bacterial cell, whereas EPS extends support in multiple functions like adhesion, biofilm formation, cell-cell interaction and protection from extreme environment. [7] The function of CPS as virulence factors has encouraged research on these polymers and commercial applications have not been reported yet. On the contrary EPS have tremendous commercial interest due their sustainable production from renewable resources, their material properties, their

biodegradability and often their biocompatibility. A diverse range of bacteria and archea produces EPS. [8]

Through medium and large-scale fermentation, broad ranges of bacterial polysaccharides are already produced in bulk quantities across the globe. Table 1 summarizes the properties and applications of bacterial EPS. Among all the bacterial polysaccharides that have been extensively studied, bacterial cellulose (BC) is a promising candidate that has been utilized in various fields that includes biomedical sciences, electronics and optoelectronics, food and packaging etc. Based on the availability and properties, it is evident that bacterial cellulose hold tremendous potential for a sustainable future.

Bacterial Cellulose

BC has captured substantial interest by virtue of its remarkable structural and physio-mechanical properties. BC is also known as bacterial nanocellulose (BNC) or biocellulose that is produced by *Glucanoacetobacter*. [9] Figure 2 (c) shows the *Glucanoacetobacter* forming cellulose nanofibers (CNF) and nanoribbons (shown by black arrows). *Glucanoacetobacter* is an acetic acid bacteria that is gram negative, aerobic, rod-shaped with high motility and ubiquity. They are usually associated with the fermentation of carbohydrates on damaged fruits, flowers, and in unpasteurized or unsterilized juice, beer, and wine. Synthesis of BC involves extrusion of glucose chains produced within the cell, through the minute pores of cell wall to form cellulose ribbons that

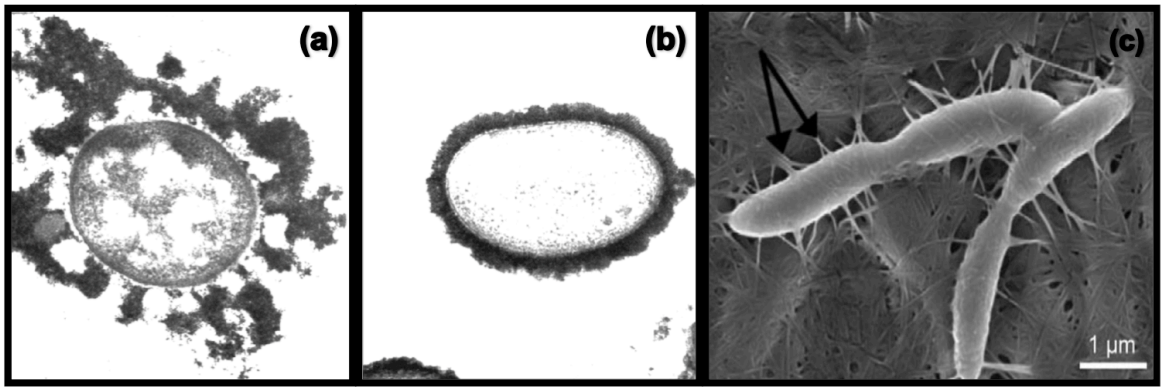

Fig 2: (a & b) Morphology of CPS and EPS producing bacteria respectively; (c) Cellulose production by *Glucanoacetobacter*.

(adapted with permission from Cuthbertson L et al. 2009; Klemm D. et al. 2011)

subsequently form highly porous matrix. [11] When cultured under special conditions, the bacteria has the ability to produce pure cellulose in the form of thick gel, "pellicle" that is composed of ~97% water, CNF and nanoribbons. [10] The vital functions of BC include, adaptation to different living environments, protection from foes, irradiation, dehydration, lack of nutrients and oxygen depletion. [9]

EPS	Components	Charge	Molecular weight	Main properties	Main applications	Market (metric tons)	Market value (US$)	Price (US$)/kg
Xanthan	Glucose Mannose Glucuronic acid Acetate Pyruvate	Anionic	(2.0-50) x 10^6	• Hydrocolloid - High viscosity yield at low shear rates even at low concentrations; - Stability over wide temperature, pH and salt concentrations ranges	• Foods • Petroleum industry • Pharmaceuticals • Cosmetics and personal care products • Agriculture	96 000	235 millions	3 - 5
Gellan	Glucose Rhamnose Glucuronic acid Acetate Glycerate	Anionic	5.0 x 10^5	• Hydrocolloid -Stability over wide pH range • Gelling capacity • Thermoreversible gels	• Foods • Pet food • Pharmaceuticals • Research: agar substitute and gel electrophoresis	N.A.	15 millions	55-66
Alginate	Guluronic acid Mannuronic acid Acetate	Anionic	(0.3-1.3) x 10^6	• Hydrocolloid • Gellling capacity • Film-forming	• Food hydrocolloid • Medicine - Surgical dressings - Wound management -Controlled drug release	30 000	N.A.	5-20
Cellulose	Glucose	Neutral	~10^6	• High crystallinity • Insolubility in most solvents • High tensile strength • Moldability	• Foods (indigestible fiber) • Biomedical -Wound healing -Tissue engineered blood vessels -Audio speaker diaphragms	N.A.	N.A.	5.8-12
Dextran	Glucose	Neutral	10^6 - 10^9	• Non-ionic • Good stability • Newtonian fluid behavior	• Foods • Pharmaceutical industry: Blood volume expander • Chromatographic media	2 000	N.A.	N.A.
Curdlan	Glucose	Neutral	5x10^4 - 2x10^6	• Gel-forming ability • Water insolubility • Edible and non-toxic • Biological activity	• Foods • Pharmaceutical industry • Heavy metal removal • Concrete additive	N.A.	N.A.	55
Hyaluronan	Glucuronic acid Acetylglucosmine	Anionic	2.0x10^6	• Biological activity • Highly hydrophilic • Biocompatible	• Medicine • Solid culture media	N.A.	1 billion	100 000
Succinoglycan	Glucose Galactose Acetate Pyruvate Succinate 3-hydroxybutyrate	Anionic	LMW <5x10^3 HMW >1x10^6	• Viscous shear thinning aqueous solutions • Acid stability	• Food • Oil recovery	N.A.	N.A.	N.A.
Levan	Fructose	Neutral	3.0x10^6	• Low viscosity • High water solubility • Biological activity: Anti-tumor activity Anti-inflammatory • Adhesive strength • Film-forming capacity	• Food (prebiotic) • Feed • Medicines • Cosmetics • Industry	N.A.	N.A.	N.A.
GalactoPol	Galactose Mannose Glucose Rhamnose Acetate Succinate Pyruvate	Anionic	(1.0-5.0) x 10^6	• Viscous shear thinning solutions in aqueous media • Film-forming • Emulsifying capacity • Flocculating capacity	Hydrocolloid for use in: (1) -Food and feed -Cosmetics -Pharmaceuticals and medicine -Oil recovery • Coatings • Packages	–	–	–
FucoPol	Fucose Galactose Glucose Acetate Succinate Pyruvate	Anionic	(2.0-10.0) x 10^6	• Viscous shear thinning solutions in aqueous media • Film-forming • Emulsifying capacity • Flocculating capacity • Biological activity due to fucose content	• Hydrocolloid for use in: (1) -Food and feed -Cosmetics -Pharmaceuticals and medicine -Oil recovery • Source of fucose and fuco-oligosaccharides	–	–	–

Table 1: Vastly studied bacterial EPS. (adapted with permission from Freitas et al. 2011)

BC structure, production and chemical modification

BC is a complex anionic and highly crystalline polysaccharide composed of glucose units combined in long chains of β – 1, 4 – glycosidic bonds. Molecular formula of BC is identical to that of plant cellulose, but with unique and complex 3-D porous networks. BC demonstrates tremendous features such as high purity, high degree of polymerization (up to 8000), high crystallinity (of 70-80%), high water content to 99%, and high mechanical stability, which is quite different from the natural cellulose. [12, 13] Nuclear magnetic resonance (NMR) spectroscopy revealed that all naturally occurring cellulose was a complex of I_α and I_β forms, and 65% of I_α content was found in BC. [14] On the basis of X-ray diffraction (XRD) investigations, BC was found to show uniplanar orientation depending on the drying procedure it also exhibited an additional axial orientation component. [15]

An effective cellulose production relies on several aspects such as the strain of *Glucanoacetobacter* used, the material of support and its surface morphology, media ingredients, temperature, pH, continuous aeration and carbon source glucose. Fermentation is a very versatile process for producing BC and since fermentation parameters have a high impact upon the viability and economics of the bioprocess, their optimization holds great importance for process development. [7, 16] Figure 3 demonstrates the production of BC under different conditions. Basically, BC has been synthesized through two routes, static and agitated cultures. Static culture involves BC production at the air-interface as an assembly of reticulated crystalline ribbons that integrates into a pellicle and thickens with time. The growth of pellicle ceases when all the cells entrapped in the pellicle die or become inactivated due to shortage of oxygen supply. [17, 18] Most widely used BC for commercial purposes is produced by agitated fermentation that produces smaller pellets instead of BC sheets. [11, 18] Very high productivity was observed in the case of agitated cultures due to high cell density and better contact with continuous supply of oxygen. For the economic production of BC, efforts are still made to identify inexpensive raw materials.

Now, BC possesses immense potential owing to the biotechnological production and its specific nanoscale structure. Certain properties, processing and material formation is not achievable with synthetic polymers as well as plant cellulose. On the other hand, BC can be exploited to achieve controlled super molecular structure, shaping of BC during biosynthesis and effective post modification or processing. [19, 20] However, strict microbial fermentation environment does not allow introducing some additives to achieve biosynthetic modifications. Hence, chemical modifications of BC are an alternative to achieve certain remarkable features while retaining its superior mechanical properties. The structural similarity with the plant cellulose allows us to follow similar modifications attempted earlier like carboxymethylation, acetylation, phosphorylation etc., to attain a wide range of BC derivatives. [13] Figure 4 illustrates generalized routes to modify BC. The modification is aimed at the enhancement of BC performance and applications depending on the requirement of different fields. With the introduction of novel functional groups into BC chain, it can demonstrate hydrophobicity,

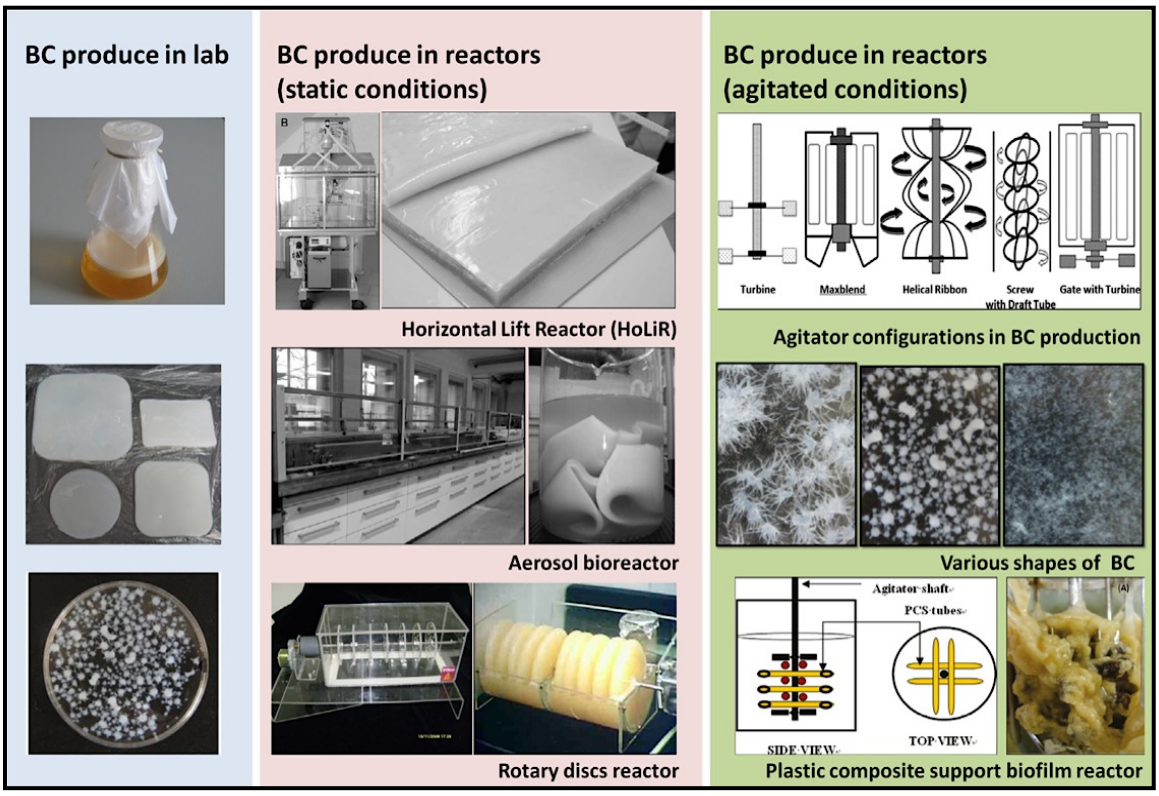

Fig 3: BC production under different conditions (adapted with permission from Shi et al. 2014)

optical properties and ion adsorption capacity. [13] The chemical modification of BC can provide new opportunities for the progress of novel nanostructured materials with well-planned functionalities for various applications in different fields.

Applications of BC composites

Being a multifunctional material, combination of BC with different materials can yield wide range of BC composites that exhibit additional properties for specific applications. [11, 15] BC composites have opened up new avenues in several fields challenging the synthetic polymers in current use due to their biodegradable and often biocompatible nature. Figure 5 depicts present applications of BC and its composites in diverse applications in varied fields. BC applications include acoustic transducer diaphragm, paper manufacturing that involves packaging and composite papers, filtration material, dialysis membrane, pharmaceutical applications that include, wound dressing, drug delivery, artificial blood vessel formation, bone regeneration, nasal septal perforation, substrate for immobilization, as food, and in electronic applications like, electronic paper, biosensors and photo catalytic applications. [25]

Recent years have seen tremendous growth in BC and its composite based applications in biomedical sciences. Numerous innovative applications exploit its biocompatibility and chirality for immobilization of proteins, antibodies, and heparin and for the separation of enantiomeric molecules as well as the formation of cellulose composites with synthetic polymers and biopolymers. [21] Nontoxicity, high water holding capacity and non-hypersensitive nature of BC makes it an outstanding biomaterial for cosmetics industries. [22] Several studies have been conducted over a period of time to show that BC and its composites have the ability to support cell growth. [23, 24] Apart from being cell growth supporting material, modified BC films can be act as an anti-proliferative and anti-adhesion material. [25]

One of the major biomedical applications that BC is used for is in wound healing. A wound could be state where anatomical structure and

function of skin is disrupted. It is dynamic process that encompasses several immune cells, extracellular matrix molecules and soluble molecules. The host response to an injury sustained erupts instantaneously and the key phases associated with a normal skin wound healing are Coagulation & inflammatory stage, proliferative stage and remodeling stage, [26, 27, 28] which is continuous and overlapping. Since ancient ages, wound dressings have undergone significant changes. For an effective wound healing, use of a suitable material to cover the wound played a vital role, which used to be plant fibers, animal fats and honey pastes. [29] With the advent of new biopolymers and fabrication techniques, an ideal wound dressing design should consider the characteristics of wound type, wound healing time, physical, chemical and mechanical properties of dressing material, which would deliver the best results of wound repair. [30] Depending on their function in the wound (debridement, antibacterial, occlusive, absorbent, adherence), type of material employed to produce the dressing (e.g. hydrocolloid,

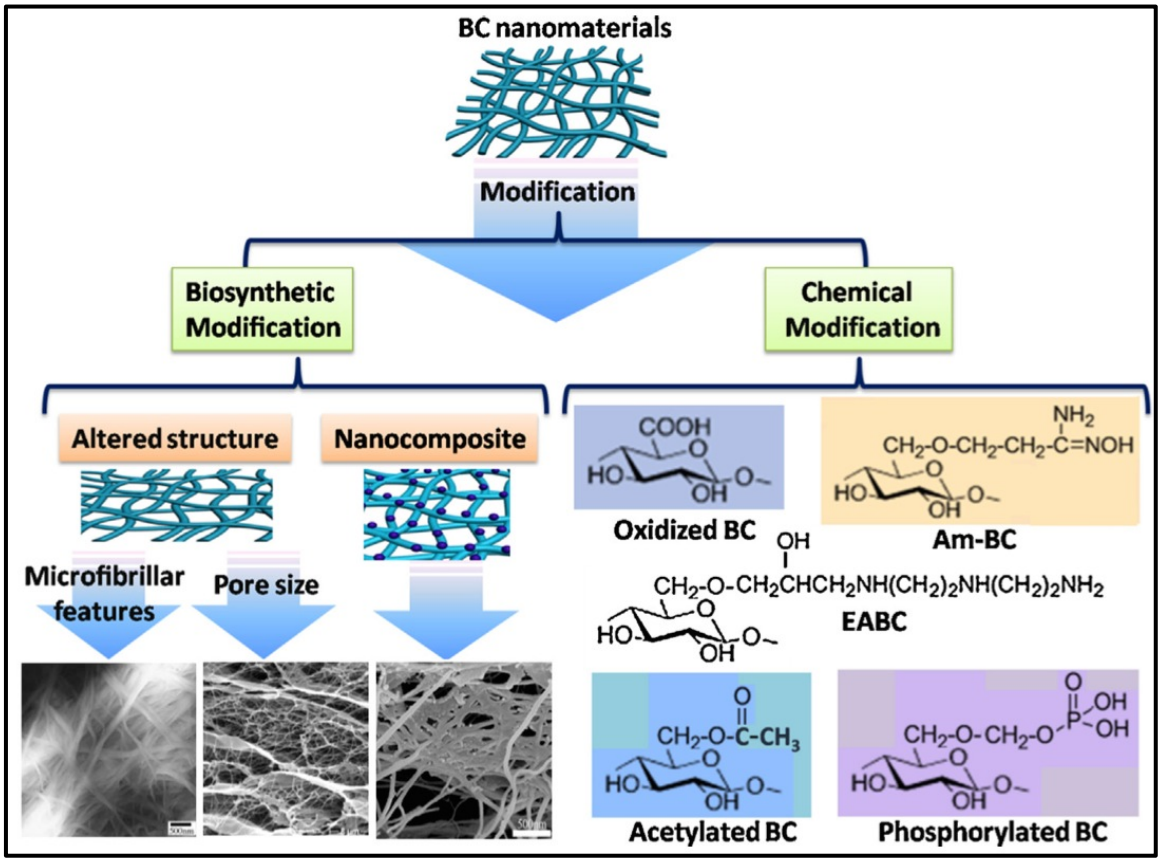

Fig. 4: Schematic representation of BC modification. (adapted with permission from Hu et al. 2014)

alginate, collagen) and the physical form of the dressing (ointment, film, foam, gel), wound dressings can be classified. [28] Applications of BC as a wound dressing material have proven to be highly effective in the recent attempts. [22, 25] Provisional skin substitutes have been developed, called "Biofills", that are cost effective and have been applied on burn wounds and other wounds, which exhibited faster healing, immediate pain relief, reduced infection rate, improved exudate retention with reduced time. [31, 25] Cellulose films – cotton gauge composites demonstrated higher water absorbency than the native cellulose, which could be exploited for wound dressings. [32] The fusion of nanotechnology and biopolymers has set high expectations in terms of material quality and applications. A variety of BNC-nanoparticle composites such as vanadium, gold, nickel, silver, cadmium sulfide have been synthesized in the last 5 years, for several biomedical applications as described in table 2. Other than the nanoparticles different polysaccharides (both natural and modified forms), drugs, proteins and peptides have also been incorporated into it to enhance or achieve additional bioactive properties. BC composites have emerged as potential contenders in tissue engineering fields as

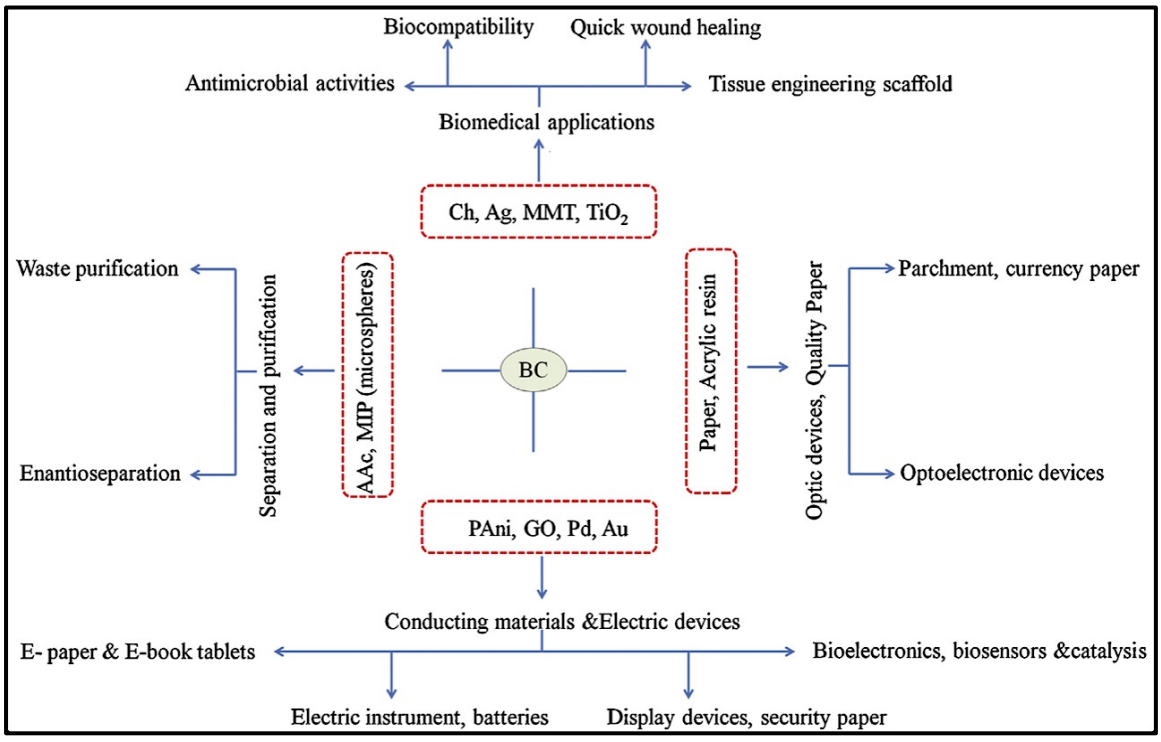

Figure 5: Applications of BC in different fields

well. BC sheets can be prospective biomaterial scaffold for tissue engineering of artificial cornea. BC sheets were found to support the growth and proliferation of corneal stromal cells, wherein the growth was observed on the surface and core of BC scaffolds. In another study a porous BC scaffolds were found to aid the differentiation of urine derived stem cells in a 3D culture system. This ability of BC may assist in the development of a tissue-engineered urinary conduit, which would be

Incorporated element	Application
Vanadium oxide nanoparticles	Used in fabrication of transparent, conductive, and photochromic vanadium nanopapers
Gold nanoparticles	Used as template for the enzyme immobilization and biosensor fabrication
Nickel nanoparticles	Used to improve BC material property for magnetographic printing and sensor application or even as magnetic tissue scaffolds
Cadmium sulfide nanoparticles	Deposition of CdS nanoparticles onto the substrate of hydrated BC can be developed as robust visible light responsive photocatalysts
Silver nanoparticles	Widely apply in wound dressing due to its antimicrobial ability
Comb	Widely apply in manufacturing electrical paper due to comb nanotube possessed with good electrical conductivity
Carboxylmethylcellulose	Role in modifying BC material property
hydroxypropylmethyl cellulose	Used to improve rehydration ability of BC during fermentation
Protein and peptide	Cellulases can be incorporated into BC, and control its biodegradation by pH variation. Some peptides, for example, microbial peptide can combine with BC to develop antimicrobial film
Sodium carbonate	Sodium carbonate incorporated with BC exhibits higher chemical stability, which serves as a critical factor in paper manufacturing
Xyloglucan	Xyloglucan was added to aggregate bacterial cellulose nanocrystals suspensions resulting in smooth model surfaces
poly(L-lactic) acid	Incorporation of poly (L-lactic) acid was demonstrated to improve mechanical property of BC
Chitosan	Chitosan was used to increased cell adhesion, and developed as scaffold for cell immobilization
Hydroxyapatite	Because of good biocompatibility of hydroxyapatite, hydroxyapatite-treated BC can be developed as a potential scaffold to promote cell proliferation
Drugs	Drug incorporated BC can be developed as wound dressing material as drug carrier in releasing drugs

Table 2: Biomedical applications of BNC composites (adapted with permission from Lin et al. 2013)

particularly useful for patients with bladder cancer who need bladder replacement. [33, 34, 25] Furthermore, there are reports available on the proliferation of chondrocytes on porous BC scaffold that was evaluated for cartilage regeneration. In this case, slightly fused nanoparticles were incorporated during biosynthesis of BC. [35]

BC promises numerous applications in food industries owing to high purity, ability to form different shapes and textures with *in situ* change in color and flavor. BC can be applied as thickening agents, salads, deserts (low calorie), and fabricated food. [36] Expansion of bacterial cellulose production took place with the import of *Nata de coco* (a desert) into Japan from Philippines. Food and Drug Administration (USA) in 1992 classified BC as "generally recognized as safe" (GRAS). Figure 6 illustrates applications of BC in food industries. Also, BC can be used as a stabilizing and suspending agent.

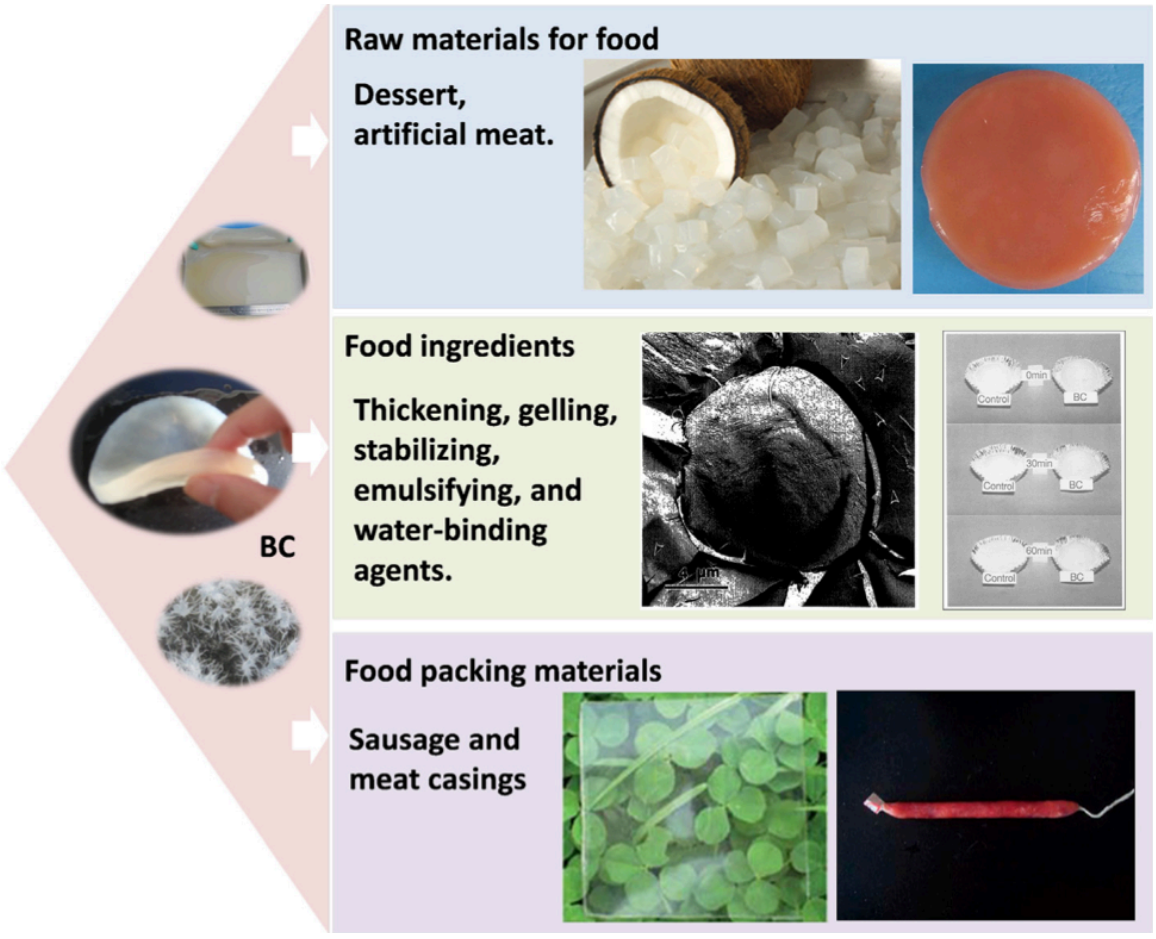

Figure 6: Various applications of BC in food industries.
(adapted with permission from Shi et al. 2014)

Superior water holding capacity and cation exchange properties are important traits of BC, which allows it to be used as a fat replacement and additional dietary fiber source, thus, lowering cholesterol in food. [39, 40] With the increasing awareness about the use of green materials and environmental concerns, renewable biomaterials are gaining a lot of attention from the food packaging industries. The recent trend in food packaging industries is the use of edible films. Candidly, edible films are used to prevent the exchange of moisture, lipid, gas, solute, or aroma compound migration between foods and their environments. They are made up of carbohydrates or proteins. [40] Cellulose derivatives are vital candidates in this field owing to their good film forming capacity. Modified BC membrane showed better barrier properties that the original BC membrane. Blending BC with biodegradable poly(lactic acid) can improve the mechanical properties without affecting the transparency and biocompatibility. [41, 42] Antimicrobial agents such as metallic nanoparticles (Ag, Au, ZnO, Cu) have been incorporated, which can sustain the activity of food storage. [37] Although there are promising applications of BC in food industries, they have not received much attention.

The versatility of BC applications extends beyond the biomedical and food industries. Functional nanocomposites or nanohybrids are generating a lot of interest due to their biofunctionality and tunable performance. As a result of their superior qualities, it has found relevant applications in composite reinforcement, sewage purification and paper industries. [44] To improve of the mechanical and electrical properties, BC matrix has been integrated with unique carbon materials. BC – carbon nanotube (CNT) thorough dip coating method into a MWCNT solution enhanced the conductivity of the composite material. [45] An increase in young's modulus and tensile strength was observed in the BC – GO nanocomposite films, which was 10% and 20% respectively. The electrically conductive and flexible BC/GO composite film with desirable mechanical properties is vital for advanced biochemical and electrochemical devices. [44]

Future of flexible transparent films is brighter than ever and its applications are getting wider, with applications in the flexible consumer electronics, smart clothing, energy harvesting and sensors. Apart from the retention of their high throughput in transmittance, conductivity and flexibility, some other requirements also need to be addressed that includes lower cost, lighter weight, large-scale production and environmental friendly substrate. The inability of traditional transparent conductive films to meet flexibility need, demands a reliable flexible substrate [45, 49] An attempt to make flexible transparent films using metal oxide semiconductors, conducting polymers, graphene, CNT's and metallic nanowires has been successfully deposited on flexible substrate through filtration, spin-coating, Langmuir-Blodgett assembly and dip coating. [45, 46, 47, 48] Among the contenders for flexible substrates, BC holds great potential owing to its small co-efficients of thermal expansion. [50] Despite their very high transparency, plastics fall short in the contentment because of their large co-efficients of thermal expansion and environment unfriendly nature. [51] Figure 7 illustrates the flexible BC sheets, where the nanofiber networks of BC headed to excellent reinforcement of resin substrate, thereby fabricating composites with significantly higher mechanical strength and lower co-efficient of thermal expansion. From left, BC sheet, BC – acrylic resin and BC – epoxy resin.

Being electrically non-conducting in nature, it is essential to treat

Figure 7: Transparent and flexible BC sheet. (adapted with permission from Yano et al. 2005)

BC with some conductive materials. Once conductive or semi conductive BC sheets are formed, they are immobilized with electrochromic dyes and attached to electrodes that results in a reversible color change. These display devices are highly flexible, biodegradable having contrast and high reflectivity. [52] Organic light emitting diode (OLED) devices based on flexible bacterial cellulose membranes have already been well recognized and have been successfully fabricated on cellulose and acrylic resin nanocomposite. These devices are useful in numerous applications including e-newspapers, e-book tablets, rewritable maps, dynamic wallpapers, and learning tools. [13, 11] Vapor deposition technique was employed to fabricate each layer of the OLED. The principle behind this technique is that, reacting material will evaporate and crystallize into the form of epitaxial thin film, depositing onto the substrate surface. This deposition technique is quite reliable for creating thin film with uniform thickness. [53] Figure 8 shows the OLED on BC nanocomposite that had captivating features of flexibility, optical transparency, high light transmittance of up to 80% and dimensional stability in terms of CTE of as low as 18 ppm/K that met the requirements of OLED substrate. [53]

The BC-PAni composite produced a high degree of conductivity and was therefore proposed for application in biosensors, flexible

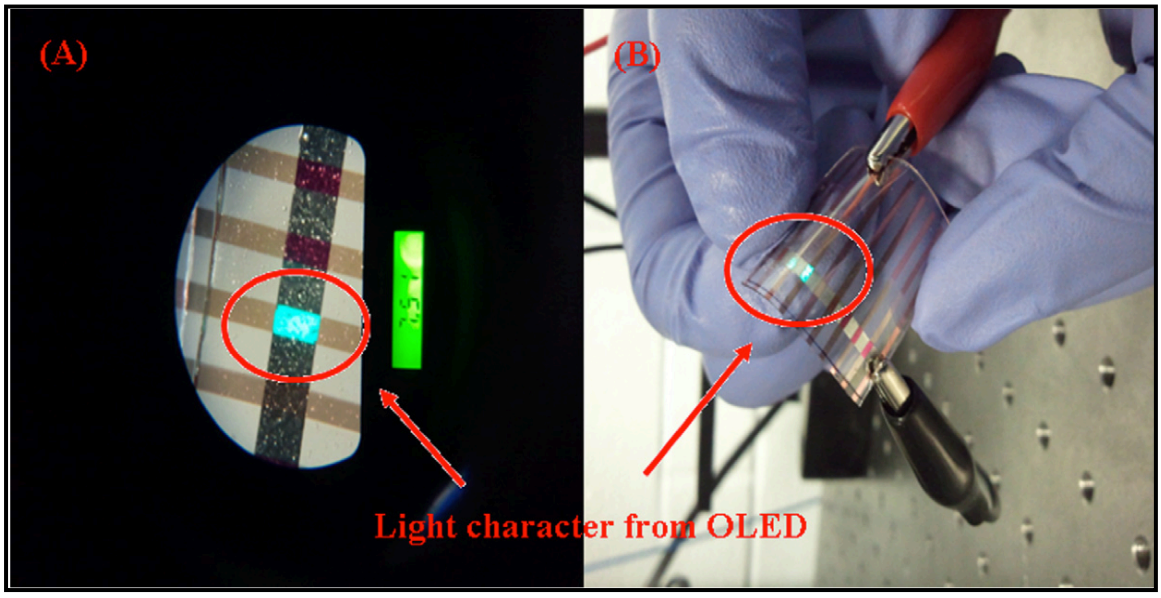

Figure 8: OLED on BC nanocomposite. (adapted with permission from Ummartyotin et al. 2012)

electrodes, flexible displays, and other electronic applications. [13] BC composites with GO and MWCNT greatly enhanced the conductivity while imparting increased mechanical properties. The application of these composites lies in designing bio-electrodes, biosensors, electronic devices, and biochemical and electrochemical devices. [43, 44]

An effective method for the construction of flexible BC membranes with photoluminescence properties was developed recently, which has promising applications in optics, electronics and biology. Flexible luminescent CdSe/BC and CdS/BC membranes have been fabricated by the *in situ* synthesis of the CdSe and CdS nanoparticles on the BC nanofibers, wherein nanoparticles were homogeneously dispersed in the BC matrix. The resulting nanocomposites exhibited good photoluminescence properties and excellent mechanical properties. [54]

BC has also been used as purification or separation membrane for the wastewater treatment. Right combination with certain materials like modified BC produced using acrylic acid (AAc) has ion exchange capacity. The BC-AAc composite membranes possessed electrochemical properties comparable to commercial membranes, as well as excellent absorption capability for heavy metals, binding with metal ions, and separation of trace metals. Use of BC composite with biodegradable materials for such purposes is effective since their disposal does not cause environmental problems. [55, 11]

Conclusion

With the increasing cognizance about environmental issues and limitation of fossil fuels science and technology will continue to shift towards renewable and environmental friendly materials. BC membranes produced by gram-negative, acetic acid bacteria (*Gluconacetobacter*) exhibits a broad range of bioactivities and applications. With the ever-increasing demand for biomaterials, BC will have a significant role to play in different fields of application because of insignificant toxicity issues related to it. To meet the growing demand of BC, a robust and feasible industrial production and supply is crucial. Despite of the relatively

simple fermentation process, new engineering processes are needed to produce desired BC with specific material properties. Moreover, genetic and biochemical investigations are also necessary to enhance BC production at molecular biological level and commercial purposes. Another aspect to be considered is to create controlled, reliable, reproducible, production techniques that will be essential for FDA approval for new applications, which will make BC available for broad range of biomedical applications in which it is lagging behind.

References

1. Black JG. Microbiology: Principles and explorations. 7th edition, **2008**, John Wiley & Sons, Inc.
2. Prescott LM, Harley JP, Klein DA. Microbiology. 7th edition, **2008,** McGraw Hill.
3. C. Whitfield. Bacterial extracellular polysaccharides; *Canadian J Microbio.* 34(4), 415–420 (**1988)**.
4. L. Bacakova, K. Novotna, and M. Parizek. Polysaccharides as cell carriers for tissue engineering: the use of cellulose in vascular wall reconstruction; *Physiological Research* 63 (Suppl. 1), S29–S47 **(2014)**.
5. F. Freitas, V. D. Alves, and M. A. Reis. Advances in bacterial exopolysaccharides: from production to biotechnological applications; *Trends in Biotechnology* 29(8), 388–398 **(2011)**.
6. L. Cuthbertson, I.L. Mainprize, J. H. Naismith, and C. Whitfield. Pivotal roles of the outer membrane polysaccharide export and polysaccharide co-polymerase protein families in export of extracellular polysaccharides in gram-negative bacteria; *Microbio. and Mol. Bio. Reviews* 73(1),155–177 **(2009)**.
7. E. T. Öner. Microbial production of extracellular polysaccharides from biomass; *Green Energy and Technol.* 35–56 **(2013)**.
8. B. H. A. Rehm. Bacterial polymers: biosynthesis, modifications and applications; *Nature Reviews Microbio* 8, 578–592 (**2010)**.

9. D. Klemm, F. Kramer, S. Moritz, T. Lindstrom, M. Ankerfors, D. Gray, and A. Dorris. Nanocelluloses: a new family of nature-based materials; *Angewandte Chemie* International *Edition* 50(24), 5438-66 **(2011)**.
10. R. J. Moon, A. Martini, J. Nairn, J. Simonson, and J. Youngblood. Cellulose nanomaterials review: structure, properties and nanocomposites; *Chemical Society Reviews* 40, 3941-3994 **(2011)**.
11. N. Shah, M. Ul-Islam, W. A. Khattak, and J. K. Park. Overview of bacterial cellulose composites: A multipurpose advanced material; *Carbohydr. Poly.* 98, 1585-1598 (**2013)**.
12. H. S. Barud, T. Regiani, R. F. C. Marques, W. R. Lustri, Y. Messaddeq, and S. J. L. Ribeiro. Antimicrobial bacterial cellulose-silver nanoparticles composite membranes; *J Nanomat.* Article ID 721631 **(2011)**.
13. W. Hu, S. Chen, J. Yang, Z. Li, and H. Wang. Functionalized bacterial cellulose derivatives and composites; *Carbohydr. Poly*. 1043-1060 **(2014)**.
14. D. L. VanderHart, and R. H. Atalla. Studies of Microstructure in native celluloses using solid-state ^{13}C NMR; *Macromolecules* 17, 1465-1472 **(1984)**.
15. F. Lina, Z. Yue, Z . Jin, and Y. Guang. Bacterial cellulose for skin repair materials. DOI: 10.5772/24323. **(2011)**
16. B. Nicolaus, M. Kambourova, and E. T. Öner. Exopolysaccharides from extremophiles: from fundamentals to biotechnology; *Environ.l Technol.* 31, 1145-1158 **(2010)**.
17. W. Borzani, and S. J. Souza. Mechanism of the film thickness increasing during the bacterial production of cellulose on non-agitated liquid media; *Biotechnology Letters* 17, 1271-1272 (**1995)**.
18. R. Mormino, and H. Bungay. Composites of bacterial cellulose and paper made with a rotating disk bioreactor; *App. Microbio. Biotechnol.* 62, 503-506 **(2003)**.

19. D. Klemm, D. Schumann, F. Kramer, N. Hebler, D. Koth, and B. Sultanova. Nanocellulose materials – different cellulose, different functionality; *Macromolecular Symposia* 280, 60–71 **(2009)**.
20. D. Klemm, D. Schumann, F. Kramer, N. Hebler, M. Hornung, H. P. Schmauder, and S. Marsch. Nanocelluloses as innovative polymers in research and applications; *Adv. Poly. Sci.* 205, 49–96 **(2006)**.
21. D. Klemm, B. Heublein, H. P. Fink, and A. Bohn. Celluloses: fascinating biopolymer and sustainable raw material; *Angewandte Chemie* International *Edition* 44, 3358–3393 **(2005)**.
22. B. Stanislaw, K. Halina, K. Alina, K. Katarzyna, Marek Ko, Manu de G. Wound dressings and cosmetic materials from bacterial nanocellulose. In: Bacterial nanocellulose; Perspectives in nanotechnology, CRC Press, New York, 157–174 (**2012)**.
23. H. Backdahl, G. Helenius, A. Bodin, U. Nannmark, B. R. Johansson, B. Risberg, and P. Gatenholm. Mechanical properties of bacterial cellulose and interactions with smooth muscle cells; *Biomaterials* 27, 2141–2149 **(2006)**.
24. Z. Cai, and J. Kim J. Bacterial cellulose/poly (ethylene glycol) composite: characterization and first evaluation of biocompatibility; *Cellulose* 17, 83–91 **(2010)**.
25. S. P. Lin, I. L. Calvar, J. M. Catchmark, Liu JR, A. Demirci, and K. C. Cheng. Biosynthesis, production and applications of bacterial cellulose; *Cellulose* 20, 2191–2219 (**2013)**.
26. S. Rawat, R. Singh, P. Thakur, S. Kaur, and A. Semwal. Wound healing agents from medicinal plants: a review; *Asian Pacific J Tropical Biomed.* 2, S1910–S1917 **(2012)**.
27. W. K. Stadelmann, A. G. Digenis, and G. R Tobin. Physiology and healing dynamics of chronic cutaneous wounds. *The American J Surgery* 176, 26S–38S **(1998)**.
28. J. S. Boateng, K. H. Matthews., H. N. E. Stevens, and G. M. Eccleston Wound healing dressings and drug delivery systems; a review; *J Pharma. Sci*. 97, 2892–2923 **(2008)**.

29. G. Majno. The Healing Hand: Man and Wound in the Ancient World; Harvard University Press, Cambridge **(1975)**.
30. S. Thomas. Wound Management and Dressing. Pharmaceutical Press; London **(1990)**.
31. R. Jonas and L. F. Farah. Production and application of microbial cellulose; *Polymer Degradation and Stability* 59, 101–106 **(1998)**.
32. A. Meftahi, R. Khajavi, A. Rashidi, M. Sattari, M. E. Yazdanshenas, and M. Torabi. The effects of cotton gauze coating with microbial cellulose. *Cellulose* 17, 199–204 **(2010)**.
33. J. Hui, J. Yuanyuan, W. Jiao, H. Yuan, Z. Yuan, and J. Shiru. Potentiality of Bacterial Cellulose as the Scaffold of Tissue Engineering of Cornea; 2nd international Conference on Biomedical Engineering and Informatics, Tianjin, China **(2009)**.
34. A. Bodin, S. Bharadwaj, S. Wu, P. Gatenholm, A. Atala, and Y. Zhang. Tissue-Engineered Conduit Using Urine-Derived Stem Cells Seeded Bacterial Cellulose Polymer in Urinary Reconstruction and Diversion; *Biomaterials* 31, 8889–8901 **(2010)**.
35. J. Andersson, H. Stenhamre, H. Bachdahl, and P. Gatenholm. Behavior of Human Chondrocytes in Engineered Porous Bacterial Cellulose Scaffolds; *J Biomed. Mat. Res.* Part A 94, 1124–1132 **(2010)**.
36. A. Okiyama, M. Motoki, and S. Yamanaka. Bacterial cellulose IV. Application to processed foods; Food Hydrocoloids 6, 503–511 **(1993)**.
37. Z. Shi, Y. Zhang, G. O. Phillips, and G. Yang. Utilization of bacterial cellulose in food; *Food hydrocolloids* 35, 539–545 (**2014**).
38. S. B. Lin, L. C. Chen, and H. H. Chen. Physical characteristics of surimi and bacterial cellulose composite gel; *J food proc. Eng.* 34, 1363–1379 **(2009)**.
39. C Chau, P. Yang, C. Yu, and G. Yen. Investigation on the lipid-and cholesterol- lowering abilities of biocellulose; *J Agri. Food Chem* 56, 2291–2295 **(2008)**.

40. K. Vu, R. Hollingsworth, E. Leroux, S. Salmieri, and M. Lacroix. Development of edible bioactive coating based on modified chitosan for increasing the shelf life of strawberries; *Food Research International* 44, 198–203 **(2011)**.
41. L. C. Tomé, L. Brandão, A. M. Mendes, A. J. Silvestre, C.P. Neto, and A. Gandini. Preparation and characterization of bacterial cellulose membranes with tailored surface and barrier properties; *Cellulose* 17, 1203–1211 **(2010)**.
42. L. Xiao, Y. Mai, F. He, L. Yu, L. Zhang, and H. Tang. Bio-based green composites with high performance from poly (lactic acid) and surface- modified microcrystalline cellulose; *J Mat. Chem*. 22, 15732–15739 **(2012)**.
43. Y. Feng, X. Zhang, Y. Shen , K. Yoshino, and W. A. Feng. Mechanically strong, flexible and conductive film based on bacterial cellulose/graphene nanocomposite; *Carbohyd. Poly.* 87, 644–649 **(2012)**.
44. S. H. Yoon, H. J. Jin, M. C. Kook, Y. R. Pyun. Electrically conductive bacterial cellulose by incorporation of carbon nanotubes; *Biomacromolecules* 7, 1280–1284 **(2006)**.
45. K. Gao, Z. Shao, X. Wu, X. Wang, J. Li, Y. Zhang, W. Wang, and F. Wang. Cellulose nanofibers/reduced grapheme oxide flexible transparent conductive paper; *Carbohyd. Poly.* 97, 243–251 **(2013)**.
46. K. Nomura, H. Ohta, A. Takagi, T. Kamiya, M. Hirano, and H. Hosono. Room-temperature fabrication of transparent flexible thin-film transistors using amorphous oxide semiconductors; *Nature* 432, 488–492 **(2004)**.
47. C. Y. Kao, B. Lee, L. S. Wielunski, M. Heeney, I. McCulloch, and E. Garfunkel. Doping of conjugated polythiophenes with alky silanes; *Adv. Fun. Mat*. 19, 1906–1911 **(2009)**.
48. H. Chang, G. Wang, A. Yang, X. Tao, X. Liu, and Y. Shen. A transparent, flexible, low-temperature, and solution-processible graphene composite electrode; *Adv. Fun. Mat.*, 20, 2893–2902 **(2010)**.

49. A. Kumar, and C. Zhou. The race to replace tin-doped indium oxide: Which material will win? ACS Nano 4, 11–14 **(2010)**.
50. H. Yano, J. Sugiyama, A. N. Nakagaito, M. Nogi, T. Matsuura, M. Hikita, and K. Handa. Optically transparent composites reinforced with bacterial nanofibers; *Adv. Mat.* 17, 153–155 **(2005)**.
51. M. Nogi, S. Iwamoto, A. N. Nakagaito, and H. Yano. Optically transparent nanofiber paper; *Adv. Mat.* 21, 1595–1598 **(2009)**.
52. J. Shah, and R. M. J. R. Brown. Towards electronic displays made from microbial cellulose; *App. Microbio.Biotechnol.* 66, 352–355 **(2005)**.
53. S. Ummartyotin, J. Juntaro, M. Sain, and H. Manuspiya. Development of transparent bacterial cellulose nanocomposite film as substrate for flexible organic light emitting diode (OLED) display; *Industrial crops and Products* 35, 92–97 (**2012**).
54. X. Li, S. Y. Chen, W. L. Hu, S. K. Shi, W. Shen, X. Zhang. In situ synthesis of CdS nanoparticles on bacterial cellulose nanofibers; *Carbohyd. Poly.* 76, 509–512 **(2009)**.
55. Y. J. Choi, Y. Ahn, M. S. Kang, H. K. Jun, I. S. Kim, and S. H. Moon. Preparation and characterization of acrylic acid-treated bacterial cellulose cation-exchange membrane; *J Chem.Technol. Biotechnol*. 79, 79–84 **(2004)**.

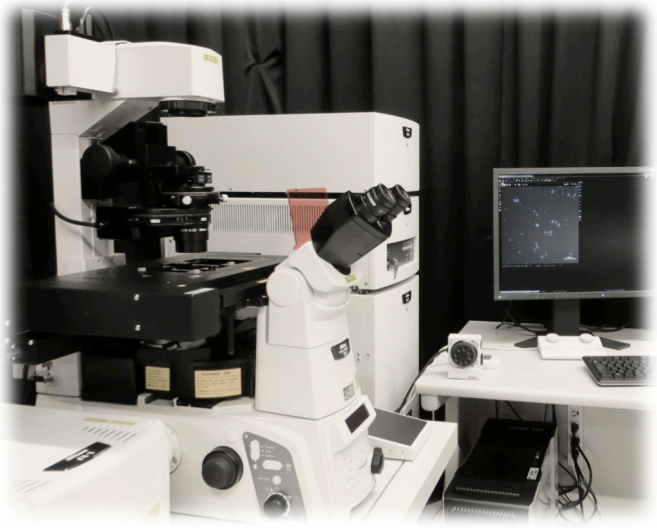

2

Bioinstrumentation

"Chance favors the prepared mind "

- Louis Pasteur

Modern experimental research requires the combination of many traditional disciplines including biology, optics, mechanics, mathematics, electronics and chemistry. The field of bioinstrumentation has seemingly endless possibilities because of its fusion of different fields for the common purpose of developing new and exciting ways of managing and treating disease and disabilities. This chapter covers the bioinstrumentation employed for this work; it includes the list of all sophisticated instruments exploited for the characterization and analysis of bacteria, their polysaccharides and BCS film. It also elaborates the principles and procedures of different colorimetric assays used for the chemical characterization polysaccharides and in vitro cell studies.

Ultraviolet-Visible Spectroscopy (UV_VIS)

The free radical scavenging activity and drug delivery was determined calorimetrically through D-730, spectrophotometer, Beckman coulter, USA and the absorbance was measured at the wavelength appropriate wavelengths based on the assay. 'Spectroscopy' is a collective term for all the analytical techniques based on the interaction of light and matter. Typical instruments in a UV-VIS range (spectrometers) can measure the 200-1000 nanometer range of the spectrum. Spectrophotometry is employed for both qualitative and quantitative evaluation of samples, wherein the molecules containing π-electrons or non-bonding electrons (n-electrons) can absorb the energy in the form of ultraviolet or visible light to excite these electrons to higher anti-bonding molecular orbitals as illustrated in Figure 1. An absorption spectrum will depict a number of absorption bands corresponding to structural groups within the molecule. Different molecules have a tendency to absorb radiation at different wavelengths. The wavelengths showing the maximum absorption band will indicate the structure of the molecule or ion and the extent of absorption is proportional with the amount of species absorbing the light.

Quantitative measurements are based on Beer's Law, which is described as follows:

$$A = ec\,l$$

where A = absorbance [no units, because it is calculated as $A = \log10(I0/I)$, where $I0$ is the incident light's intensity and I is the light intensity after it passes through the sample]; e = molar absorbance or absorption coefficient [in $dm^3\ mol^{-1}\ cm^{-1}$ units]; c = concentration (molarity) of the compound in the solution [in mol dm^{-3} units]; l = path length of light in the sample [in cm units]. The visible regions of the spectrum are: Violet: 400-420 nm; Indigo: 420-440 nm; Blue: 440- 490 nm; Green: 490-570 nm; Yellow: 570-585 nm; Orange: 585-620 nm; Red: 620-780 nm. [1, 2] The wavelength and intensity of the electromagnetic radiation absorbed or emitted can be recorded to get a spectrum.

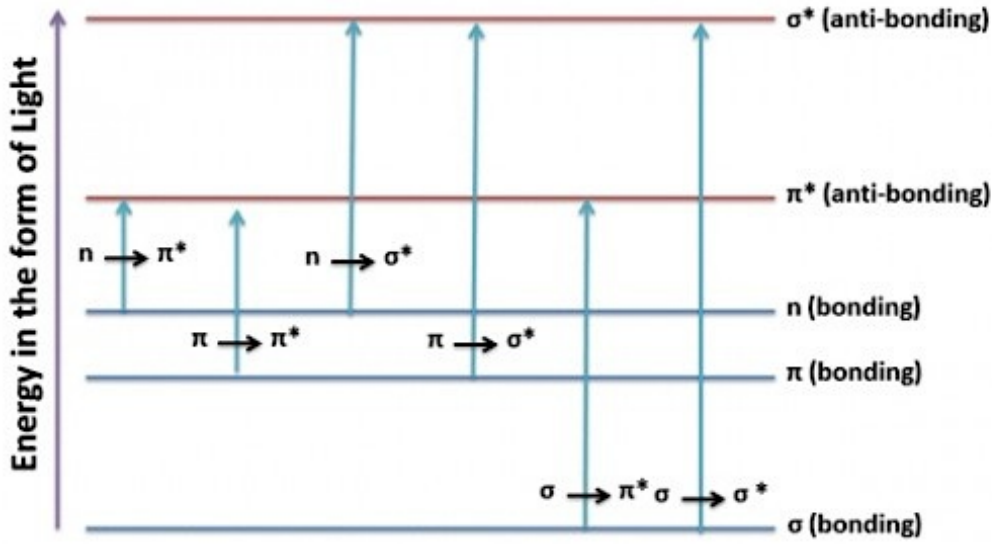

Fig 1: Different transitions between the bonding and anti-bonding electronic states when light energy is absorbed in UV-Visible Spectroscopy.

X-ray Photoelectron Spectroscopy (XPS)

XPS is also known as Electron Spectroscopy for Chemical Analysis (ESCA), is a powerful research tool for the study of the surface of solids. The technique is widely used to study the properties of atoms, molecules, solids, and surfaces. The success of XPS technique is associated with studies of the physical and chemical phenomena on the surface of solids, where x-rays are bombarded to excite the emission of electrons and simultaneously measure the kinetic energy. [3]

XPS irradiates the sample surface with a low energy (~1.5 KeV) X-ray to generate photoelectric effect. Figure 2 shows the diagram of XPS. This X-ray excites the electrons of the sample atoms and if their binding energy is lower than the X-ray energy, they will be emitted from the parent atom as a photoelectron. Only the photoelectrons at the extreme outer surface (10-100 Angstroms) can escape the sample surface, making this a surface analysis technique. The energy spectrum of the emitted photoelectrons is determined by means of a high-resolution electron spectrometer. The sample analysis is conducted in a vacuum chamber, under the best vacuum conditions achievable, typically ~10^{-10} torr. XPS is very surface-sensitive, with a typical "sampling depth" of only a few nanometers from 1-10 nm. The instrument is capable of analyzing

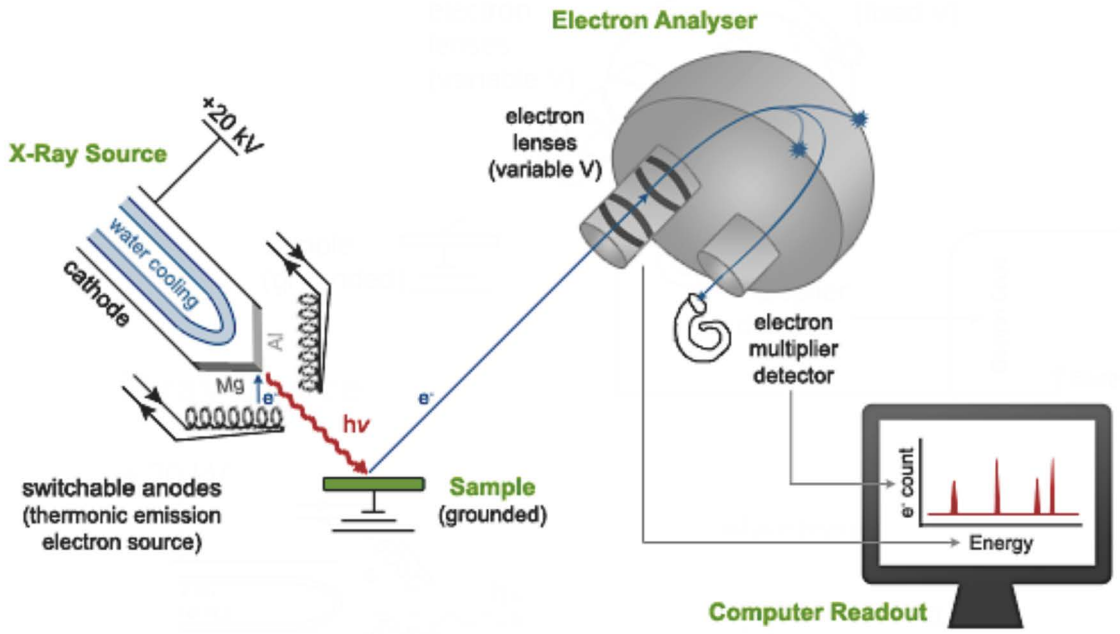

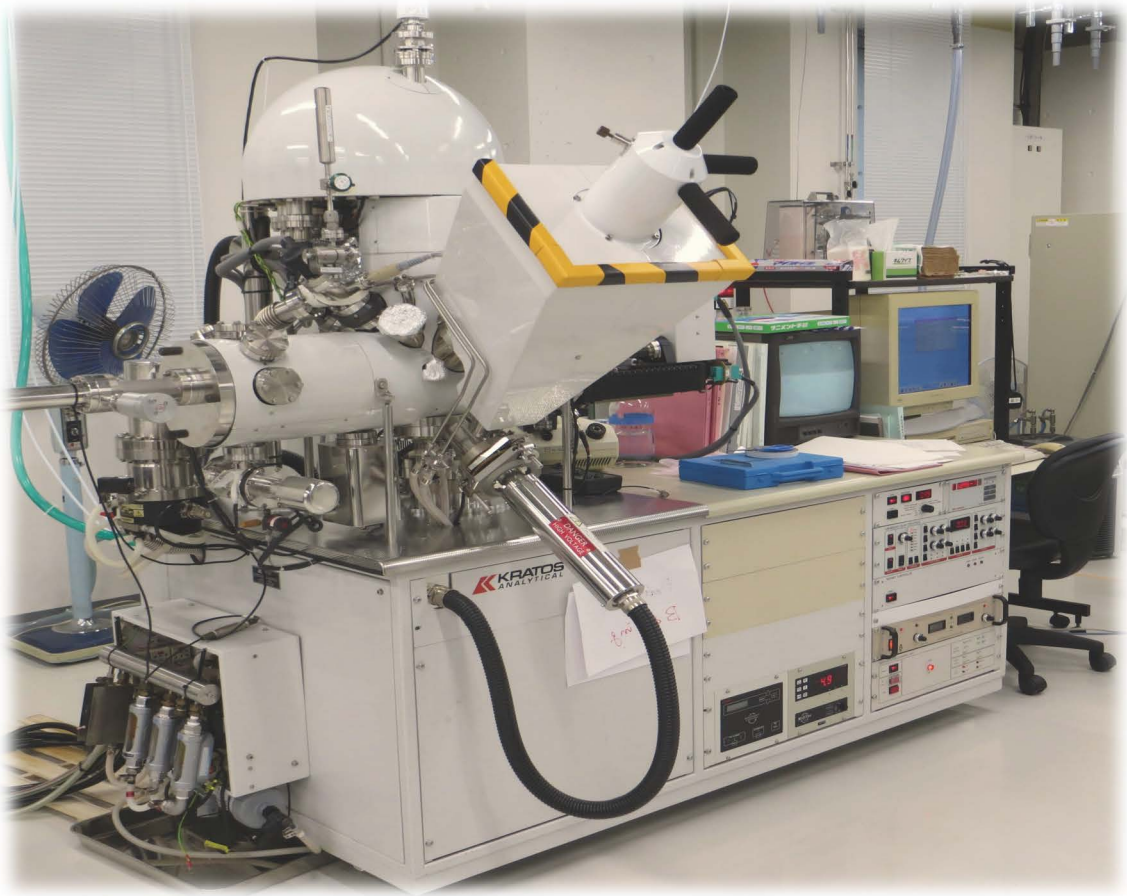

Fig 2: X-ray Photoelectron Spectroscopy Principle (Top); Kratos-Axis-His, Shimadzu, Japan (Bottom)

the samples that contains elements with atomic number above 3.

A typical XPS spectrum is a plot of the number of electrons detected versus the binding energy of the electrons detected. Each element produces a characteristic set of XPS peaks at characteristic binding energy values that directly identify each element that exist in or on the surface of the material being analyzed. The characteristic peaks obtained corresponds to the electron configuration of the electrons within the atom, e.g., 1s, 2s, 2p, 3s, etc. Binding energies of the photoelectrons depend on the chemical environments of the exact peak position of the chemical state of these elements. Depth profiling can be performed by means of etching the surface of the material to obtain information at larger depths (1–2 μm). This can be achieved by alternative sputtering with Ar^+ ions and then recording the spectrum.[3, 4]

Fourier Transform Infrared Spectroscopy (FTIR)

The infrared spectra were performed on a Perkin Elmer Spectrum 100 FT-IR system (Perkin Elmer, USA). The range of Infrared region is 12800 ~ 10 cm^{-1} and can be divided into near-infrared region (12800 ~ 4000 cm^{-1}), mid-infrared region (4000 ~ 200 cm^{-1}) and far-infrared region (50 ~ 1000 cm^{-1}). Figure 3 shows the image of FTIR.

FTIR is used to determine the structures of molecules with the molecules' characteristic absorption of infrared radiation. Infrared spectrum is molecular vibrational spectrum. When exposed to infrared radiation, sample molecules selectively absorb radiation of specific wavelengths, which causes the change of dipole moment of sample molecules. Consequently, the vibrational energy levels of sample molecules transfer from ground state to excited state. The frequency of the absorption peak is determined by the vibrational energy gap. The number of absorption peaks is related to the number of vibrational freedom of the molecule. The intensity of absorption peaks is related to the change of dipole moment and the possibility of the transition of energy levels. Therefore, by analyzing the infrared spectrum, one can readily obtain abundant structure information of a molecule. Most

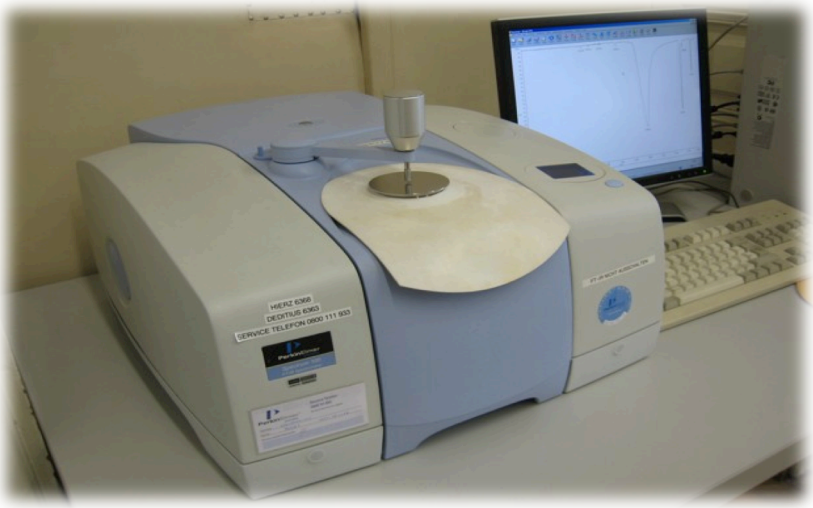

Fig 3: Perkin Elmer Spectrum 100 FT-IR system

molecules are infrared active except for several homonuclear diatomic molecules such as O_2, N_2 and Cl_2 due to the zero dipole change in the vibration and rotation of these molecules. What makes infrared absorption spectroscopy even more useful is the fact that it is capable to analyze all gas, liquid and solid samples. The common used region for infrared absorption spectroscopy is 4000 ~ 400 cm^{-1} because the absorption radiation of most organic compounds and inorganic ions is within this region. [6]

Energy Dispersive X-ray Spectroscopy (EDX/EDS/EDAX)

EDS is an analytical technique used for the elemental analysis or chemical characterization of a sample. It relies on the investigation of an interaction of some source of X-ray excitation and sample. EDS makes use of the X-ray spectrum emitted by a solid sample bombarded with a focused beam of electrons to obtain a localized chemical analysis. All elements from atomic number 4 (Be) to 92 (U) can be detected in principle, though not all instruments are equipped for 'light' elements (Z < 10). Qualitative analysis involves the identification of the lines in the spectrum and is fairly straightforward owing to the simplicity of X-ray spectra. Quantitative analysis (determination of the concentrations of the elements present) entails measuring line intensities for each element in the sample and for the same elements in calibration standards of known

composition. By scanning the beam in a television-like raster and displaying the intensity of a selected X-ray line, element distribution images or 'maps' can be produced. Also, images produced by electrons collected from the sample reveal surface topography or mean atomic number differences according to the mode selected. [7] The SEM, which is closely related to the electron probe, is designed primarily for producing electron images, but can also be used for element mapping, and even point analysis, if an X-ray spectrometer is added. Thus, there is a considerable overlap in the functions of these instruments.

Raman Spectroscopy

Raman spectroscopy is a complementary method to evaluate vibrational transitions. It is basically a light scattering technique, which is inelastic. The principle of the Raman spectroscopy involves sending a monochromatic light (only one color and not a mixture) on the sample to study and analyze the scattered light. The incidental photons are destroyed and their energy is used for creating scattered photons and creating (Stokes process) or destroying (anti-Stokes process) vibrations in the studied sample. Figure 4 depicts the principle of raman spectroscopy and the image of Nicolet iS50/Raman, Thermo Scientific, Japan.

For Raman analysis, a sample is illuminated with a laser beam and light from the illuminated spot is collected with a lens and sent through a monochromator. Wavelengths close to the laser line due to elastic Rayleigh scattering are filtered out while the rest of the collected light is dispersed onto a detector. The Raman effect occurs when light impinges upon a molecule and interacts with the electron cloud and the bonds of that molecule. For the spontaneous Raman effect, which is a form of light scattering, a photon excites the molecule from the ground state to a virtual energy state. When the molecule relaxes it emits a photon and it returns to a different rotational or vibrational state. The difference in energy between the original state and this new state leads to a shift in the emitted photon's frequency away from the excitation wavelength.

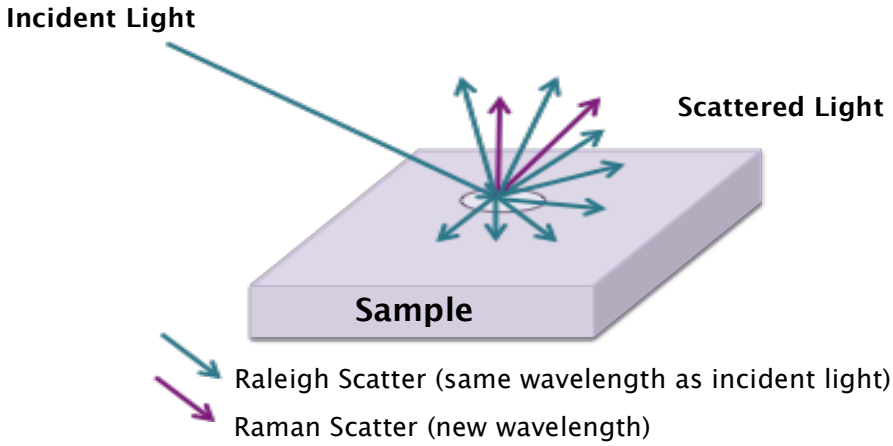

Fig 4: Raman Spectroscopy Principle [8]; Nicolet Si50/Raman, Thermo Scientific, Japan.

Raman spectroscopy is commonly used in chemistry, since vibrational information is specific to the chemical bonds and symmetry of molecules.

Zeta Sizer

Zetasizer ZS measures the size of particles and molecules of 1 nm to several microns using dynamic light scattering and it measures zeta potential as well as electrophoretic mobility using electrophoretic light scattering. Zetasizer performs the size measurements using a process called Dynamic light scattering (DLS), zeta potential using laser Doppler micro-electrophoresis and detection of molecular weight through static light scattering. Figure 5 depicts the image of a Zetasizer. **Dynamic**

Fig 5: Zetasizer ZS90, Malvern, Japan

Light Scattering is used to measure particle and molecule size. This technique measures the diffusion of particles moving under Brownian motion, and converts this to size and a size distribution using the Stokes-Einstein relationship. Non-Invasive Back Scatter technology (NIBS) is incorporated to give the highest sensitivity simultaneously with the highest size and concentration range. **Laser Doppler Micro-electrophoresis** is used to measure zeta potential. An electric field is applied to a solution of molecules or a dispersion of particles, which then move with a velocity related to their zeta potential. This velocity is measured using a patented laser interferometric technique called M3-PALS (Phase analysis Light Scattering). This enables the calculation of electrophoretic mobility, and from this the zeta potential and zeta potential distribution. **Static Light Scattering** is used to determine the molecular weight of proteins and polymers. In this technique, the scattering intensity of a number of concentrations of the sample is measured, and used to construct a Debye plot. From this the average molecular weight and second virial coefficient can be calculated, which gives a measure of molecule solubility. [9]

Rheometer

Viscosity is a measure of a fluid's resistance to flow. Viscometer/ Rheometer is a precise torque meter, which is driven at discrete rotational speeds. The drive mechanism to a rotating cone senses the resistance to rotation caused by the presence of sample fluid between the cone and a stationary flat plate. The resistance to the rotation of the cone produces a torque that is proportional to the shear stress in the fluid. This reading is easily converted to absolute centipoise units (mPa·s) from pre-calculated range charts. Alternatively, viscosity can be calculated from the known geometric constants of the cone, the rate of rotation, and the stress related torque. These instruments provide precise shear profiles necessary to determine viscosity and develop rheological data. Figure 6 depicts the image of a rheometer. On the basis of viscosity fluids can be classified as Newtonian and Non-Newtonian fluids, wherein Newtonian fluids are those that can be characterized using a single coefficient of viscosity for a specific temperature. Where as most of the fluids change their viscosity with relative change of flow or strain rate. Such fluids are collectively called as Non- Newtonian fluids.

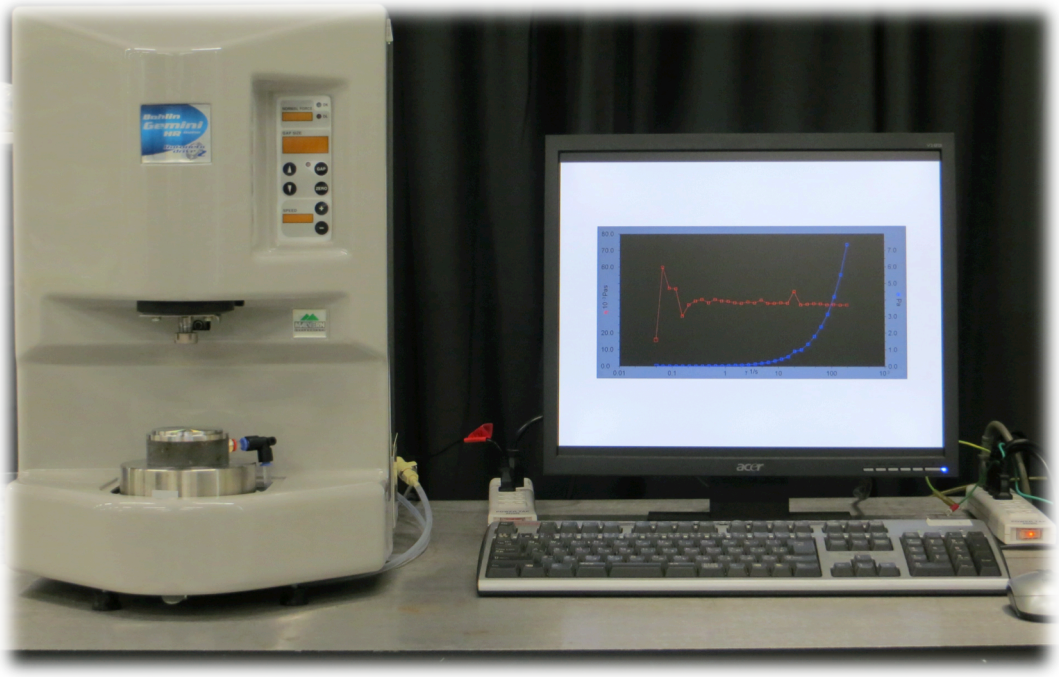

Fig 6: Bohlin Gemini II Rheometer, Malvern, Japan.

Thermogravimetric Analysis (TGA)

Thermal gravimetric analysis often serves as a maiden diagnostic tool, since it measures the weight loss seen in a material with the increase in temperature. Figure 7 shows the image of TGA-50. Usually, stoichiometric, heat stability, and compositional information can be obtained by studying the change in mass as a function of temperature. Also by recording the specific temperature point, where maximum rate of weight loss occurs, it is possible to identify the composition of the polymer. While, identifying the degradation temperature, the apparatus should have the ability to quantify loss of water, loss of solvent, loss of plasticizer, decarboxylation, pyrolysis, oxidation, decomposition, weight % filler, amount of metallic catalytic residue remaining on carbon nanotubes, and weight % ash. Dry specimens weighing 5 to 10 mg of were placed in a clean dry pan. The chamber was purged with either nitrogen or air and the sample was heated from 25°C to 1000°C at a constant rate of 20°C per minute. In thermogravimetry a continuous graph of mass change against temperature is obtained when a substance is heated at a uniform rate or kept at constant temperature. A plot of mass (M) change versus temperature (*T*) is referred to as the thermogravimetric curve (TG curve).

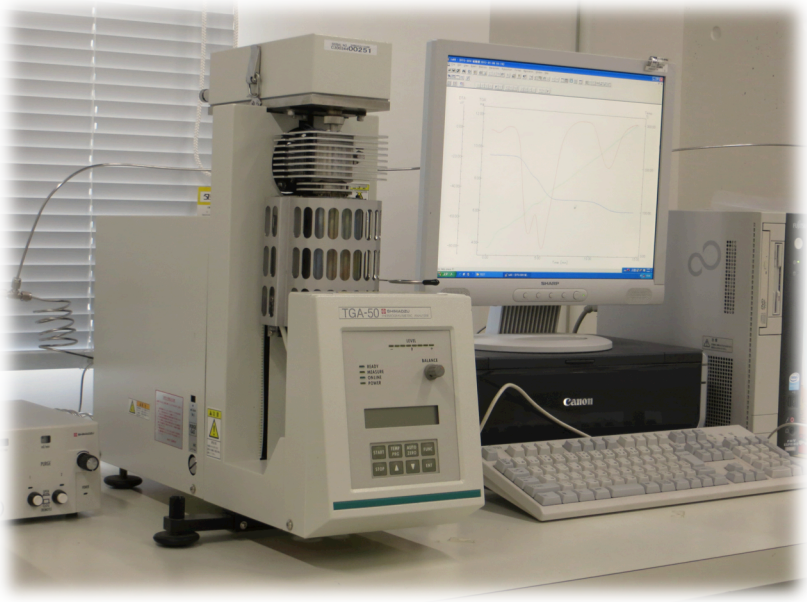

Fig 7: TGA-50, Shimadzu, Japan

Mechanical strength testing

The tensile properties of BCS films were characterized using a Universal Testing Machine (Instron 3345, UK) equipped with a 500 N load-cell. Figure 8 illustrates the tensile strength mechanism. [11]

Mechanical properties including elasticity, yield strength, ultimate tensile strength and ductility are usually part of material specifications and are obtained by tensile testing. The ability to resist breaking under tensile stress is one of the most important and widely measured properties of materials used in structural applications. Properties in longitudinal direction are measured by clamping the strip sample and straining it until break while measuring the required force. Tensile tests, combined with the construct dimensions, result in stress-strain curves. The stress can be defined as an engineering stress, equaling the measured force divided by the initial cross-sectional area defined as the force divided by the deformed cross-sectional area. The force per unit area (MPa or psi) required to break a material in such a manner is the ultimate tensile strength or tensile strength at break. For most tensile testing of

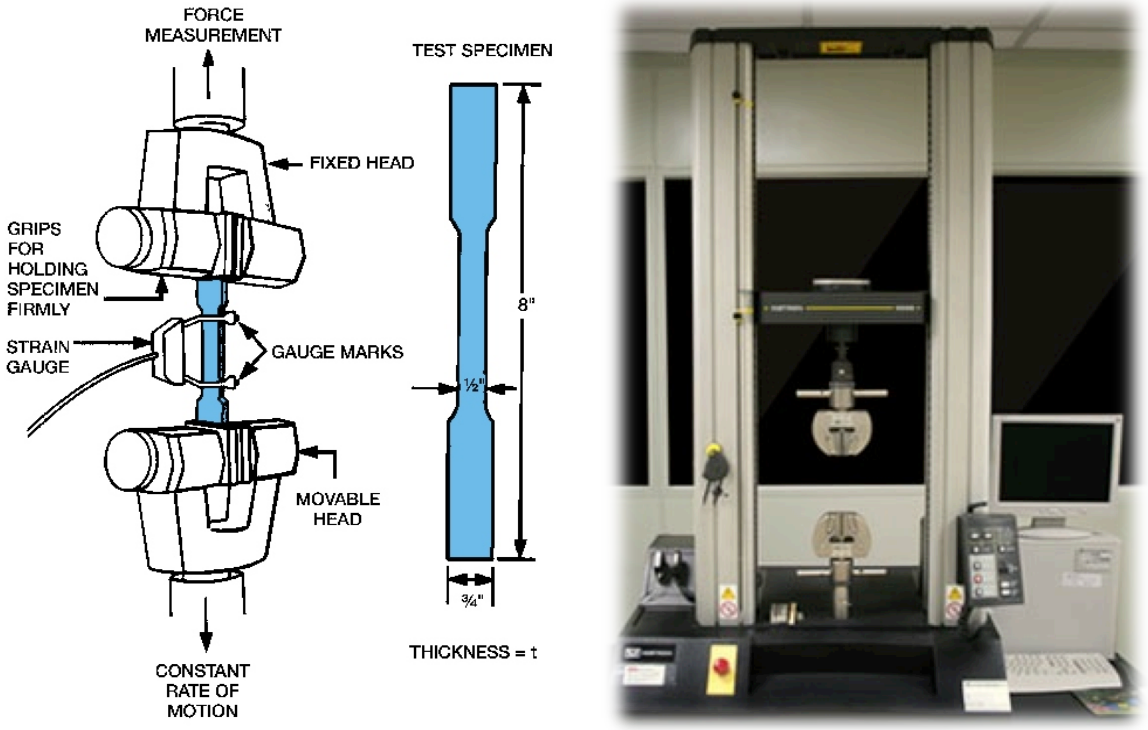

Fig 8: Universal Testing Machine (Instron 5566, UK)

materials, the initial portion of the test, the relationship between the applied force, or load, and the elongation the specimen exhibits is linear. In this linear region, the line obeys the relationship defined as "Hooke's Law" where the ratio of stress to strain is a constant, or

$$\frac{\sigma}{\varepsilon} = E$$

E is the slope of the line in this region where stress (σ) is proportional to strain (ε) and is called the "Modulus of Elasticity" or "Young's Modulus".

Scanning Electron Microscopy (SEM)

The SEM uses a beam of electrons to scan the surface of a sample to build a three-dimensional image of the specimen. Sample preparation can be minimal or elaborate for SEM analysis, depending on the nature of the samples and the data required. Minimal preparation includes acquisition of a sample that will fit into the SEM chamber and some accommodation to prevent charge build-up on electrically insulating samples. Most electrically insulating samples are coated with a thin layer

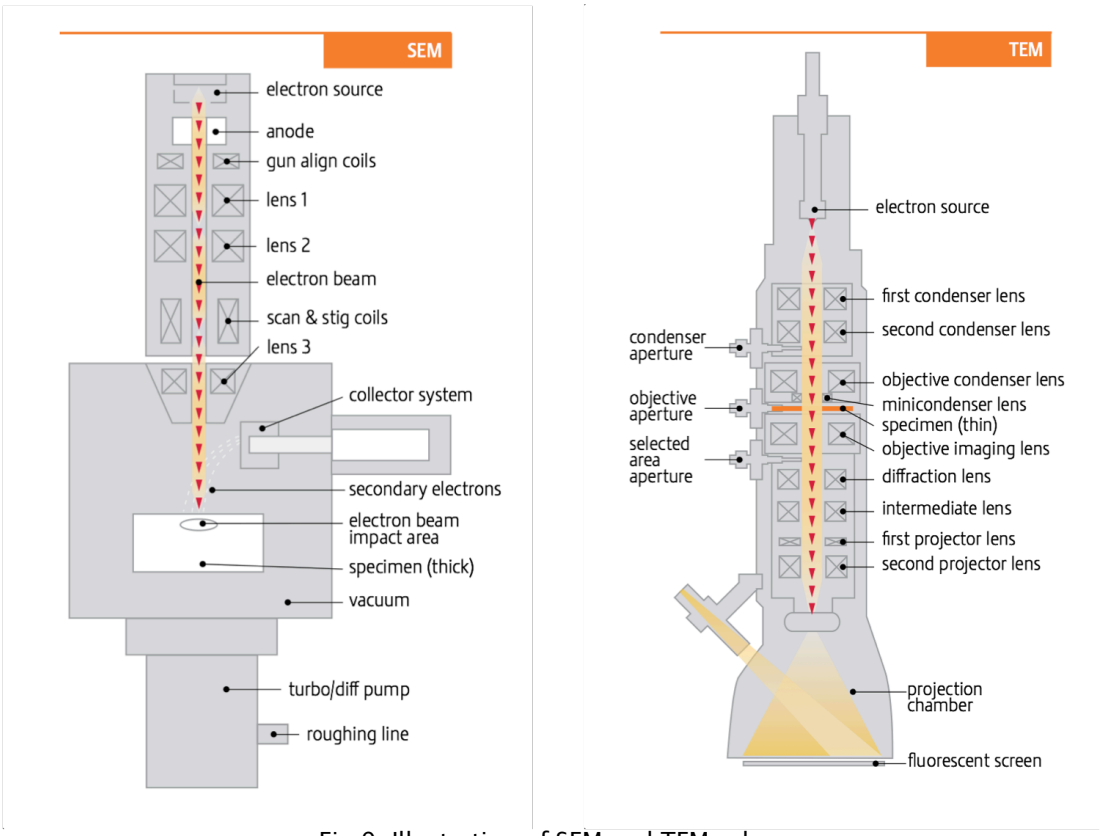

Fig 9: Illustration of SEM and TEM scheme

SEM – JSM-7400F, JEOL, Japan

TEM – JEM-2200FS, JEOL, Japan

of conducting material, commonly carbon, gold, or some other metal or alloy. The choice of material for conductive coatings depends on the data to be acquired: carbon is most desirable if elemental analysis is a priority, while metal coatings are most effective for high-resolution electron imaging applications. Figure 9 shows the schematic diagram of SEM and TEM [12]. When the electron beam hits the sample, the interaction of the beam electrons from the filament and the sample atoms generates a variety of signals. Depending on the sample, these can include secondary electrons (electrons from the sample itself), backscattered electrons (beam electrons from the filament that bounce off nuclei of atoms in the sample), X-rays, light, heat, and even transmitted electrons (beam electrons that pass through the sample). The signals that derive from electron-sample interactions reveal information about the sample including external morphology (texture), chemical composition, and crystalline structure and orientation of materials making up the sample. Secondary electrons and backscattered electrons are commonly used for imaging samples: secondary electrons are most valuable for showing morphology and topography on samples and backscattered electrons are most valuable for illustrating contrasts in composition in multiphase samples.

Transmission Electron Microscopy (TEM)

The requirement of TEM in diverse field is attributed to the minute details that can be captured through this instrument. It is used to examine the structure, composition or properties of samples. For a conventional TEM analysis, a specimen has to be reasonably dried and thin for ensuring electron transparency. In general, a sample has to follow certain conditions including a complete lack of water (as high vacuum conditions are used), an ability to remain stable when exposed to e-beam damage and the presence of both electron transparency and electron opacity zones. TEM reveals information about sample morphology, crystallographic data using electron diffraction, and compositional analysis using energy dispersive or wavelength dispersive

spectroscopy. The TEM uses a high energy electron beam transmitted through a very thin sample to image and analyze the microstructure of materials with atomic scale resolution. The electrons are focused with electromagnetic lenses and the image is observed on a fluorescent screen, or recorded on film or digital camera. The electrons are accelerated at several hundred kV, giving wavelengths much smaller than that of light: 200kV electrons have a wavelength of 0.025Å. However, whereas the resolution of the optical microscope is limited by the wavelength of light, that of the electron microscope is limited by aberrations inherent in electromagnetic lenses, to about 1-2 Å. The high resolution imaging mode of the microscope images the crystal lattice of a material as interference pattern between the transmitted and diffracted beams. This allows one to observe planar and line defects, grain boundaries, interfaces, etc. with atomic scale resolution. The brightfield/darkfield imaging modes of the microscope, which operate at intermediate magnification, combined with electron diffraction, are also invaluable for giving information about the morphology, crystal phases, and defects in a material. [12]

Atomic Force Microscopy (AFM)

The atomic force microscope (AFM) is one kind of scanning probe microscopes (SPM). SPMs are designed to measure local properties, such as height, friction, magnetism, with a probe. To acquire an image, the SPM raster-scans the probe over a small area of the sample, measuring the local property simultaneously. AFMs operate by measuring force between a probe and the sample. Normally, the probe is a sharp tip, which is a 3-6μm tall pyramid with 15-40nm end radius. Though the lateral resolution of AFM is low (~30nm) due to the convolution, the vertical resolution can be up to 0.1nm. To acquire the image resolution, AFMs can generally measure the vertical and lateral deflections of the cantilever by using the optical lever. The optical lever operates by reflecting a laser beam off the cantilever. The reflected laser beam strikes a position-sensitive photo-detector consisting of four-segment photo-

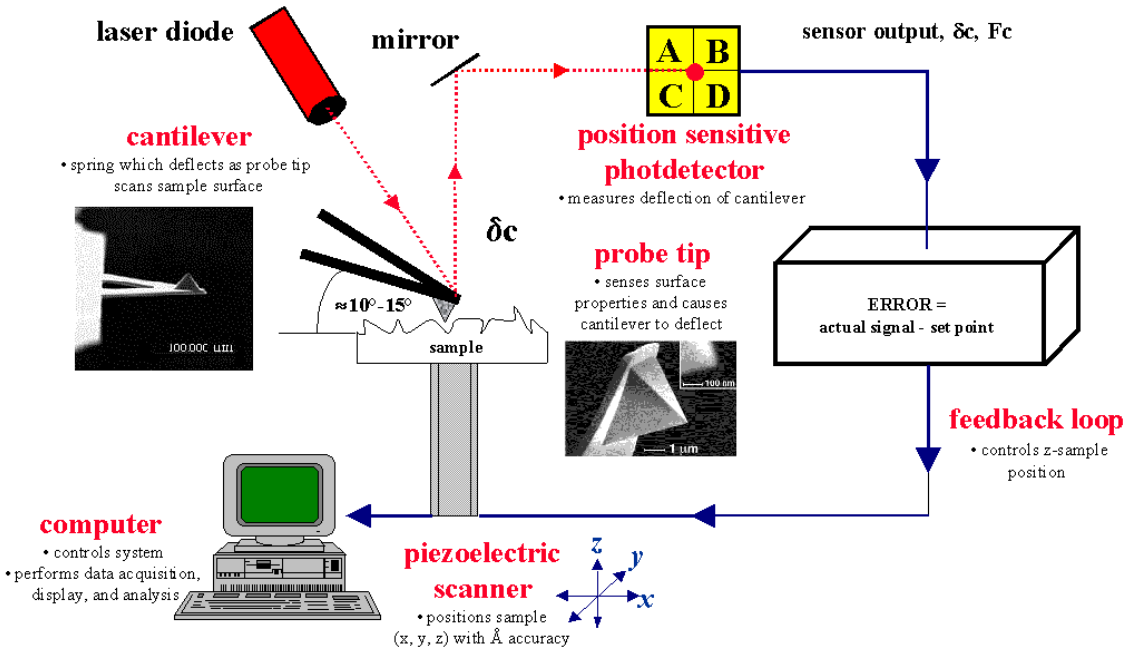

Fig 10: Illustration of AFM components and their functions

AFM-Asylum Research, MFP-3D-CF, California

detector. The differences between the segments of photo- detector of signals indicate the position of the laser spot on the detector and thus the angular deflections of the cantilever. In contact mode, AFMs use feedback to regulate the force on the sample. The AFM not only measures the force on the sample but also regulates it, allowing

acquisition of images at very low forces. The feedback loop consists of the tube scanner that controls the height of the tip; the cantilever and optical lever, which measures the local height of the sample; and a feedback circuit that attempts to keep the cantilever deflection constant by adjusting the voltage applied to the scanner. A well-constructed feedback loop is essential to microscope performance. [13] Figure 10 shows AFM schematic representation. [14]

Laser Scanning Confocal Microscopy (LSCM)

The principle of LSCM relies on the coherent light emitted by the laser system (excitation source) passes through a pinhole aperture that is situated in a conjugate plane (confocal) with a scanning point on the specimen and a second pinhole aperture positioned in front of the detector (a photomultiplier tube). As the laser is reflected by a dichromatic mirror and scanned across the specimen in a defined focal plane, secondary fluorescence emitted from points on the specimen (in the same focal plane) pass back through the dichromatic mirror and are focused as a confocal point at the detector pinhole aperture. The signal from the detector is then digitized and passed to a computer. The image of the sample is digitally built up by scanning the sample in the X and Y directions and then special software is used to reconstruct a digital image. Figure 11 depicts the working of LSCM. [15, 16, 17]

Nikon Eclipse Ti, Inverted Microscope system, Japan

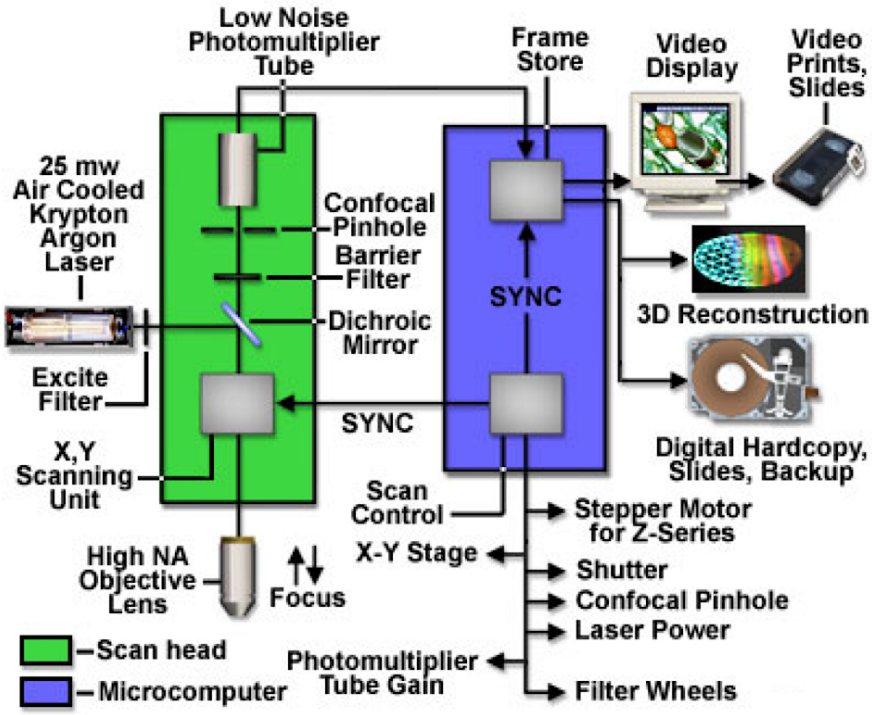

Fig 11: Principle of confocal microscopy

Summary

Since, the advent of nanotechnology, it has seen a tremendous growth with a wider applications. With increasing knowledge and application of advanced functional materials, polymers and composites, need for new tools with improved functionalities becomes a necessity. Simultaneous progress in instrumentation industries with newer, faster, simpler and more efficient characterization techniques for nanomaterial, nanocoatings and nanocomposites are required. However, large extent of it depends on the cost, ease of handling and performance.

References

1. S. L. Ustone. Ultraviolet/Visible Light Absorption Spectrophotometry in Clinical Chemistry. Encyclopedia of Analytical Chemistry, 1699-1714, **(2000).**
2. http://pharmaxchange.info/press/2011/12/ultraviolet-visible-uv-vis-spectroscopy-principle/

3. D. Zemlyanov. "Introduction to X-ray Photoelectron Spectroscopy and to XPS Applications," http://nanohub.org/resources/2668, **(2007).**
4. J. F. Moulder, W. F. Stickle, P. E. Sobol, K. D. Bomben. Handbook of X-ray Photoelectron Spectroscopy, published by Perkin-Elmer Corp., , Eden Prairie, MN, USA, **(1992)**.
5. http://www.chem.queensu.ca/people/faculty/horton/research.html
6. http://chemwiki.ucdavis.edu/Physical_Chemistry/Spectroscopy/Vibrational_Spectroscopy/Infrared_Spectroscopy/How_an_FTIR_Spectrometer_Operates.
7. J. C. Russ. Fundamentals of Energy Dispersive X-ray Analysis, Butterworths. London, (**1984).**
8. http://www-che.engr.ccny.cuny.edu/courses/che5535/lecture5/sld002.htm
9. http://www.malvern.com/en/products/product-range/zetasizer-range/zetasizer-nano-range/zetasizer-nano-zs/
10. H. H. Winter. Rheometry with Capillary Rheometers. Chapter in Encyclopedia of Life Support Systems (EOLSS) UNESCO- Publishers Co Ltd 6.197. Gallegos C, Walters K (ed), **(2008)**.
11. http://www2.warwick.ac.uk/fac/sci/wmg/globalcontent/courses/ebm/mant/materials/properties_of_materials/
12. http://www.fei.com/Introduction-to-Electron-Microscopy/
13. http://www.nanoscience.gatech.edu/zlwang/research/afm.html
14. http://research.mui.ac.ir/images/stories/test/photo/lab/afm/afm-r3jgkw.gif
15. http://www.microscopyu.com/articles/confocal/pawley39steps.html
16. B. Matsumoto. Cell Biological Applications of Confocal Microscopy. *San Diego: Academic Press.* PP.507, **(2002).**
17. Diaspro A. Confocal and Two-Photon Microscopy: Foundations, Applications, and Advances. New York: Wiley-Liss. PP.567, **(2002).**

3

Large Scale Fermentation and Characterization of Bacterial Cellulose

"Imagination is more important than knowledge "

- Albert Einstein

BC is an exopolysaccharide produced by bacteria, which has unique structural and mechanical properties as discussed in the chapter 1. Owing to its biocompatibility and biodegradability, BC gives plenty of room for researchers across the globe to use it for diverse applications such as in biomedicine, bionanoelectronics, food and packaging. Furthermore, BC has a distinct advantage over plant cellulose in terms of purity. This chapter is focused mainly on the cultivation, collection and purification of BC through fermentation of *Komagataeibacter sucrofermentans*. The entire process starts with the microbial cultivation. A pre-culture is prepared and is transferred to the jar fermenter, through which controlled agitated conditions are provided for bacterial growth and BC production. Thereafter, BC pellicles are harvested and purified through alkali treatment. Post purification, BC is subjected to various physical and chemical characterizations like electron microscopy and XPS, respectively.

Introduction

Cellulose is a high molecular weight natural polysaccharide comprising D-glucopyranosyl repeating units, predominantly produced by plants. [1] However, some microorganisms like the bacteria (*Acetobacter*, *Agrobacterium*, *Achromobacter*, *Aerobacter*, S*arcina, Azotobacter*, *Rhizobium, Pseudomonas, Salmonella, Alcaligenes and Sarcina ventriculi)*, fungi (Oomycetes) and algae (Green algae, Brown algae, Red algae and Golden algae) have the ability to produce cellulose. [2] Cellulose is insoluble in water and almost inexhaustible source of raw material available on earth. [3] Both bacterial cellulose (BC) and plant cellulose have similar molecular formula $(C_6H_{10}O_5)_n$, but differ in their physical and chemical properties. [4] BC has unique characteristics that include high purity (free of hemicellulose and lignin), high crystallinity and remarkable mechanical properties, due to the uniform ultrafine-fiber network structure, the high planar orientation of the ribbon-like fibers when compressed into sheets, the good chemical stability, and the high water holding capacity. [5-7] Fibrils of BC are very thin, with a width of only one-hundredth that of plant cellulose. [8] Numerous bacterial extracellular polysaccharides (EPS) have been reported over recent decades with an extensive study on their composition, structure, biosynthesis and functional properties. Only a few EPS (e.g. bacterial cellulose) have emerged as industrially important biopolymer with significant commercial value. [9] Among several bacteria reported to produce EPS, *Glucanoacetobacter* is counted upon as the most important genus because of its ability to produce very high yield of BC. The unique properties of BC open up wide industrial applications in food, pharmaceutical, textile, paper, cosmetics, medicines for wound dressing, acoustic transducer diaphragm, filtration etc. [10]

Recently, lot of focus has been shed on the mass production of BC owing to its varied fields of applications that includes optimization of culture conditions, media composition, strain improvement or scaling up process. [11] Factors mainly affecting cellulose production are growth media, environmental conditions and formation of byproducts. Current

methods employed in BC production include static culture, [12] agitating culture, [13] and airlift reactor. [14]

Continuous and semi-continuous fermentation are also looked upon as a route to achieve large-scale production of BC. The key is to produce maximum BC with desired form and properties. To enhance production of BC two vital aspects are to be considered the genetic and engineering point of view. The later includes the reactor design, nutrient selection, process control and optimization and the former includes the cloning of BC synthesis geneto speculate genes for better production of BC. [8] Addition of supplements during cultivation or employing chemical modifications to BC to obtain its derivatives has gained a lot of interest. Chemical or physical surface modifications are regularly enforced to achieve specific medical applications. [15] Carboxymethylation, acetylation, phosphorylation, succinylation, benzoylation, acetylation and carbanilation are some of the chemical methods that have been reported to modify BC. Chemical modifications can be attained through both homogeneous and heterogeneous reactions. But, unfortunately the focus on chemical modifications of BC is not enough. [16]

The present study involves the production of BC through agitating culture method using the strain *K. sucrofermentans* JCM 9730 strain. Post fermentation the acquired BC was homogenized and subjected to alkali treatment with NaOH to complete the purification process. The purified BC was freeze-dried and subjected to various characterizations that include electron microscopy, XPS, and FTIR.

Materials and Methods

All the chemicals used were of analytical grade and were used as received. Dialysis membrane from Spectrum Laboratories Inc. (Rancho Dominquez, USA) has an approximate molecular weight cut off of 500 Da. Carbon coated Formvar grids, 0.05% Ruthenium red solution, 2.5% Glutaraldehyde, 0.05% Sodium cacodylate, 2.5mM MgCl2.6H2O (pH 7.4), 1% OsO4, Ethanol, Embedding resin, Gelatin capsule, TI blue solution, Lead citrate, Poly-L-lysine coated slides.

Bacterial strain and Morphology

Komagataeibacter sucrofermentans JCM 9730^T strain was purchased Riken Bioresource Center, Japan and was cultured as per the instructions on the product information sheet. The bacterial culture was revived using the acetobacter medium (Glucose 100g, Yeast extract 10g, Calcium carbonate 30g, Agar 15g in 1L DW). The petri-plates containing bacterial culture were incubated at 28°C. Colonies are white-creamy and smooth with entire margin or rough. It is a gram-negative rod that is non-motile and measures 0.5-0.8 X 1.0-3.0 μm in size with the ability to produce BC, an exopolysaccharide (EPS). [17]

Bacterial Fermentation and Purification

Bacterial culture was cultivated in Hestrin-Schramm (HS) medium as mentioned elsewhere. [18] The following composition of media was used: glucose, 20g; Bacto peptone, 5g; Bacto yeast extract, 5 g; disodium phosphate (anhydrous), 2.7g; citric acid monohydrate, 1.15g in 1 L of distilled water. pH was adjusted to 6.0 with HCl or NaOH and was sterilized by autoclaving. The pre-culture was transferred to the fermenter post sterilization. The following conditions were optimized on the fermenter for the cellulose production: Agitation, 100 rpm; pH, 6.0; temperature, 28°C; DO, 3ppm. SI antifoam was used to prevent the excess foam during fermentation. The bacterial cellulose pellicles were harvested after 10 days and subjected to purification. The purification was carried through the alkali extraction method described elsewhere [19] The cellulose pellicles obtained post fermentation was homogenized in distilled water using the high-pressure homogenizer for 5 mins. The homogenized sample was centrifuged at 13,800 g for 10 mins at 10°C and the supernatant was discarded. The cellulose paste was mixed thoroughly for homogeneity and was placed in a beaker with alkaline solution of 0.30 mol/dm^3 NaOH preheated to 90°C. The mixture was heated for 25 mins and rapidly cooled down in an ice bath. Then, the samples were washed with distilled water and pH of the sediments was

adjusted to 7. Subsequently, BC freeze-dried and the samples were stored in airtight tubes and refrigerated until further analyses were done.

SEM Analysis

For Scanning Electron Microscopy (SEM) images the bacterial sample was sputter coated with Pt and the images were obtained on a JEOL, JSM-7400F scanning microscope at room temperature.

- Cells from mid-exponential-phase cultures were bound to poly-l-lysine-coated slides during the fixation process, which was carried out overnight at 4 °C in an atmosphere saturated with glutaraldehyde vapor.
- After washing in 0.1 M sodium cacodylate, 0.05% (w/v), ruthenium red was added for 4 h.
- The cells were dehydrated in an ethanol series (30, 50, 70, 90 and 100%, v/v) at room temperature, each dehydration step taking 20 min.
- The samples were dried and sputter-coated with platinum.
- Electron micrographs were obtained by using SEM.

TEM Analysis

Samples were negatively stained for Transmission Electron Microscopy (TEM) images, which were obtained on a JEOL, JEM-2200FS transmission electron microscope.

- For negative staining, carbon-coated formvar grids were placed facedown over a droplet of mid-exponential phase culture in HS medium.
- After 4 min, the grid was removed, blotted briefly with filter paper and, without drying, transferred to 0.05% (w/v) ruthenium red solution (pH 7.2), then blotted quickly, air-dried and examined using TEM under 200 kV.

FTIR Analysis

The chemical structure of BC was analyzed and through Fourier Transform Infrared (FTIR) (Perkin Elmer) with a resolution of 4 cm^{-1} in the region of 4000 to 400 cm^{-1}.

XPS Analysis

Elemental analysis was determined using X-ray photoelectron spectroscopy KRATOS with a basic pressure of 1.7 x 10^{-8} and mono-Al anode with pass energy of 40 (survey scan) X-ray source.

Results and Discussion

BC was successfully synthesized through fermentation process using *Komagataeibacter sucrofermentans* JCM 9730^{T} strain in HS medium. Several routes to fermentation exist in the modern era. Two main types of fermentation process are agitated and static.

Static fermentation has been employed in *nata de coco* food industries for many years. It has shown good results due to low shear force during fermentation that contributes to enhanced productivity. However, optimization of culture conditions becomes vital during the entire process, since cellulose membrane itself can become a barrier for substrates and oxygen necessary for the cells to produce cellulose. Hence, controlled fermentation conditions become a vital aspect to improve the BC yield production. [20, 21]

In the present study, BC production was carried out in a jar fermenter under controlled conditions. Figure 1 shows the BC pellicles in jar fermenter. Small sphere-like BC pellicles were visible after 24-48 hours post inoculation, which further increased in size with time. The pellicles formed were of different sizes. They had a tendency to accumulate inside a bag-like membrane that is formed during the process. The BC sphere-like pellicles were collected after 10 days. BC sphere-like pellicles were collected and subjected to purification by alkali treatment method. We have used 0.30 mol/dm^3 of NaOH that was adequate to remove most of the contaminants from BC. The results agree

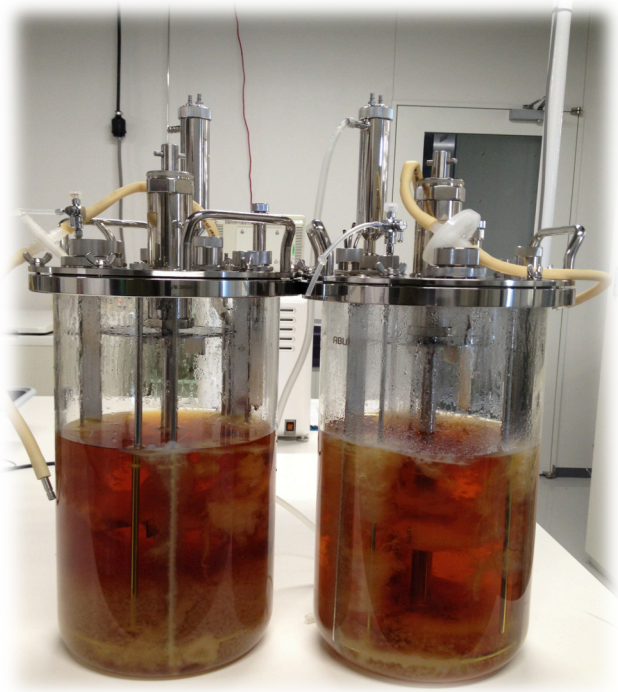

Fig: 1 BC production in jar fermenter

with the earlier reports, where sphere-like cellulose particles have been reported. [21] But unlike their results, sphere-like pellicles were observed in the fermenter when rotational speed was set at 100. However, The variation of flask sizes and media volumes resulted in different aeration and media fluid motion dynamics, which would affect shear forces in the media as well as oxygen dissolution rate. Based on this data, it appeared that the dominant factor influencing both sphere-like formation and cellulose yield for a strain capable of producing sphere-like particles of cellulose was the fluid dynamics, which could relate particularly to shear forces on the surface of the forming particles.

In the present study the following parameters were set for the production of BC,

- Rotational speed – 100 rpm
- Temperature – 28 °C
- pH – 6.0
- Dissolved oxygen – 10 ppm
- No. of days – 10

Electron Microscopic studies were conducted for the observation of BC sphere-like pellicles. For the SEM studies the samples were fixed to the poly-l-lysine-coated slides and then sputter coated with platinum. Figure 2 shows SEM images of BC at different magnifications. From the figure it is evident that each cell produces nano-fibrils, which assemble into a gelatinous membrane that form a sphere-like BC pellicle. This pellicle contains pure cellulose and bacterial cells entrapped between the nano-fibrils. Bacterial cells were found all over the BC mat with an average size of ~ 2-3 micrometers.

Detailed images of the bacteria and cellulose fibrils were visualized though the TEM images. Figure 3 shows the TEM images of *Komagataeibacter sucrofermentans* and BC fibrils secretion. The average size of the BC fibrils was noted to be ~ 10-20 nm. Also, the secretion of cellulose by bacterial cells was visible in the images. From the TEM

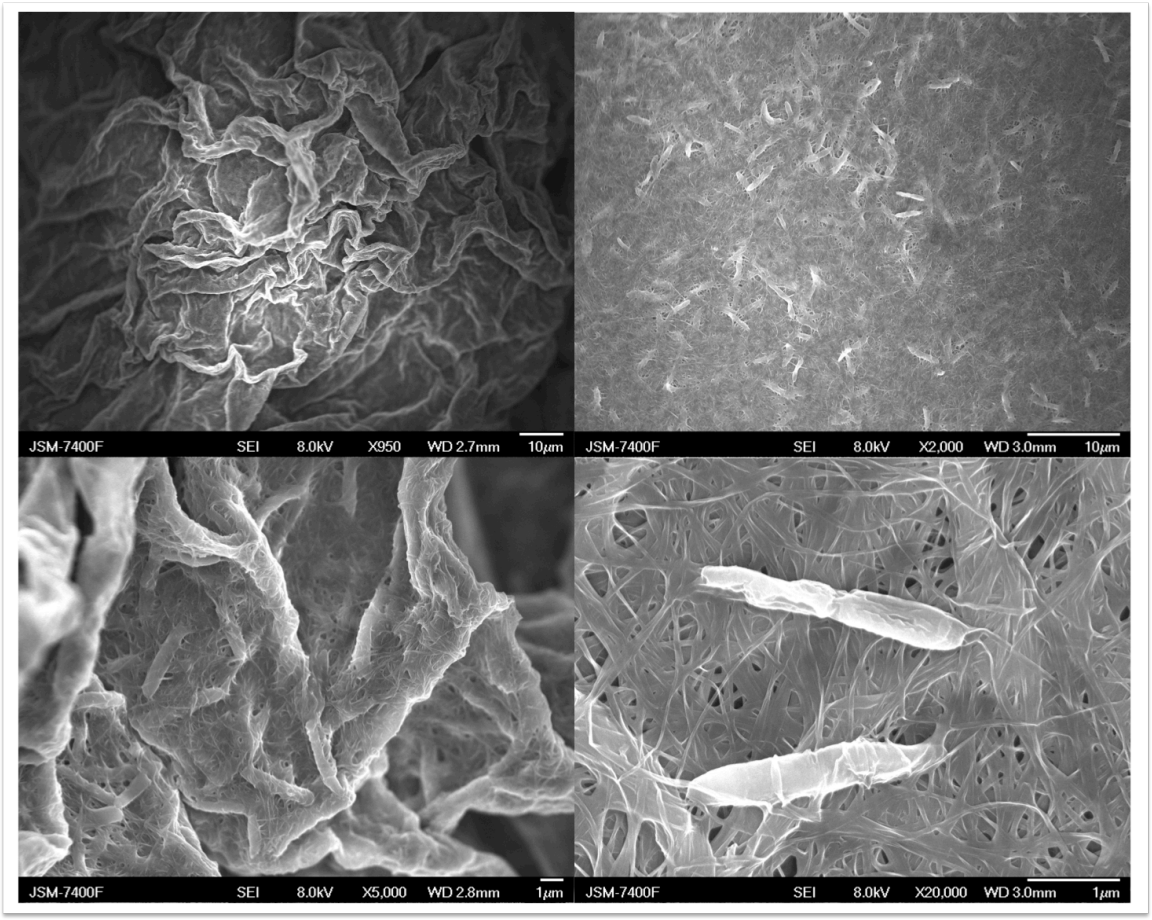

Fig 2: SEM images of BC at different magnifications

Images the bacterial morphology was clearly visible noted, which can also be related with the SEM results.

Subsequently, BC sphere-like pellicles were washed and purified through alkali treatment method. Though the alkali treatment method has been prevalent for years to purify BC, the suitable concentration still remains a mystery. While most studies use high concentrations of alkali, we have adapted much lower concentration 0.30 mol/dm^3 of NaOH, which was adequate to purify BC from most contaminants. After the purification process, the color of BC changed from yellow to white. The pure BC appeared to be like a sponge and was able to hold adequate water. This purification method is simple and requires only water and/or low concentration of alkali for the removal of bacterial cellulose impurities. This is in contrast with the isolation procedures for other celluloses, which involve ~20 steps, high temperature of treatment (160-180°C), and a number of chemical reagents some of which are toxic or produce toxic by-products. [19] Successive chapters will detail about the pure BC and its related applications.

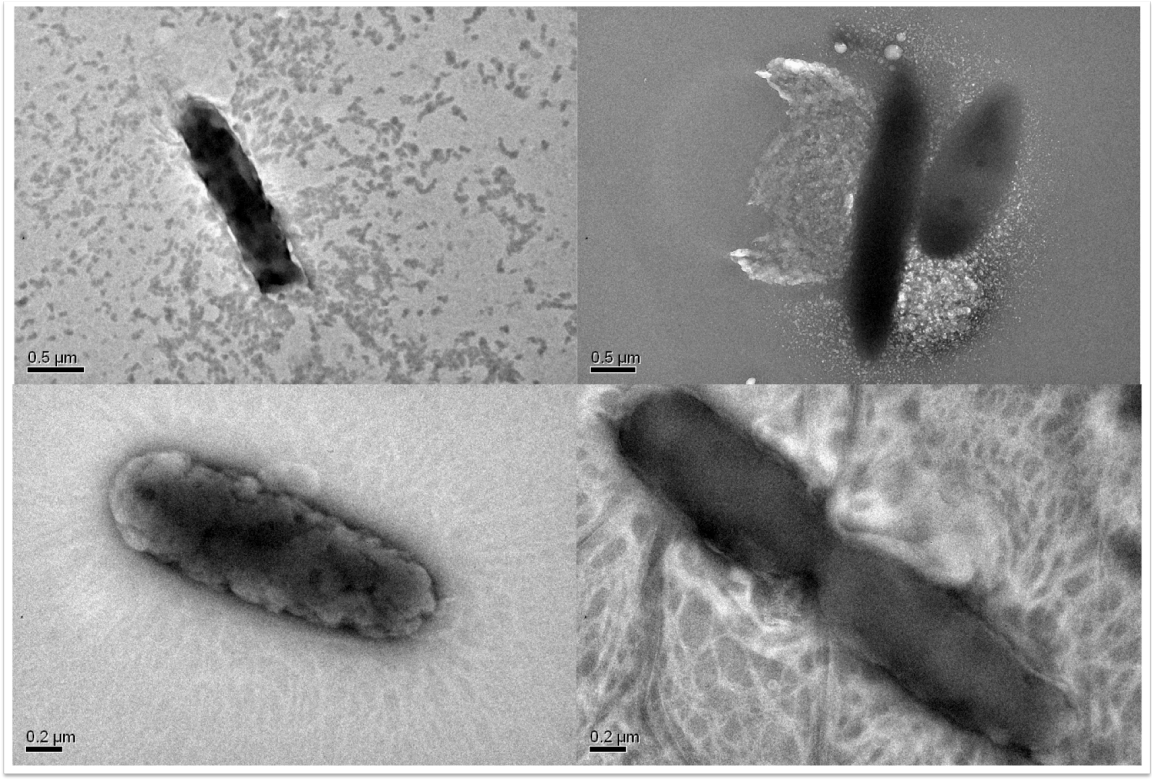

Fig 3: TEM images of *Komagataeibacter sucrofermentans* and BC fibrils secretion

XPS analysis was performed to know the composition of BC. Figure 4 (a & b) shows the wide spectra and the decovulated spectra of carbon and oxygen, respectively. BC is a homopolysaccharide composed of β-D- glucopyranose units. Each monosaccharide unit contains five carbon atoms linked to one of oxygen and another carbon linked to two oxygen atoms. Thus, one expects a curve resolved XPS C 1s signal to consist of only two peaks (C2 and C3). The carbon composition, C1/C2/C3/C4 for the pure cellulose is expected to be [0:83:17:0]. [22]

In the present study, XPS results showed peaks at carbon peaks at 285.4, 287.38, and 284.09, which were attributed to C-OH, C=O and C-C bonds respectively. The current XPS results were similar to the previous report by Li et al. [23] The oxygen peak at 532.42 was attributed to the OH groups of BC and the nitrogen peak may be ascribed to the BC matrix. The results confirmed the BC sample. Further analysis was done through FTIR to know the chemical structure of BC.

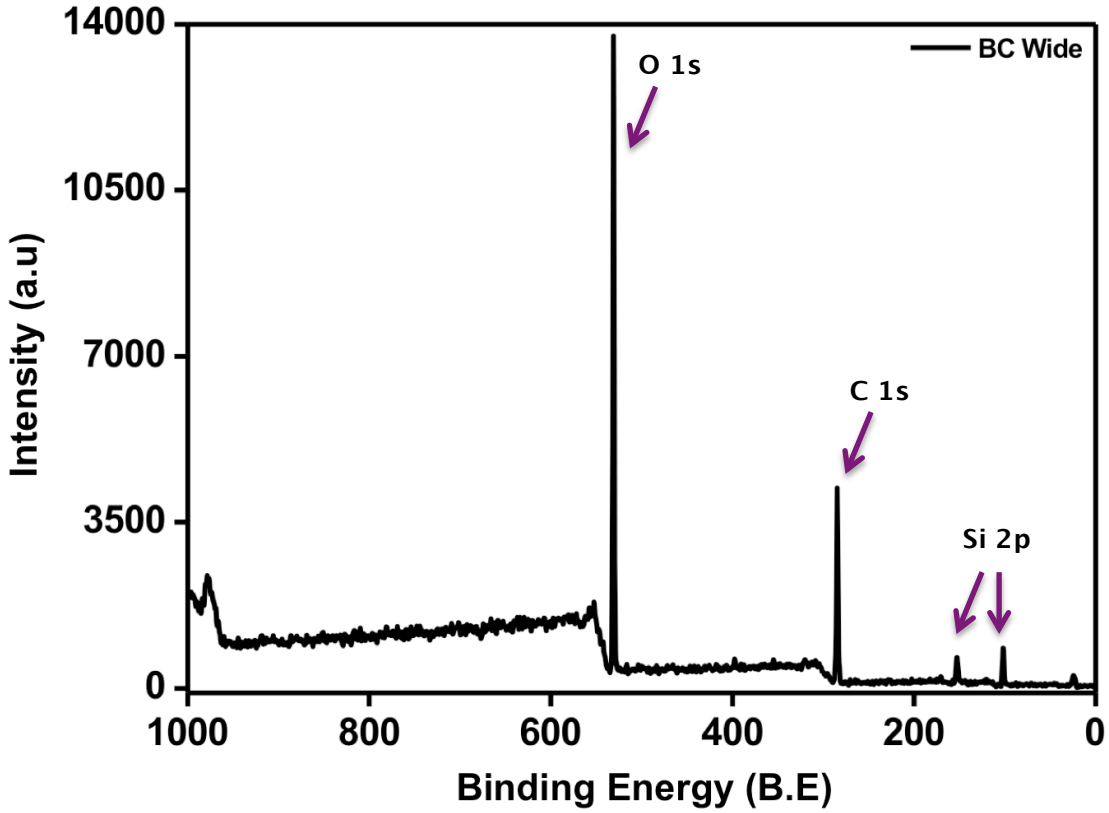

Fig 4: XPS wide spectra of bacterial cellulose

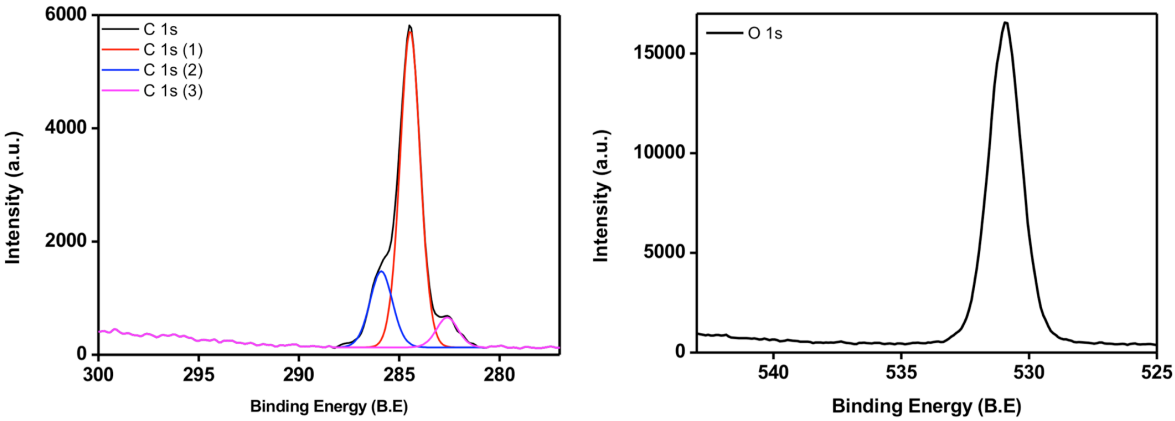

Fig 4 (b): Deconvulated peaks of C 1s and O 1s

The broad band in the 3400–3200 cm^{-1} regions in BC was due to the characteristic OH stretch as shown in Figure 5. The absorption peaks at 2896, 1649 and 1428 cm^{-1} was due to the CH stretching of $-CH_2$, glucose carbonyl of cellulose and $-CH_2$ symmetric bending respectively. The absorption band at 900 cm^{-1} is attributed to C–O–C stretching of β-(1,4) glycosidic linkages and the increased peak intensity in this region is attributed to the amorphous nature of sample. [24]

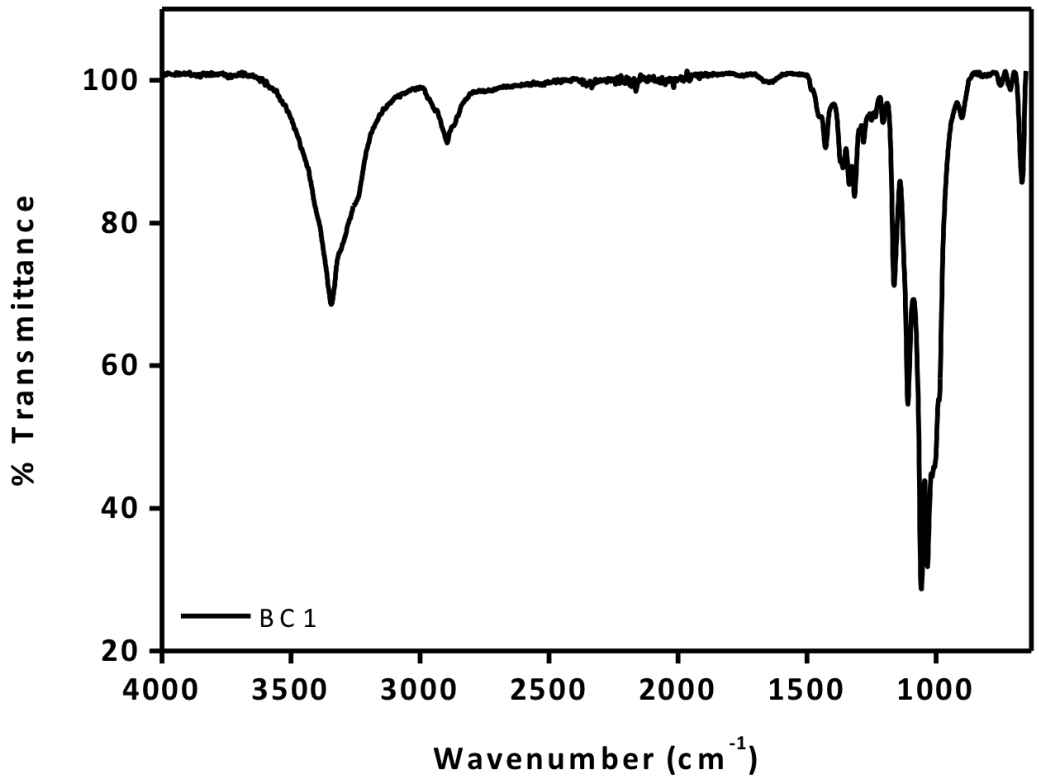

Fig 5: FTIR spectra of bacterial cellulose

Conclusion

In the era of declining forests, global climate changes, continuing expansion of industrialization, it is reasonable to consider the consequences of an alternative source of cellulose. This is an excellent opportunity to take advantage of new development since the intense interest in *Nata de coco* and other microbial cellulose products now is fueled by the demand for the product. The increasing demand for BC outpaces its supply, largely because of lack of investment in fermentation related research to optimize microbial cellulose production on a large scale. Hence, it would be ideal if more investment were made in the microbial fermentation, as it may reduce the vital issues surrounding the world in future.

In the present study, *Komagataeibater sucrofermentans* bacterial strain was procured from Riken Bioresource Center. Bacterial cells were revived and then a pre-cultured. Pre-culture was inoculated into the jar fermenter to initiate the bacterial fermentation process to synthesis BC under controlled conditions for better yield. BC sphere-like pellicles were harvested after 10 days of incubation and were subsequently purified. After purification, BC was characterized both physically and chemically using electron microscopy, XPS and FTIR. The results confirmed the presence of pure cellulose, which could be applied for various applications in biomedicine, bionanoelectronics, food and packaging. Perhaps this chapter about bacterial cellulose will provide a stimulus for the renewal of interest in combining traditional cellulose technology with bionanotechnology development to create growth in a new, exciting field.

References

1. D. Klemm, B. Heublein, H. P. Fink, A. Bohn. Cellulose: fascinating biopolymer and sustainable raw material. *Angew.Chem.,Int. Ed.* 44, 3358–3393 **(2005)**.
2. R. Prashant, Chawla, B. Ishwar, Bajaj, A. Shrikant. Survase and S.

3. R.M. Brown. Cellulose structure and biosynthesis: what is in store for the 21st century? *J Polym. Sci. Pol. Chem.* 42(3), 487–495 **(2004)**.
4. F. Yoshinaga, N. Tonouchi, and K. Watanabe. Research progress in production of bacterial cellulose by aeration and agitation culture and its application as a new industrial material; *Biosci. Biotechnol. Biochem.* 61. 219–224 **(1997)**.
5. A. Svensson, E. Nicklasson, T. Harrah, B. Panilaitis, D.L. Kaplan, M. Brittberg, and P. Gatenholm. Bacterial cellulose as a potential scaffold for tissue engineering of cartilage; *Biomaterials* 26, 419–431 **(2005)**.
6. P. Ross, R. Mayer, and M. Benziman. Cellulose biosynthesis and function in bacteria. *Microbiol. Rev.* 55, 35–38 **(1991)**.
7. D. Klemm, D. Schumann, U. Udhardt, and S. Marsch. Bacterial synthesized cellulose – Artificial blood vessels for microsurgery; *Progress in Polymer Science* 26(9), 1561–1603 **(2001)**.
8. M. Shoda and Y. Sugano. Recent advances in bacterial cellulose production; *Biotechnol. Bioprocess Eng*. 10, 1–8 **(2005)**.
9. B. H. A. Rehm, (ed.) Microbial production of biopolymers and polymer precursors: applications and perspectives; *Caister Academic Press.* **(2009)**
10. S. P. Lin, I. L. Calvar, J. M. Catchmark, J. R. Liu, A. Demirci, K. C. Cheng. Biosynthesis, production and applications of bacterial cellulose; *Cellulose* 20, 2191–2219 **(2013)**.
11. W. Czaja, D. Romanovicz, R. M. Brown. Structural investigations of microbial cellulose produced in stationary and agitated culture; *Cellulose* 11, 403–411 **(2004)**.
12. D. Kralisch, N. Hessler, D. Klemm, R. Erdmann, and W. Schmidt. White biotechnology for cellulose manufacturing— The HoLiR concept. *Biotechnol. Bioeng.* 105(4), 740–747 **(2010)**.
13. Z. Yan, S. Chen, H. Wang, B. Wang, and J. Jiang. Biosynthesis of bacterial cellulose/multi-walled carbon nanotubes in agitated culture; *Carbohydr. Polym.* 74(3), 659–665 **(2008)**.
14. H. J. Song, H. Li, J. H. Seo, M. J. Kim, and S. J. Kim. Pilot-scale production of bacterial cellulose by a spherical type bubble column

bioreactor using saccharified food wastes. *Korean J Chem. Eng.* 26(1), 141-146 **(2009)**.

15. S. Bauer, P. Schmuki, K. V. D. Mark, and J. Park. Engineering biocompatible implant surfaces: Part I: Materials and surfaces; *Prog. Mater. Sci.* 58(3), 261−326 **(2013)**.
16. Z. Qin, L. Ji, X. Yin, L. Zhu, Q. Lin, J. Qin. Synthesis and characterization of bacterial cellulose sulfates using a SO_3/Pyridine complex in DMAc/LiCl; *Carbohyd. Polym.* 101, 947-953 **(2013)**.
17. Y. Yamada, P. Yukphan, H. T. L. Vu, Y. Muramatsu, D. Ochaikul, S. Tanasupawatand, and Y. Nakagawa. Description of *Komagataeibacter* gen. nov., with proposals of new combinations (*Acetobacteraceae*); *J. Gen. Appl. Microbiol.* 58, 397-404 **(2012)**.
18. S. Hestrin, and M. Schramm. Synthesis of cellulose by *Acetobacter xylimum II*. Preparation of freeze-dried cells capable of polymerizing glucose to cellulose; *Biochem.J* 58(2), 345-352 **(1954)**.
19. M. E. Embuscado, J. N. BeMiller and J. S. Marks. Isolation and partial characterization of cellulose produced by *Acetobacter xylinum*; *Food Hydrocolliods* 10(1), 75-82 **(1996)**.
20. R. M. Brown Jr. Emerging technologies and future prospects for industrialization of microbially derived cellulose. In: Harnessing Biotechnology for the 21st Century Ed. M.R Ladisch and A Bose. Proceedings of the Ninth International Biotechnology Symposium and Exposition. Crystal City, Virginia. *American Chemical Society*, Washington, D.C., 76-79 **(1992**).
21. Y. Hu, and M. J. Catchmark. Formation and characterization of sphere-like bacterial cellulose particles produced by *Acetobacter xylinum* JCM 9730 strain; *Biomacromolecules* 11; 1727-1734 (**2010)**.
22. C. M. G. Carlsson and G. Strom. Reduction and oxidation of cellulose surfaces by means of cold-plasma; *Langmuir* 7; 2492-2497 **(1991).**
23. J. Li, Y. Z. Wan, L. F. Li, H. Liang, and J. H. Wang. Preparation and characterization of 2,3-dialdehyde bacterial cellulose for potential biodegradable tissue engineering scaffolds. Materials Science and

Engineering C: Biomimetic and Supramolecular Systems, 29;1635-1642 **(2009).**

24. M. Ul-Islam, N. Shah, J. H. Ha and J. K. Park. Effect of chitosan penetration on physico-chemical and mechanical properties of bacterial cellulose; Korean J. Chem. Eng. 28;1736-1743 (**2011**).

4

Evaluation of Antioxidant Property and Cytotoxicity of Bacterial cellulose Sulfate

"Science is organized knowledge. Wisdom is organized life"

- Immanuel Kant

Modified cellulose is being used for various biomedical applications, food and packaging industries, thus the evaluation about environmental friendly nature is must after modification. Present study was attempted to synthesize bacterial cellulose sulfate and develop a highly transparent film. Thereafter, evaluate its cytotoxicity, hemocompatibility, antioxidant property that has received lesser attention compared to the other chemically modified cellulose. Bacterial cellulose was produced by *Komagataeibacter sucrofermentans* by controlled agitated method and later was purified by alkali treatment method. Acetosulfation of bacterial cellulose was carried out to functionalize it with sulfate groups. Confirmation of successful sulfation was done through XPS, FTIR and FT Raman spectroscopy. The degree of sulfation was found to be 0.28. The cytotoxicity results infer that bacterial cellulose sulfate is non-toxic, blood compatible and biocompatible. Also, no significant difference in the antioxidant levels was observed in L929 cells or liver homogenate. Thus, the *ex vivo* and *in vitro* studies show that varying concentrations of BCS used here is deemed safe for biomedical applications, edible films, food and packaging.

Introduction

The abundance of cellulose in nature provides an effective platform to utilize this renewable material in different industries for wide applications. Lots of cellulose-based materials are being developed owing to their biocompatibility and biodegradability to replace their synthetic counterparts. The major source of cellulose is plants (cotton and wood), however certain microorganisms are also capable of producing cellulose. The advantage of bacterial cellulose (BC) over plant cellulose is the absence of hemicelluloses, which negatively affects the cellulose crystallinity index. [1] Apart from BC, cotton is another major candidate known for its high purity. [2] However, there are certain drawbacks in cotton cultivation, which includes extreme vulnerability to climatic change. Though it is resilient to higher temperatures, it is sensitive to water availability. Moreover, there is threat of pests and pathogens that may directly affect its production. Also the time taken for the production of cotton is 4-6 months, which is considerably longer than the microbial cellulose production. BC production has somehow not captured enough interest, though it has slight edge over the plant cellulose. Though, it possesses remarkable mechanical properties and high crystallinity that makes it an attractive candidate for various applications in biomedical sciences, electronics and optoelectronics, food and packaging industries, [3-5] still its effective production is not widespread. Furthermore, purification is simple and not energy consuming or chemical intensive process, which can aid in the prevention of environmental problems caused due to the byproducts of wood pulping. [6] The only major production of BC is in the food industry as *nata de coco*, a desert that originated from Philippines. Hence, if the mass production of BC could be adapted as a source of cellulose for other applications, it is quite possible to synthesize highly crystalline cellulose in a short time.

One of the major issues associated with cellulose is its insolubility in most solvents, which limits the applications of cellulose to a great extent. To combat this issue the scientific community has formulated

several methodologies over the years like chemical modification of cellulose for specific applications. [7] Homogeneous and heterogeneous reactions have yielded several types of chemical modifications that include acetylation, phosphorylation, succinylation, benzoylation carboxymethylation and carbanilation. Cellulose sulfate (CS) produced through sulfation process is a half ester of cellulose and have several advantages over cellulose in their properties. CS is water-soluble and possesses antiviral, antibacterial and anticoagulant properties owing to a broad range of degrees of substitution ascribed to sulfate groups. [8] Apart from that it possesses good biocompatibility, film-forming ability and is biodegradable. These properties have paved way for CS in applications related to drug delivery, bioseparation and cell encapsulation. [9] Hence, owing to the simplicity in preparation, affordable cost and well-matched for large-scale production, CS turns out to be an incipient candidate for active packaging and edible films. [10] Recently, for the first time bacterial cellulose sulfate (BCS) has been developed through direct sulfation method using SO_3/Pyridine complex in DMAc/LiCl, [11,12] however, possible immunogenic property of bacterial polysaccharides demands thorough investigation for specific bioactive mechanisms.

An integral part of aerobic metabolism is the generation of reactive oxygen species (ROS) that include free radicals, superoxide anion, hydroxyl radical and non-radical molecules like, hydrogen peroxide, and singlet oxygen etc. due to gradual reduction of O_2through high energy exposure or electron transfer chain. [13] At high concentrations ROS are hazardous to organisms and when excess free radical generation occurs, the cell is in a state of “oxidative stress”. [14] The consequences of excessive free radicals include oxidation of proteins, peroxidation of lipids, damage nucleic acids, enzyme inhibition, necrosis and cell death. [13-15] Antioxidants play a vital role in hindering the formation and scavenging of free radicals along with other potentially toxic oxidizing species. Biologically active polysaccharides can revitalize and restore the

the natural antioxidant defense mechanism. [16]

In the present work, we have functionalized BC with sulfate group owing to the immense potential of sulfur containing polysaccharides in biomedical field. Post sulfation, we have developed a highly transparent film with good integrity that can be used as edible film, active food packaging film and for biomedical applications. One of the major aspects of this study was to evaluate the antioxidant potential of BCS samples by analyzing different factors involved in formation of oxidative stress in mammalian cells and tissues respectively. The study also includes the evaluation of hemocompatibilty, anticoagulant activity and cell viability to elucidate the bioactive potential of BCS film.

Materials and Methods

All the chemicals/reagents used were of analytical grade and were used as received. Dialysis membrane from Spectrum Laboratories Inc. (Rancho Dominquez, USA) has an approximate molecular weight cut off of 500 Da.

BC Fermentation and Purification

Komagataeibacter sucrofermentans was cultivated in Hestrin-Schramm (HS) medium as mentioned elsewhere. [17] Briefly, the following media composition was used for cultivation: glucose, 20g; Bacto peptone, 5 g; Bactoyeast extract, 5 g; disodium phosphate (anhydrous), 2.7g; citric acid monohydrate, 1.15g in 1 L of distilled water. pH was adjusted to 6.0 with HCl or NaOH and was sterilized by autoclaving. The bacterial sphere-like cellulose aggregates were collected after 10 days. Alkali extraction method described elsewhere, was employed to purify the BC sample. [18] The cellulose pellicles were homogenized for 5 mins and centrifuged at 13,800 g for 10 mins at 10°C. Supernatant was discarded and the cellulose paste was mixed thoroughly for homogeneity. Cellulose paste was treated with 0.30 mol/dm^{3}NaOH preheated to 90°C and was heated for 25 mins and rapidly cooled down in an ice bath. Subsequently, samples were washed with distilled water

and pH of the sediments was adjusted to 7.

Acetosulfation of BC

Acetosulfation of BC was carried out as mentioned elsewhere. [19] 1g of BC was suspended in 50 ml of anhydrous DMF for over 14 h. 0.35 ml of cholorosulphuric acid and 4.7 ml of acetic anhydride in DMF was dropped in cellulose suspension under vigorous stirring. The suspension was maintained at 50°C for 5 h and then cooled to room temperature. This reaction agent was then poured into saturated ethanolic solution of anhydrous sodium acetate. The precipitate was collected and washed with 4% sodium acetate solution in ethanol. Deacetylation was done with 1M ethanolic solution of NaOH for 15 h and pH was adjusted to 8 with acetic acid/ethanol (50/50, w/w). The final product was washed with ethanol and dissolved in water.The sample was filtered and dialyzed against demineralized water.

The degree of sulfation (DS) value was calculated according to the equation (1) given by [20],

$$DS = \frac{S\% \,.\, 162.1}{3207 - 102.1 \,.\, S\%} \quad (\mathbf{1})$$

Electron Microscopy

BC and BCS samples were sputter coated with platinum. Scanning Electron Microscopy (SEM) images of the BC and BCS samples were obtained on a JEOL, JSM-7400F scanning microscope at room temperature. Bacterial sample was negatively stained for Transmission Electron Microscopy (TEM) images, which were obtained on a JEOL, JEM-2200FS transmission electron microscope.

XPS, FTIR and FT Raman

The elemental analysis for the presence of Carbon, Nitrogen, Oxygen and Sulfur were determined through X-ray photoelectron spectroscopy (XPS) KRATOS, with a basic pressure of 1.7 x 10^{-8} and mono-Al anode with pass energy of 40 (survey scan) X-ray source.

The chemical structure characterization was analyzed through Fourier Transform Infrared (FTIR) (Perkin Elmer) with a resolution of 4 cm^{-1} in the region of 4000 to 400 cm^{-1}. FT raman spectroscopy was performed to illustrate the introduction of sulfate groups into the BC sample. FT raman spectra was recorded on a Nicolet iS50/Raman, Thermo Scientific Spectrometer. A semi-conductor laser with an exciting line of 1064 nm was applied as light source for excitation of Raman scattering. The raman spectra was recorded in a range between 4000-150 cm^{-1} using an spectral resolution of 4 cm^{-1}. A laser output of 0.50 W with a focal spot size of 60 μm (diameter) was used. The peak integration was carried out with OMNIC iS50Raman software version 9.1.0. Beckman coulter 730 spectrophotometer (USA) was used to record the percentage of transmittance of BCS film.

Total Carbohydrate and Total Protein Assay

Total carbohydrates in BCS samples were quantified through Phenol-Sulfuric acid method against glucose standard as stated elsewhere. [21] Total protein in BCS sample was quantified by bicinchonic acid assay (BCA) method against bovine serum albumin standard. [22]

Cell Viability Assay

Alamar blue reduction assay that quantifies metabolically active cells with their ability to convert resazurin to fluorescent resorufin, was used to study the *in vitro* cytotoxicity of BCS sample at different concentrations. Standard assay protocol was followed for the study. Briefly, L929 (mouse fibroblast like cells) and KUSA (mouse mesenchymal stem cells) were seeded separately and incubated at 37°C in 5% CO_2 environment to obtain ~5-8 x 10^{-3} cells per well. Fresh media was replaced after 24 hours of incubation and different concentrations of BCS sample were added to the wells. The study was carried out for 24 and 72 hours in triplicates. After the incubation period in the respective cases, 10% of alamar blue dye was added to each well and incubated for 4 hours. Thereafter, fluorescence was measured at 580-610 nm, using

multi detection microplate reader (Dainippon Sumitomo Pharma, Powerscan HT.[23]

Cellular Absorption Studies

Sypro ruby dye (Biofilm matrix stain) was used to tag different concentrations of BCS sample to study the absorption and adhesion to mammalian cells using confocal microscopy. BCS samples tagged with dye were incubated with L929 cells for 24 hrs. Post incubation, unbound BCS was washed with 1x PBS and cells were treated with Hoechst dyefor 30 mins. After incubation, cells were observed under confocal laser scanning microscope, using 488 nm laser lines for sypro ruby and 405 nm for Hoechst. [16]

Hemocompatibility and Anticoagulant Assay

Hemolytic activity of different concentrations of BCS sample was evaluated following standard protocols using human RBCs as mentioned elsewhere. [24] Briefly, serum was removed from the fresh human whole blood stabilized in ethylenediaminetetraacetic acid (EDTA) through centrifugation at 200g for 5 minutes. Sterile isotonic PBS was used to wash the residual RBCs for ~5 times and then to dilute it 10 folds after the last wash. The diluted RBC suspension was added to BCS sample with different concentrations and incubated for 2 hours. Post incubation the intact RBCs were removed by centrifugation. Optical density of the supernatant was measured using spectrophotometer with (A) absorbance of hemoglobin at 570 nm and absorbance of reference at 620 nm. The hemolysis percentage was calculated as per equation (2),

$$\%\, Hemolysis = \frac{Sample\ A_{570-620} - Negative\ Control_{570-620}}{Positive\ Control_{570-620} - Negative\ Control_{570-620}} \times 100 \quad (\mathbf{2})$$

To examine the whole blood clotting time, different concentrations of BCS sample were incubated with 100 µl of citrated whole blood for 5 minutes at room temperature. 50 µl of incubated blood was placed on a

glass slide and 25 µl of 50 mM calcium chloride ($CaCl_2$) was added and gently rocked. Time from the addition of $CaCl_2$till the appearance of first clot was recorded. [25]

Antioxidant studies – Preparation of tissue homogenate and cells

Standard protocols with slight modifications were used to evaluate antioxidant properties. 10 % of fresh liver homogenate was prepared in ice-cold saline using a rotor stator homogenizer at 1000 rpm. The resulting homogenate was used for further analysis. L929 cells homogenate and mice liver homogenate were used to evaluate the antioxidant property of BCS sample. DMEM media was used to culture L929 cells and were incubated at 37°C in 5% CO_2 environment. Upon reaching confluent growth, cells were trypsinized and collected. The collected cells were diluted with saline to attain 2 x 10^5 cells/ml and were treated with varying concentrations of BCS sample. Optical density measurements were recorded using spectrophotometer to know the effect of oxidative stress and amount of BCS in inhibiting it.

Protein Assay

BCA method was followed to determine the protein content in L929 cells and liver homogenate against bovine serum albumin standard as described by [22] Briefly, 0.1 ml of L929 cells and liver homogenate were added to 1.9 ml of BCA test reagent A and B mixture and incubated in dark for 30minat 37°C. OD values were recorded at 562 nm.

Reduced Glutathione Assay

Reduced Glutathione assay (GSH) was initiated by adding 0.2 ml of L929 cells and liver homogenate to 0.8 ml of 5% Trichloroacetic acid (TCA) respectively. The mixture was centrifuged at 3500 rpm for 10 min at 4°C. 0.5 ml of supernatant was added to 4 ml of 0.2 M PBS. 0.5 ml of 2 mM 5-5' Dithiobis(2-nitrobenzoic acid) (DTNB) was added to the reaction mixture just before recording the OD values at 412 nm. [26]

Lipid Peroxidation Assay

Lipid Peroxidation assay (LPO) was performed by adding 0.2 ml of L929 cells and liver homogenate to a reaction mixture containing 1.5 ml of 0.8% thiobarbituric acid (TBA), 8.1 ml of sodium dodecyl sulfate (SDS), 1.5 ml acetic acid and 0.6 ml of distilled water. The reaction mixture was kept in boiling water bath for 1 hour and cooled to room temperature. 1 ml of distilled water was added to the tubes and centrifuged at 3500 rpm for 10 min at 4 $^{\circ}$C. The OD values were noted at 532 nm. [27]

Superoxide Dismutase Assay

Superoxide dismutase assay (SOD) was carried out by adding 0.1 ml of L929 cells and liver homogenate to a reaction mixture containing 2.5 ml 0.1 M Trisbuffer, 0.1 ml of 1mM, 0.5 ml of 1 mM Diethylenetriamine penta acetic acid (DTPA) and 10 mM Pyrogallol. OD values were noted at 420 nm for 0, 1, 2 and 3 min. [28]

Results and Discussion

K. sucrofermentans was cultured in HS media and bacterial sphere-like cellulose was procured after 10 days of incubation at 28°C under constant agitation of 100 rpm. Figure 1 shows the images of sphere-like BC as acquired after 10 days of incubation and magnified SEM image of the pellicles. The agitated culture produced sphere-like BC that appeared to be of different sizes as reported earlier. [29] Bacterial cells were embedded in the BC fibrous matrix as shown in figure 2 (a). Negative staining using 1% Titanium-blue was performed to see the magnified image of bacteria through TEM as depicted in figure 2 (b). Bacterial cells were of ~2-3 μm size as seen through the TEM images. The average diameter of the BC fibrils was of ~10-15 nm as seen in figure 2 (c). BC was subjected to purification by alkali treatment method. A low concentration of NaOH was used to purify BC, which was quite effective in removing the bacterial cells and other contaminants. Figure 2 (d) shows the SEM image of purified BC. The image clearly infers the absence of bacterial cells that were adhered in between the fibrils.

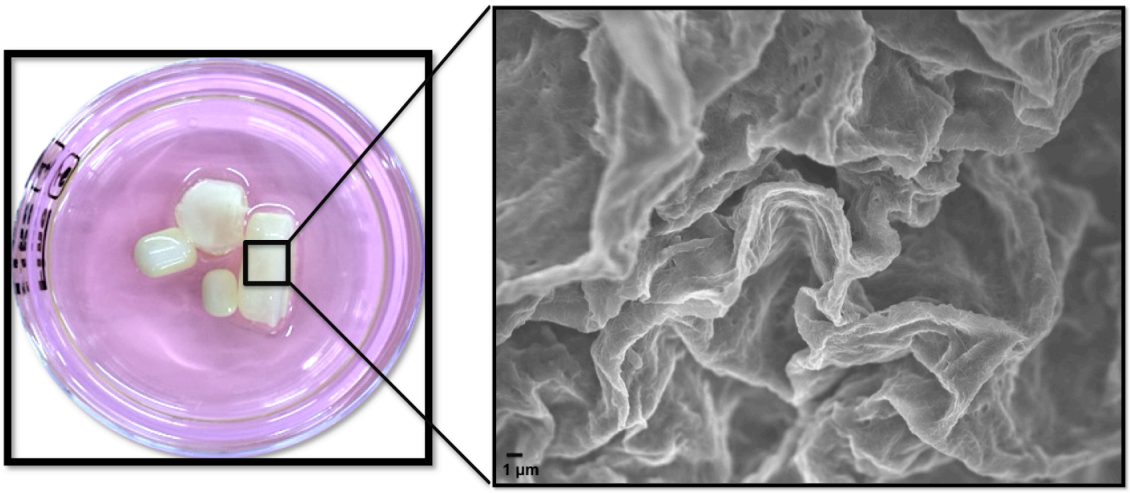

Fig. 1 Bacterial sphere-like pellicles – Macroscopic image of sphere-like BC (left) and SEM image (right).

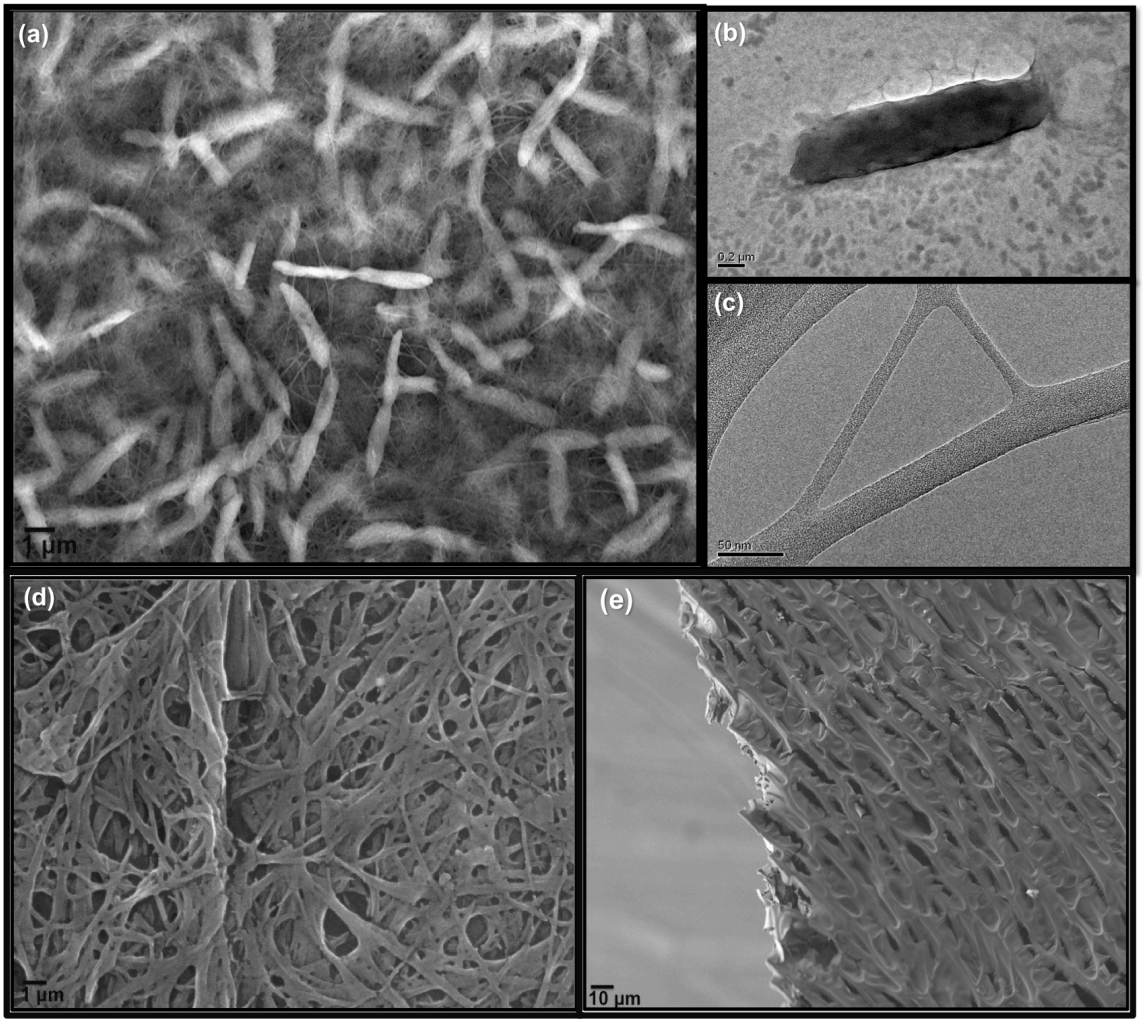

Fig. 2 SEM image (a) BC, (d) purified BC, (e) Freeze dried BCS; TEM image (b) *K. sucrofermentans*, (c) BC fibrils.

Purified BC was functionalized with sulfate groups though acetosulfation method. This quasi-homogenous reaction yielded BC sulfate. Figure 2 (e) illustrates the SEM image of freeze-dried BCS sample. The image shows that there is a complete revamp in the morphology of BC after functionalization. The fibrous structure of BC is completely lost after functionalization and insoluble BC now becomes highly soluble in water. Through the drop cast method highly transparent film were prepared in plastic plates and it was subjected to several characterizations to understand its potential for various biomedical and food packaging applications.

XPS measurements were carried out to confirm the sulfation of BC sample. Fig. 3 (a) shows the XPS spectra of BC and BCS samples with different functional groups. C 1s peaks observed in BCS sample at 285.58, 284.06 and 286.98 were attributed to C-OH, C-C and C=O bonds respectively. O1s peak was attributed to the -OH groups of cellulose and N1s was due to organic matrix. The successful functionalization of sulfate groups was inferred by the presence of a peak at 167.9. [23] S 2p peaks at 166.51, 167.76 and 166.05 were ascribed to Na_2SO_3 bonds (Moulder*et al.* 1995 [30]). The sulfur content in BCS sample was 2.31%, quantified through CasaXPS software (version 2.3.16 Pre-rel 1.4). By using the equation (1), the degree of sulfation was found to be 0.28.

FTIR spectra revealed the presence of two new peaks in BCS sample at 1217 and 810 cm^{-1} that indicated the successful sulfation of BC hydroxyl groups and were attributed to the asymmetric vibration ν_{as}(O=S=O) and C-O-S stretching vibration ν(C-O-S) respectively. [11]; [12] Broad peak at 3400-3200 cm^{-1} regions in BC and BCS were assigned to the characteristic -OH stretch as shown in Fig. 3(b). The absorption peaks at 2896, 1649 and 1428 cm^{-1} was due to the -CH stretching of $-CH_2$, O-H bending and $-CH_2$ symmetric bending respectively. [31]

FT raman spectra was analyzed to confirm the presence of sulfate groups on the functionalized BC. Molecular conformations and hydrogen bonding patterns of cellulose have been analyzed through this technique

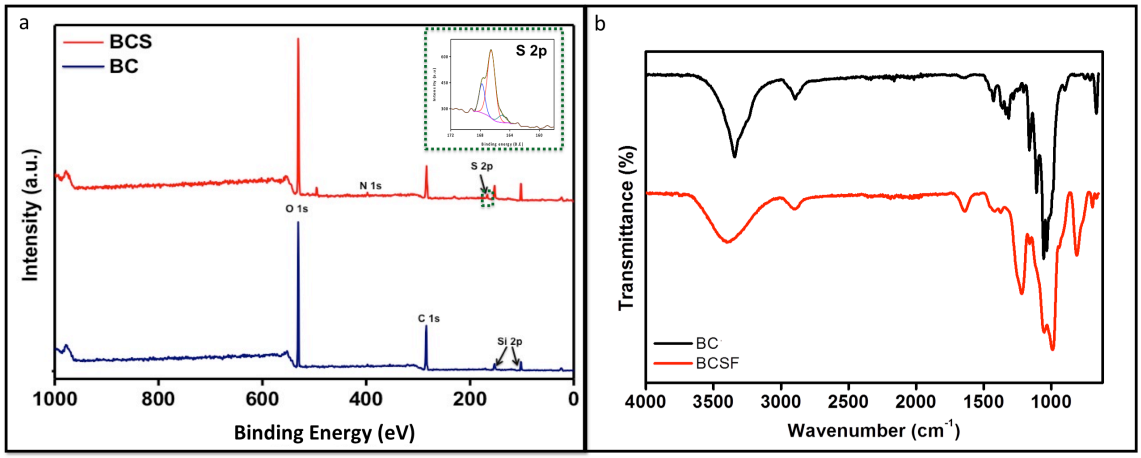

Fig. 3 (a) XPS spectra, (b) FTIR spectra of BCS film

that has proved to be advantageous. Also, FT raman spectra has been detailed for cellulose in earlier reports. [32] Fig. 4 (a) depicts the FT raman spectra of BC and BCS samples. Based on the conformation of cellulose backbone and hydrogen bonding, the spectra can be split into two regions, (a) region below 1600 cm^{-1} and (b) region above 2700 cm^{-1}, respectively.[33] The presence of sulfate groups were confirmed with the appearance of new bands from raman spectra of BCS sample at 419, 590, 824, 1076 and 1270 cm^{-1}.The bands at 419 cm^{-1} and 590 cm^{-1}occur as triplets and were attributed to the deformation vibration of SO_3 groups and deformation vibration δ(O=S=O) respectively. The band at 824 $cm^{-1}$was assigned to the ν(C–O–S) stretching and this band intensity increases with the increase in degree of sulfation. The bands at 1076 cm^{-1} and 1270 cm^{-1} were ascribed to symmetric stretching vibration ν_a(O=S=O) and asymmetric vibration of ν_{as}(O=S=O). [32]

Fig 4 (b) illustrates the transmittance spectra of BCS film, which was recorded in the wavelength range of 200 –1000 nm. The optical transparency of the film in the visible wavelength (400–800nm) was found to be 90–92%, which exhibited very high transparency. The high transparency of the BCS film offers huge advantage in edible films and food packaging industries. The figure also illustrates the flexibility of the film when folded. The integrity of the film was good, as it was not affected after peeling off from the surface of plate. Hence, the flexibility was deemed good, as the film remained unaffected even after folding for

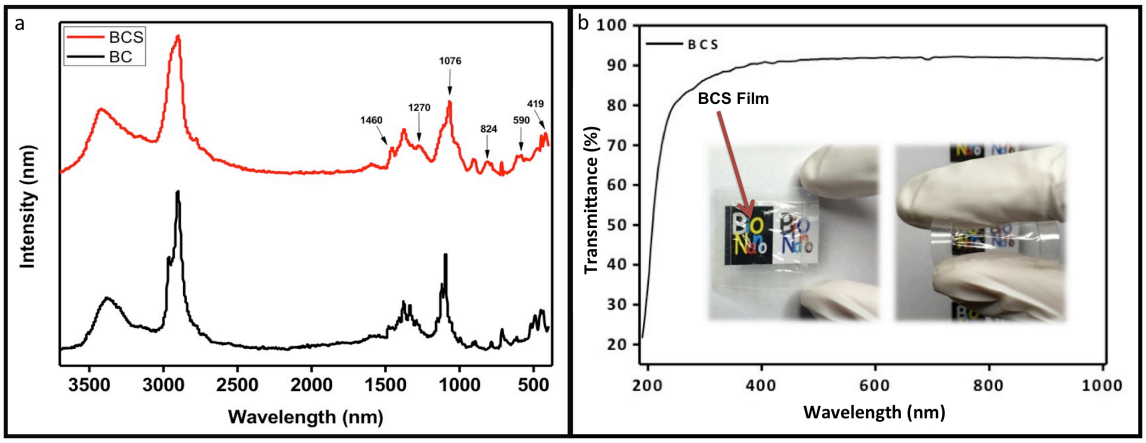

Fig. 4 (a) FT raman spectra, (b) Optical transmittance of BCS film.

>100 times.

Having confirmed the successful sulfation of BC, the total carbohydrate and protein content in the BCS sample was analyzed calorimetrically by phenol-sulfuric acid method and BCA method respectively. The total carbohydrate content of BCS sample was 75 mg/ml, which indicates significant amount of carbohydrate retention post functionalization. After purification, the total protein concentration was 0.027% per mg of BCS sample that implied higher purity of samples. To explore its potential in various biomedical and food packing applications, a thorough study on hemocompatibility, cytotoxicity, anticoagulant activity and antioxidant properties were studied.

Biocompatibility of BCS samples was confirmed through alamar blue assay by observing the cell viability percentage of L929 cells and KUSA cells upon exposure to varying concentrations BCS for 24 and 72 hours. Fig. 5 shows the cell viability percentage of L929 and KUSA cells for 24 hours and 72 hours respectively. The figure illustrates a cell viability of >85%, regardless of the cell type or incubation period. Also, there is an increasing trend observed in the cell viability percentage with the increase in the concentration of BCS sample. These results infer that BCS concentrations used in this study are not only highly biocompatible but appear to have some growth enhancing ability as well. However, there was a slight dip in the cell viability percentage in 72 hours plate initially, which could be due to media usage by respective cell lines used in the study.

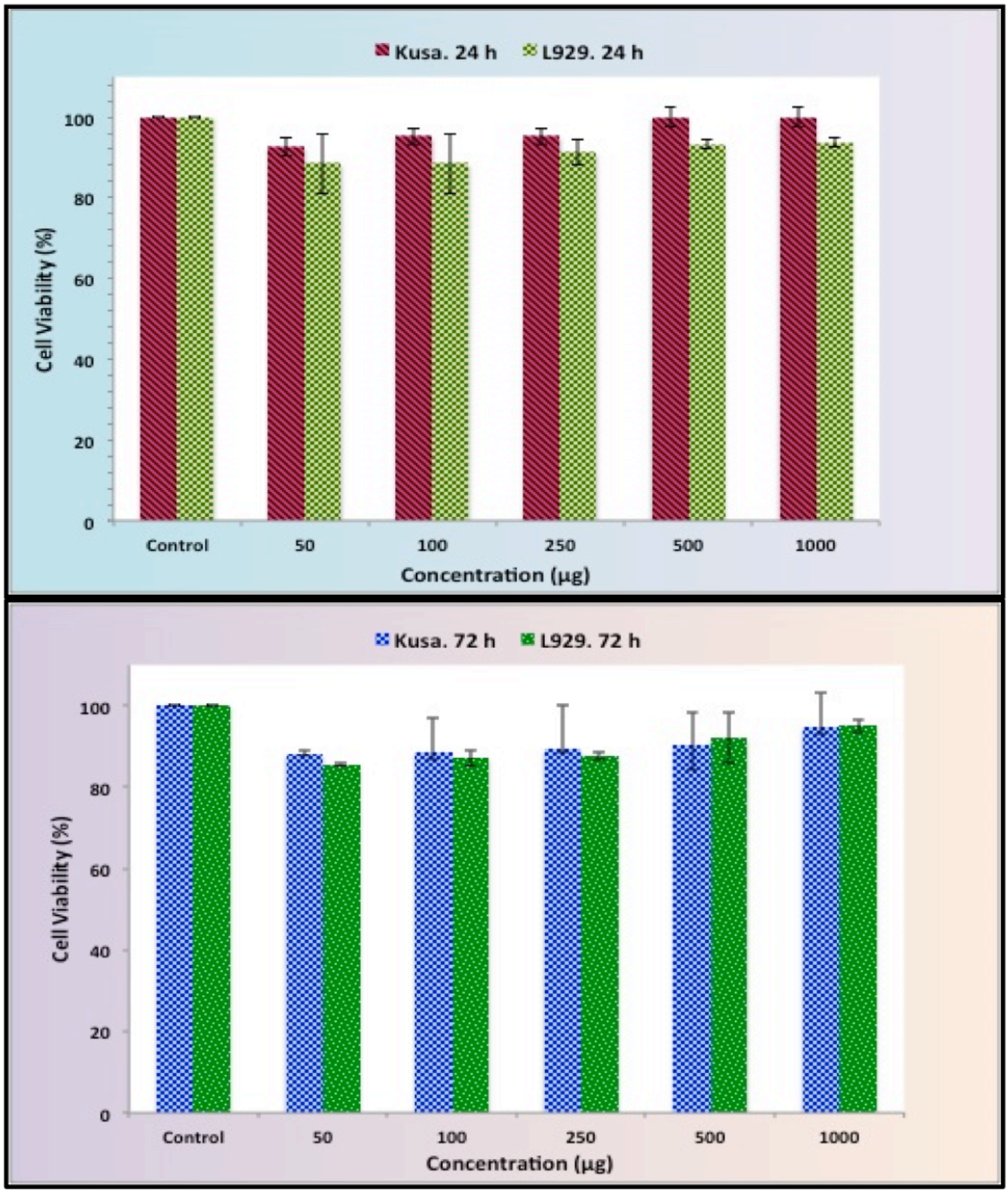

Fig. 5 Cell viability assay of KUSA and L929 with BCS sample.

Cellular absorption studies were conducted for BCS sample and the confocal images were recorded as shown in fig. 6 and 7. Sypro-ruby tagged BCS sample was treated with L929cells and incubated for 24 hours. The images illustrate that the integrity of cells remained intact and the effective absorption of BCS was observed with respect to the fluorescence inside the cell.

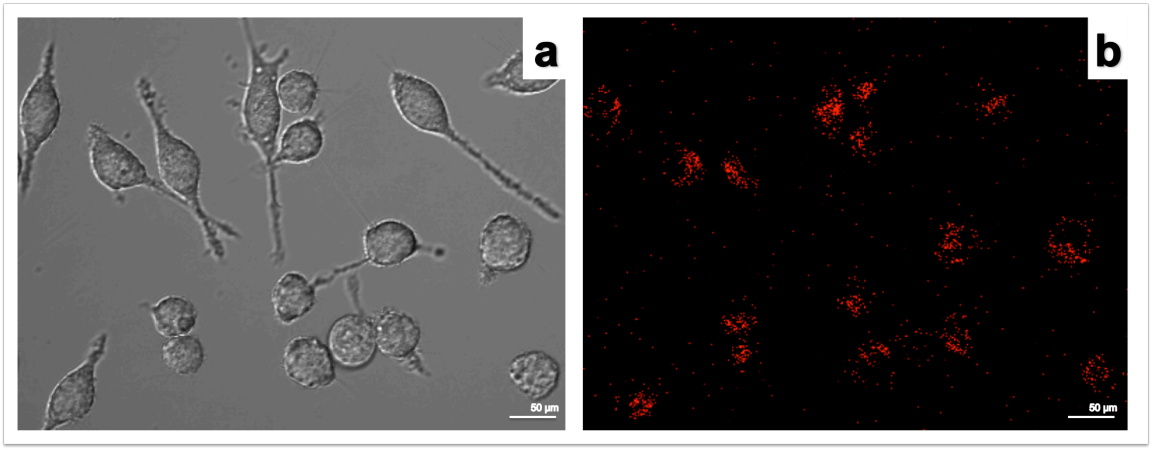

Fig. 6 (a) Bright field confocal images of L929 cells and (b) Sypro-ruby tagged BCS in L929 cells.

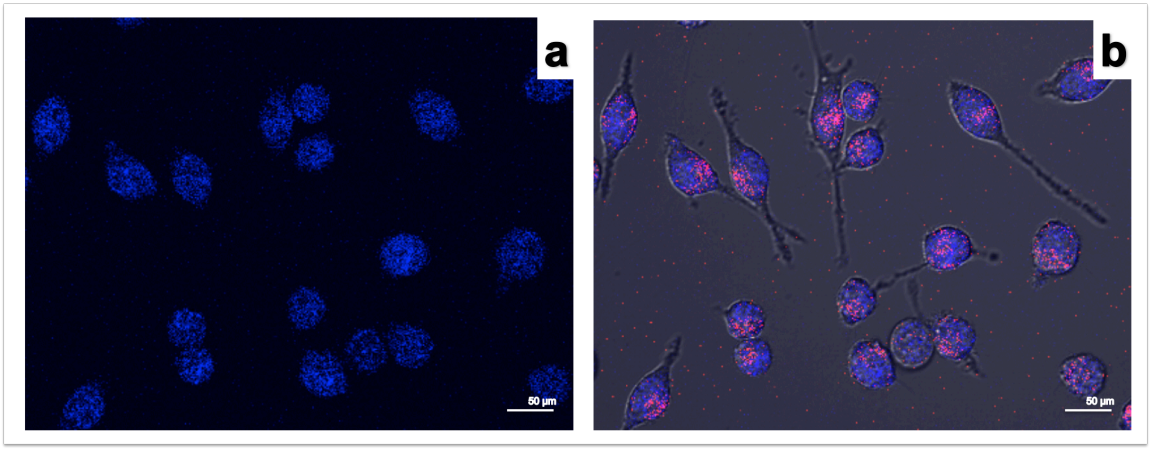

Fig. 7 (a) L929 stained with hoechst stain and (b) Merged images of L929 cells.

Using the standard protocol, the hemolytic activity of human RBCs was tested with different concentrations of BCS sample. The working principle behind this method is, when human RBCs are lysed there is a release of deep red colored hemoglobin, which can be calorimetrically determined. Deionized water, normal saline served as the positive and negative control respectively. Figure 8 depicts the hemolysis percentage measurements and whole blood clotting time. The results of hemolysis study infer that the BCS concentrations used in this study did not show hemolysis of human RBCs irrespective of increasing concentrations.

Whole-blood clotting assessment is widely opted for diagnosing clotting disorders. Fresh blood was collected from a volunteer and was subjected to analysis. Clotting time in seconds after incubation with whole blood were 280±3 seconds for all BCS concentrations used for the

study. The blood samples containing BCS coagulated at the same time as that of the control, which infers that BCS concentrations used in this study did not interfere with the coagulation cascade of human blood.

The ability of a molecule to inhibit the oxidation of other molecules renders an anti-oxidative property to it. Oxidation contributes to the production of free radicals that initiate a chain of reactions, which leads to necrosis. [34] When the production of free radicals exceeds the cell or tissue's antioxidant capacity, it results in oxidative stress that unsettles the cellular functions and leads to various pathological conditions. [15] Fig. 9 shows the levels of GSH in L929 cells and liver homogenates treated with different concentrations of BCS samples. GSH plays a crucial role in detoxification and inactivation of free radicals, oxidants and electrophiles. [35] In a healthy tissue or cell, majority of glutathione is present in the reduced form and an increased GSSG (oxidized form) concentration indicates oxidative stress. In the present study, GSH content in the control system of L929 cells amounted to 0.0115±0.0005 μmol/mg. The concentration of GSH was below the control system until 100 μg/ml BCS concentration. Thereafter, there was an increase in the levels of GSH from 250-1000 μg/ml, however a decreasing trend was also observed from 250-1000 μg/ml as shown in the figure. The results of L929 cells revealed that BCS samples until 100 μg/ml did not affect the GSH levels of cells, but when the concentration increased from 250-1000 μg/ml, it inferred a progressive antioxidant effect. In the case of liver homogenate, the control system showed 0.05 μmol/mg concentration of GSH. All the test concentrations used in the liver homogenate analysis were below the control system, which indicated the nominal GSH oxidation. The results infer that BCS concentrations used in this study does not influence the action of GSH in liver homogenate. The deviation in results may be attributed to the low concentration of proteins in cell lines.

LPO is used as an indicator of oxidative stress in cells and tissues owing to a well-established mechanism of cellular damage in plants and

animals. [36] Polyunsaturated fatty acids have vital role that includes regulation of gene expression, energy provision, cell signaling and membrane structure. However, they are susceptible to free radical-initiated oxidation, which can cause oxidative stress, where lipid peroxidation takes place with the formation of lipid hydroperoxide. [37] The present study involved L929 cells and liver homogenate treated with different concentrations of BCS sample. Fig. 10 illustrates the malondialdehyde (MDA) formation in L929 cells and liver homogenate post treatment with BCS sample. The results of L929 cell line study revealed that, MDA levels in all cells treated with different concentrations of BCS remained lesser than the control group, which was 0.95±0.002 nmol/mg. In case of the liver homogenate, the control group showed MDA level of 0.035 nmol/mg and the sample containing 50μg of BCS sample was below the control group. However, a slight insignificant increase of LPO was observed from 100-1000 μg, which was comparable with the control group. The results imply that the BCS samples showed antioxidant activity by controlling LPO and free radical generation. The inconsistency of two test systems (L929 cell lines and liver homogenate) contributes to the difference in the observed results. [16,38]

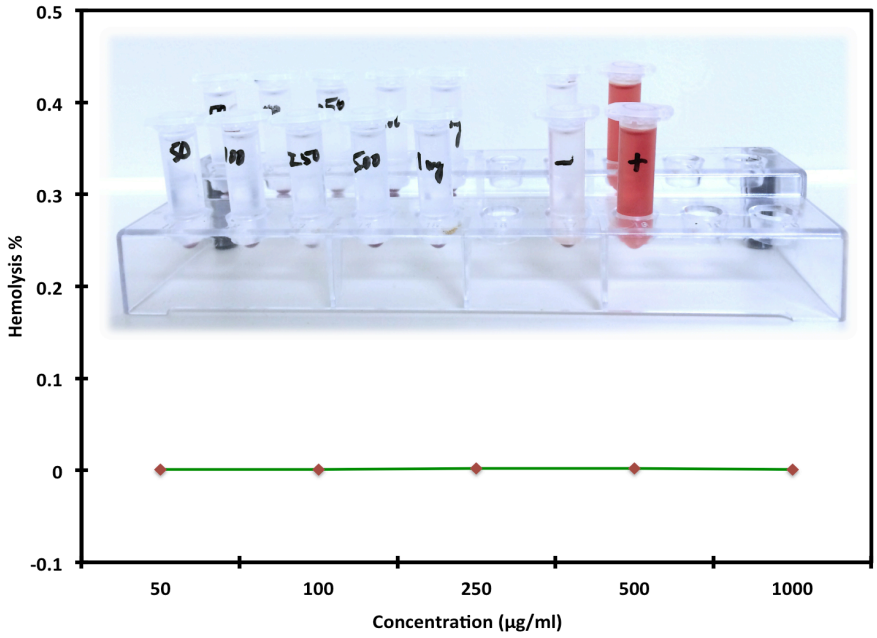

Fig 8: Hemolysis percentage of human RBCs with different concentrations of BCS.

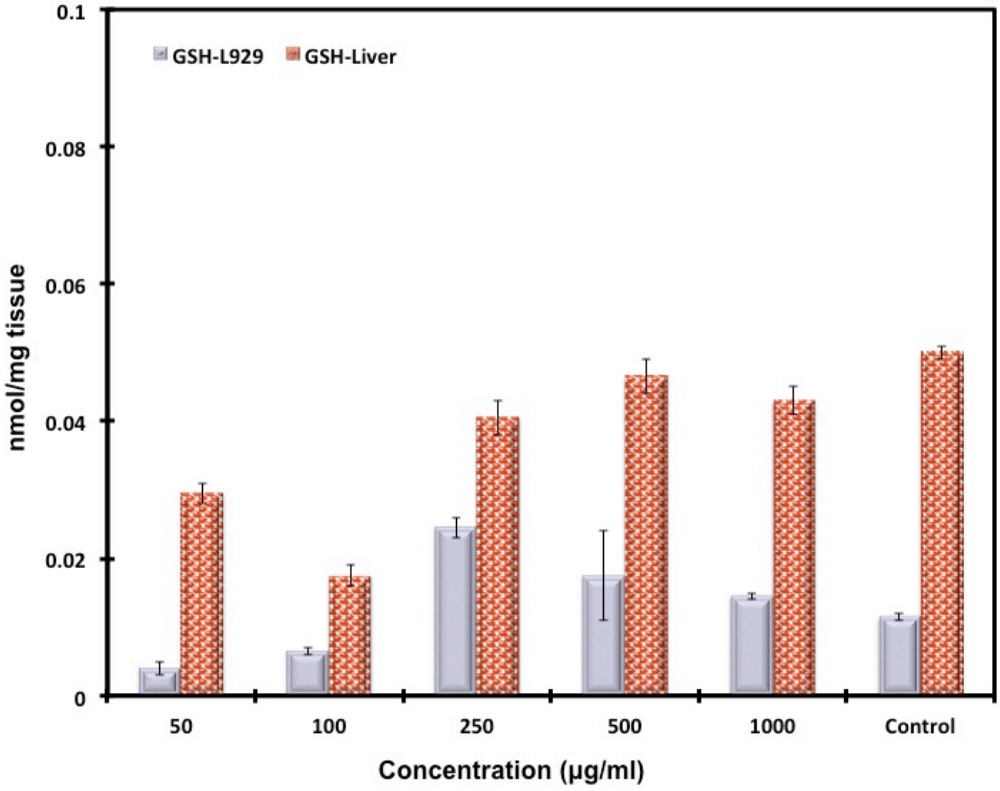

Fig 9: GSH levels in L929 cells and liver homogenate after treatment with BCS.

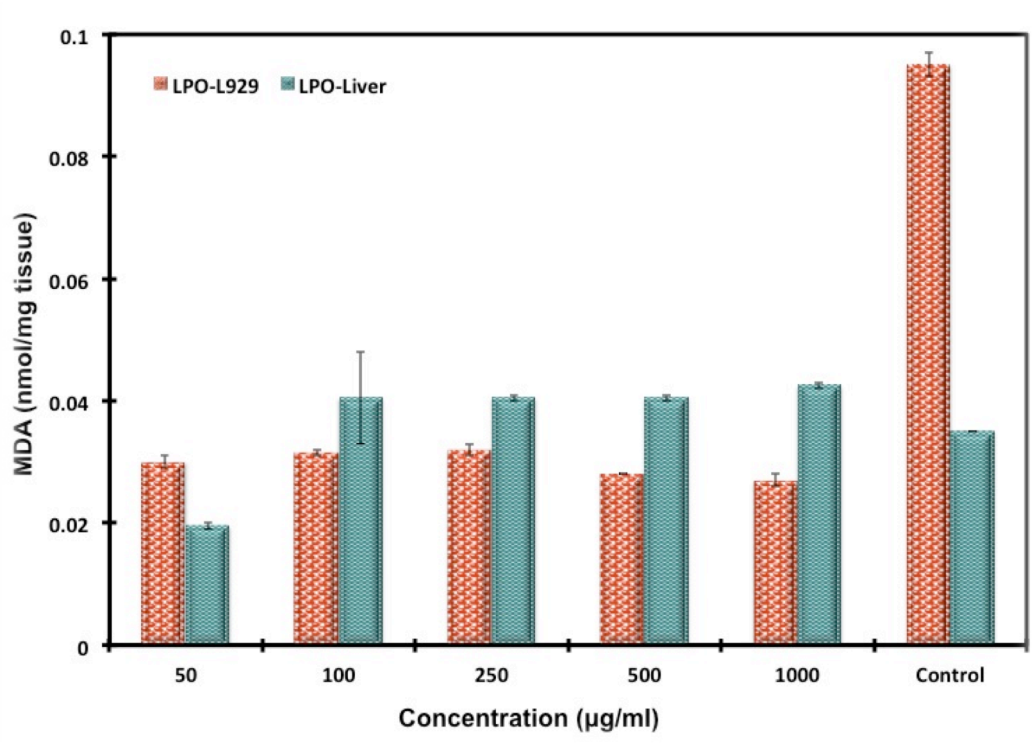

Fig 10: LPO levels in L929 cells and liver homogenate after treatment with BCS.

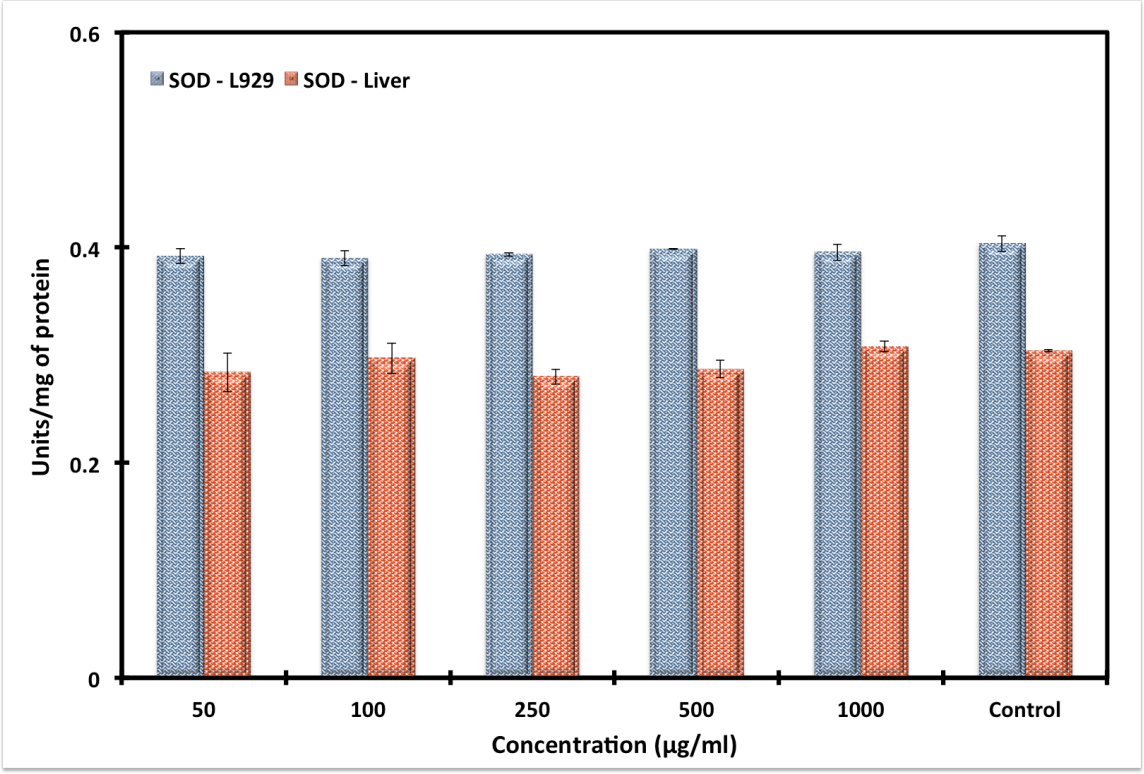

Fig 11: LPO levels in L929 cells and liver homogenate after treatment with BCS.

In a network of biological antioxidants, SOD is a vital enzyme that is endogenously induced in order to eliminate superoxide radicals by conversion to hydrogen peroxide and oxygen. [39] SOD can mutate DNA or assault enzymes that produce amino acids and other essential molecules. [28] Fig. 8 shows the SOD levels when BCS was exposed to L929 cells and liver homogenate. The L929 results showed that the control group produced 0.4035±0.0075 units of SOD per mg of protein. When the BCS was treated with the cells, there was no apparent change observed in the levels of SOD production. In case of liver homogenate the control group showed 0.304±0.001 units of SOD per mg of protein and very slight variations in levels of SOD was observed, which was deemed insignificant.

Conclusion

To summarize, BC was produced in our lab and was purified through the alkali treatment method. Thereafter, acetosulfation of BC was carried out to functionalize it with sulfate groups. Successful

sulfation of BC was confirmed with XPS, FTIR and FT raman studies. Lack of adequate information regarding acetosulfation of BC encouraged us to conduct this study. We also developed a highly transparent film, which has good integrity and flexibility. This film possesses immense potential for applications in food and biomedicine. We have evaluated the cytotoxicity, antioxidant property and hemocompatibility of BCS sample by using different concentrations to illustrate the biocompatibility and ecofriendly nature of our film. The antioxidant results infer that BCS was not involved in excessive generation of free radicals in L929 cells or liver homogenate and was comparable to the control group in this work. The cytotoxicity results showed that the cell viability of L929 and KUSA cells was >85% with an increasing trend in cell viability upon increasing concentration of BCS, which infers that it is highly biocompatible and non-toxic. The hemolytic study confirms the non-hemolytic nature of BCS, when incubated with the blood cells for 2 hours. Also, it did not interfere with the coagulation cascade of blood, which suggests that it is highly blood compatible. Thus, the *ex vivo* and *in vitro* studies show that BCS concentrations do not contribute to cells or tissue damage and is deemed safe for food packaging or biomedical applications. However, further *in vivo* evaluation is required to study its dose dependent effects with different concentrations of BCS.

References

1. N. Xu, W. Zhang, S. Ren, F. Liu, C. Zhao, H. Liao, Z. Xu, J. Huang, Q. Li, B. Yu, Y. Wang, J. Jiang, J. Qin, and L. Peng. Hemicelluloses negatively affect lignocellulose crystallinity for high biomass digestibility under NaOH and H_2SO_4 pretreatments in *Miscanthus*; *Biotechnol. Biofuels* 5, 58. **(2012)**.
2. P.J. Wakelyn, and N.R. Bertoneire. Cotton fiber chemistry and technology. CRC press. **(2006)**.
3. A. Svensson, T. Nicklasson, B. Harrah, D. Panilaitis, L. Kaplan, M. Brittberg, and P. Gatenholm. BC as a potential scaffold for tissue

engineering of cartilage; *Biomaterials* 26, 419–431 **(2005)**.

4. P. Ross, R. Mayer, and M. Benziman. Cellulose biosynthesis and function in bacteria; *Microbio. Rev.*55:35–38 **(1991)**.
5. D. Klemm, D. Schumann, U. Udhardt, and S. Marsch. Bacterial synthesized cellulose – Artificial blood vessels for microsurgery; *Prog. Poly. Sci.* 26, 1561–1603 **(2001)**.
6. J.R. Colvin. The biosynthesis of cellulose; Plant biochemistry, Academic Press Inc., New York, 543–570 **(1980)**.
7. S. Bauer, P. Schmuki, K. Von der Mark, and J. Park. Engineering biocompatible implant surfaces: Part I: Materials and surfaces; *Prog. Mat. Sci.*58: 261−326 **(2013)**.
8. K. Zhang, D. Peschel, E. Bäucker, T. Groth, and S. Fischer. Synthesis and characterisation of cellulose sulfates regarding the degrees of substitution, degrees of polymerisation and morphology; *Carbohydr. Polym.* 83, 1659–1664 **(2011).**
9. Y.L. Xie, M.J. Wang, and S.J. Yao. Preparation and characterization of biocompatible microcapsules of sodium cellulose sulfate/chitosan by means of layer-by-later self assembly; *Langmuir*25, 8999–9005 **(2009)**.
10. G. Chen, B. Liu, and B. Zhang. Characterization of composite hydrocolloid film based on sodium cellulose sulfate and cassava starch; *J Food Eng.* 125, 105–111 **(2014)**.
11. Z. Qin, L. Ji, X. Yin, L. Zhu, Q. Lin, and J. Qin. Synthesis and characterization of BC sulfates using a SO_3/Pyridine complex in DMAc/LiCl; *Carbohyd. Polym.* 101, 947–953 **(2013)**.
12. L. Zhu, J. Qin, X. Yin, L. Ji, and Q.L.Z. Qin. Direct sulfation of BC with a $ClSO_3H$/DMF complex and structure characterization of the sulfates; *Polym. Adv. Technol.* 25, 168–172 **(2013).**
13. P. Sharma, A.B. Jha, R. Dubey, and M. Pessarakli. Reactive oxygen species, oxidative damage, and antioxidative mechanism in plants under stressful conditions; *J Botony* Article ID 217037, 26 **(2012)**.

14. D. Surendran, C.S. Geetha, and P.V. Mohanan. Amelioration of melatonin on oxidative stress and genotoxiceffects induced by cis-platin*in vitro*; *Toxicol.Mech. Methods* 22, 631-637 **(2012)**.
15. V.V.S Anjana, S.K. Tinu, C.S Geetha, and P.V. Mohanan. Effect of hydroxyapatite coated bioactive glass and vinyl acetate on antioxidant defence mechanism, oxidative DNA damage and chromosomal anomalies; *Trends in Biomaterials and Artificial Organs,* **26**: 64-73 **(2012)**.
16. S. Raveendran, V. Palaninathan, N. Chauhan, Y. Sakamoto, Y. Yoshida, T. Maekawa, and D.S. Kumar. *In vitro* evaluation of antioxidant defense mechanism and hemocompatibility of mauran; *Carbohydr. Polym.*98, 108-115 **(2013 b)**.
17. S. Hestrin, and M. Schramm. Synthesis of cellulose by *Acetobacterxylimum* II Preparation of freeze-dried cells capable of polymerizing glucose to cellulose; *BiochemistryJ* 58, 345-352 **(1954)**.
18. M.E. Embuscado, J.N. BeMiller, and J.S. Marks. Isolation and partial characterization of cellulose produced by *Acetobacterxylinum*; *Food Hydrocolliods*10, 75-82 **(1996)**.
19. K. Zhang, E. Brendler, A. Geissler, and S. Fischer. Synthesis and spectroscopic analysis of cellulose sulfates with regulable total degrees of substitution and sulfation patterns via ^{13}C NMR and FT Raman spectroscopy; *Polymer* 52, 26-32 **(2010b)**.
20. M. Gericke, T. Liebert, and T. Heinze. Interaction of ionic liquids with polysaccharides, 8 - Synthesis of cellulose sulfates suitable for polyelectrolyte complex formation; *Macromol. Biosci.* 9, 343-353 **(2009)**.
21. M. Dubois, K.A. Gilles, J.K. Hamilton, P.A. Rebers, and F. Smith Calorimetric method for determination of sugars and related substances; *Anal. Chem.*28, 350-356 (1956).
22. P.K. Smith, R.I Krohn, G.T. Hermanson, A.K. Mallia, F.H.Gartner, M.D. Provenzano, E.K. Fujimoto, N.M. Goeke, B.J. Olson, and D.C. Klenk. Measurement of protein using bicinchoninic acid; *Anal. Biochem.* 150, 76-85 **(1985)**.

23. S. Raveendran, B. Dhandayuthapani, Y. Nagaoka, Y. Yoshida, T. Maekawa, and S.D. Kumar. Biocompatible nanofibers based on extremophilic bacterial polysaccharide, mauran from *Halomonas maura*; *Carbohyd. Polym.* 92,1225-1233 **(2013a)**.
24. H.C. Li, F.J. Hsieh, C.P. Chen, M.Y. Chang, P.C.H. Hsieh, C.C. Chen, S.U. Hung, C.C. Wu, and H.C. Chang. The hemocompatibilty of oxidized nanodiamondnanocrystals for biomedical applications; *Scientific Reports*3, 30-44 **(2013)**.
25. R. Shelma, and C.P. Sharma. Development of lauryl sulfated chitosan for enhancing hemocompatibility of chitosan; *Colloids Surf B*84, 561-570 **(2011)**.
26. M.S. Moron, J.W. Depierre, and B. Mannervik. Levels of glutathione, glutathione reductase and glutathione S-transferase activities in rat lung and liver; *Biochem. Biophys. Acta.* 582, 67-78 **(1979)**.
27. H. Ohkawa, M. Ohishi, and K. Yagi. Assay for lipid peroxidase in animal tissues by thiobarbituric acid reaction.; *Anal.Biochem.*193, 265-275 **(1979)**.
28. A. Nandi, and I.B. Chatterjee. Assay of superoxide dismutase activity in animal tissues; *J Biosci.* 13, 305-315 **(1988)**.
29. H.U. Yang, and J.M. Catchmark. Formation and characterization of spherelike BC particles produced by *Acetobacterxylinum* JCM 9730 strain; *Biomacromol.* 11, 1727-1734 **(2010)**.
30. J.F. Moulder, W.F. Stickle, P.E. Sobol, and K.D. Bomben. Handbook of X-ray photoelectron spectroscopy; Physical electronics, Inc. USA **(1995)**.
31. K. Zhang, E. Brendler, and S. Fischer. FT Raman investigation of sodium cellulose sulfate; *Cellulose* 17, 427-435 **(2010a)**.
32. M.S. Chargot, J. Cybulska, and A. Zdunek. Sensing the structural differences in cellulose from apple and bacterial cell wall materials by Raman and FT-IR Spectroscopy; *Sensors*11, 5543-5560 **(2011)**.
33. H. Sies. Oxidative stress: oxidants and antioxidants; *Experim. Physiol.* 82, 291-295 **(1997)**.

34. M. Arun, P.K. Silja, L.E. Sheeja, C.S. Geetha, and P.V. Mohanan. Molecular level toxicological evaluation of dental composite implanted in albino rats; *Toxicol. Environ. Chem.*9, 60-768 **(2012)**.

35. N. Dilsiz, A. Sahaboglu, M.Z. Yildiz, and A. Reichenbach. Protective effects of various antioxidants during ischemia-reperfusion in the rat retina. Graefe's Arch *Clin.Exp.Ophthalmol.*244, 627–33 **(2006)**.

36. A. Catala. Lipid peroxidation of membrane phospholipids generates hydroxy-alkenals and oxidized phospholipids active in physiological and/or pathological conditions; *Chemistry and Physics of Lipids* 157, 1-11 **(2009)**.

37. *C.J. Weydert, and J.J. Cullen. Measurement of superoxide dismutase, catalase, and glutathione peroxidase in cultures cells and tissues; Nat. Protoc.5, 51-66* ***(2010).***

38. L.R. Shen, F. Xiao, P. Yuan, Y. Chen, Q.K. Gao, L.D. Parnell, M. Meydani, J.M. Ordovas, D. Li, and C.Q. Lai. Curcumin-supplemented diets increase superoxide dismutase activity and mean lifespan in *Drosophila; Age35, 1133-1142* **(2013)**.

5

Synthesis of Bacterial Cellulose Sulfate film

"Genius is one percent inspiration & ninety nine percent perspiration "

- Thomas A. Edison

The rising consciousness about the benefits of environment friendly and biodegradable materials demand a substitute for the prevailing non-degradable and toxic materials. Towards this aspect bacterial cellulose has numerous potential applications owing to their important properties like high biocompatibility, biodegradability, and ecofriendly nature. In the present study, we have synthesized bacterial cellulose using *Komagataeibacter sucrofermentans* strain through batch fermentation and functionalized it with sulfate groups to form bacterial cellulose sulfate (BCS) that has negligible reports so far. Using this BCS, we synthesized a highly transparent film by drop cast method, which exhibited high optical transmittance of 90-92% in the visible wavelength range. BCS was thoroughly characterized, using SEM and AFM for its surface morphology; XPS, FTIR, TGA and XRD to confirm the successful functionalization of bacterial cellulose. The results inferred the successful sulfation of bacterial cellulose and the film has a smooth surface with good integrity and mechanical properties. Furthermore, cell viability studies confirmed the biocompatible nature of the sample. These properties of the film hold immense promise for applications in biomedicine, optoelectronics and food packaging.

Introduction

Optically transparent and functional materials has gained tremendous interest due to their varied applications in electronics, optoelectronics, food and packaging industries. The quest for green materials to replace the current toxic and non-degradable materials has revealed several biopolymers and cellulose as prospective candidate among them. Cellulose is the most abundant biopolymer, which is produced by plants and bacteria. Though structurally similar, the absence of hemicellulose and lignin gives bacterial cellulose (BC) a superior quality over plant cellulose. BC fibrils are very thin, with high planar orientation and uniform ultrafine-fiber network that contribute to its chemical stability and high water holding capacity. [1,2] Good mechanical strength, biocompatibility, relative thermostabilization, high sorption capacity and alterable optical appearance have opened up broad industrial platform for BC. [3] Though BC has many advantages, its insolubility in most solvents hampers its applications. To solve this issue, direct sulfation of BC has been reported recently to form cellulose sulfate (CS). CS is a half ester of cellulose that has certain advantages over cellulose in their properties such as solubility in water, rheological behavior, varied interactions with low or high molecular cations and thermo reversible gel formation, which will further develop its applications. [4-6]

Most materials currently employed for food packaging are non-degradable, which is a threat to the environment. Though numerous biopolymers have been tested to develop an ecofriendly food packaging material, poor mechanical properties has been a limiting factor. Edible food packaging films have gained lot of attention, as there is an increasing demand for green materials that can provide longer shelf life and better quality to food items. Recently in the food industries, edible food packaging films developed from cellulose were used to coat fruits, oily foods and constant soluble packaging in food industries. [7] While numerous reports exist on commercially available microcrystalline and functionalized cellulose based materials, there are negligible data

available on the use of BC thin films for food packaging. Since BC produced by *Komagataeibacter* spp. is edible (for eg: *nata de coco)*, it can be an exciting prospect for food industries owing to its inherent biocompatibility, non-toxic and biodegradable nature. BC has applications in biomedical field as wound dressing materials, artificial skin, blood vessels and bio membranes. BC membranes that would not never dry have been used for treating patients with second-degree burns. The results have proved that the skin of patients treated with BC recovered faster than those treated with conventional methods. [8] Biocompatible BC-Poly(2-hydroxyethyl methacrylate) nanocomposite translucent films have also been developed as potential dry dressings. [9]

Novel structural and functional materials based on renewable resources are capturing lot of attention since metal conductors despite their potential high conductivity are unable to meet the requirements of flexible electronic devices. BC and its applications in optoelectronics has gained a lot of attention in the last decade due to its unique characteristics like high purity, high crystallinity, flexibility, smoothness, transparency and mechanical strength. [10] Optically transparent BC membrane substrates were used for flexible organic lighting emission (FOLED) and for electronic papers. [9] The unique features of BC has inducted itself into the field of electronics, where efforts have been taken to significantly enhance the conductivity, transparency and mechanical properties of BC membranes. [11,12] For achieving transparency, transparent composites such as epoxy resins reinforced with BC have been developed that has about 70% fiber content with a low thermal co-efficient and very high mechanical strength. [13] The major drawbacks of using epoxy resins involves high cost, relative low modulus, long curing profile, reduction of properties in the presence of moisture due to the toxic content in the form of Bisphenol A. Hence, a competent substitute is required to combat the toxicity and biodegradability related issues of existing the BC composites treated epoxy resins, which may pose serious threat to environment and people.

In this chapter, we report acetosulfation of BC to form bacterial

cellulose sulfate (BCS). By the functionalization of BC with sulfate groups, we have developed a highly transparent BCS film with good mechanical properties and biocompatibility without adding any resins to improve its transparency. This highly transparent film holds tremendous potential as an incipient candidate for biomedical applications, optoelectronic substrates and food packaging industries.

Materials and Methods

All the chemicals used were of analytical grade and were used as received. Dialysis membrane from Spectrum Laboratories Inc. (Rancho Dominquez, USA) has an approx. molecular weight cut off of 500 Da.

Komagataeibacter sucrofermentans JCM 9730^T strain was purchased from Riken Bioresource Center, Japan and was revived using Acetobacter medium. Bacterial fermentation was carried out in a jar fermenter using Hestrin-Schramm (HS) medium mentioned elsewhere. [14] The BC pellicles were purified through the alkali extraction method as described elsewhere. [15] Briefly, BC obtained through downstream processing of fermentation was homogenized in distilled water using the high-pressure homogenizer (APV2000, SPX, Germany) for 5 min. The homogenized sample was centrifuged at 13,800 g for 10 min at 10°C and the supernatant were discarded. The cellulose paste was mixed thoroughly for homogeneity and was placed in a beaker with alkaline solution of 0.30 mol/dm^3 NaOH preheated to 90°C. The mixture was heated for 25 min and rapidly cooled down in an ice bath. Then, the samples were washed with distilled water and pH of the sediments was adjusted to 7 and freeze-dried.

Acetosulfation of BC was carried out as mentioned elsewhere. [16] Briefly, 2.5g of BC was suspended in 125 ml of anhydrous DMF at room temperature for over 14 h. Reaction agent consisting chlorosulfuric acid and acetic anhydride in DMF was dropped in cellulose suspension under vigorous stirring. The resulting solution was maintained at 50°C for 5 h and was then cooled to the room temperature. This reaction agent was then poured into saturated ethanolic solution of anhydrous sodium

acetate. Through centrifugation the precipitate was collected and was washed with 4% sodium acetate solution in ethanol. Deacetylation was carried out using 1M ethanolic solution of NaOH for 15 h and pH was adjusted to 8 with acetic acid/ethanol (50/50, w/w). The final product was dissolved in water, filtered, dialyzed and freeze dried. Drop cast method was adapted to form the BCS film, wherein 25% of BCS sample was drop casted onto a plastic plate and vacuum dried on a flat surface.

Scanning Electron Microscopy (SEM) images of the BC and BCS samples were obtained on a JEOL, JSM-7400F scanning microscope at room temperature. The elemental characterization was determined through X-ray photoelectron spectroscopy (XPS) KRATOS with a basic pressure of 1.7 x 10^{-8} and mono-Al anode with pass energy of 40 (survey scan) X-ray source. The chemical structure analysis was obtained through Fourier Transform Infrared (FTIR) (Perkin Elmer) with a resolution of 4 cm^{-1} in the region of 4000 to 400 cm^{-1}. The mass fraction of cellulose $I_{\alpha}f_{\alpha}^{IR}$, was estimated using an equation as mentioned elsewhere. [17]

$$f_{\alpha} = \frac{A_{750}}{A_{750} + k\,A_{710}} \qquad (1)$$

where, A_x is the integrated absorption at the corresponding wavenumber and k is the constant (k = 0.16). Powder X-ray diffraction (XRD) pattern was carried out on a Rigaku (RINT) diffractometer equipped with a rotating anode. The 2θ angle for the XRD spectra was recorded at a scanning rate of 5°/minute. Thermogravimetric analysis (TGA) of the samples was carried out using Shimadzu TGA-50. UV-vis spectroscopy was done using Beckman coulter-730 spectrophotometer over a wavelength range of 200-1000 nm.

Results and Discussion

BC required for the present study was obtained through batch fermentation process using *Komagataeibacter sucrofermentans* JCM 9730^{T} strain in HS medium. Small sphere-like BC pellicles were seen as

discussed in chapter 3. BC pellicles were collected after 10 days and were subjected to purification by alkali treatment method. In our study we have used relatively low concentration 0.30 mol/dm^3 of NaOH that was sufficient to remove most of the contaminants from BC compared to previous reports. [13,18]

Acetosulfation involves the competitive esterification of BC suspended in N, N-dimethylformamide (DMF) with a mixture of a sulfating agent [chlorosulfuric acid ($ClSO_3H$)] and acetylating agent (acetic anhydride) that upon subsequent saponification yields CS. The resulting reaction is quasi-homogenous synthesis that occurs via gradual dissolution of BC (suspended in DMF) in the reaction mixture. Deacetylation by NaOH marks the completion of acetosulfation. [5,19,20] Clear transparent solution was obtained as BCS was dissolved in water.

Bacterial Cellulose Sulfate films (BCSF) were synthesized through drop casting method and by vacuum drying the sample. Figure 1 (a), (b) depicts SEM images of BC before and after acetosulfation reaction. The SEM images reveal a remarkable change after the reaction, where all the fibrils of BC have disappeared and only a smooth film remains.

XPS measurements were carried out to confirm the sulfation of BC sample. Figure 2 illustrates the XPS spectra of BC and BCS, with atomic percentage of the elements. The presence of a peak at 167.9 eV in the BCS sample corresponds to sulfate, thus confirming the successful functionalization. [21] The figure also shows different functional groups present in BC and BCS samples. [22] Table 1 shows the atomic percentage

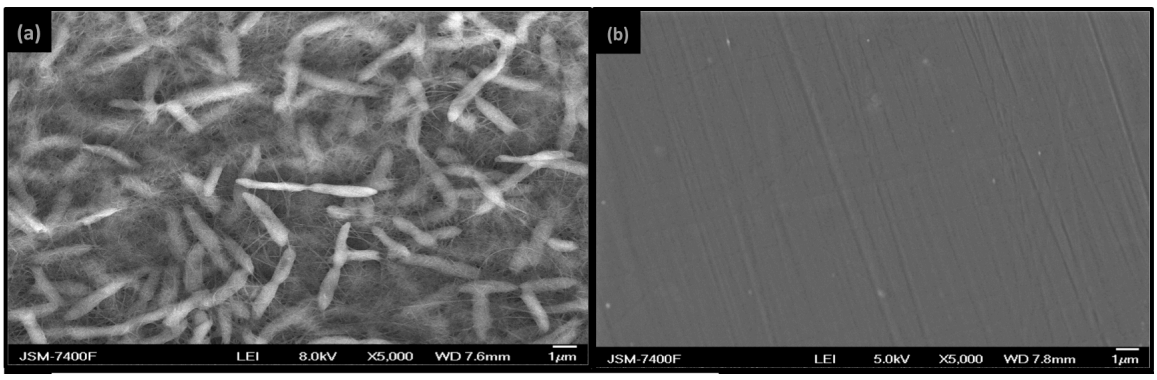

Figure 1 (a), (b) depicts SEM images of BC before and after acetosulfation reaction, respectively

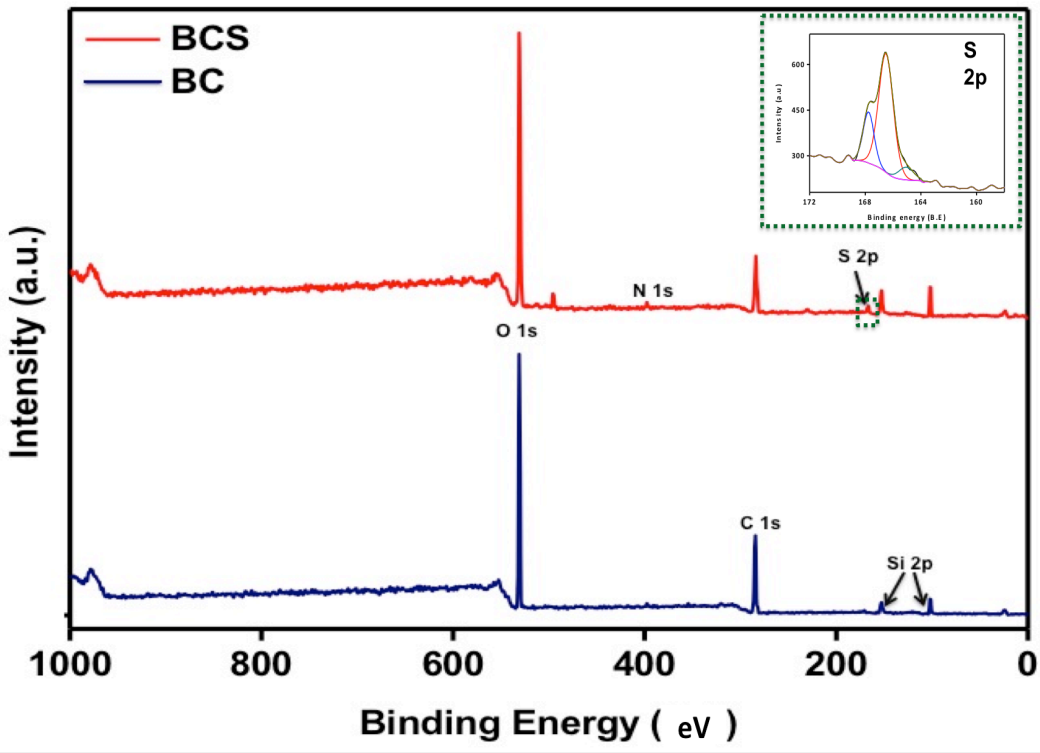

Fig 2: XPS spectra of BC and BCS

Sample	C %	N %	O %	S %
BC	50.19	0.84	48.97	-
BCS	41.24	1.42	55.03	2.31

Table 1: Elemental composition of BC and BCS

BC	Peak %	B.E (eV)	Attributed to
C 1s	72.80	285.94	C-OH group
C 1s	19.75	287.38	C=O
C 1s	7.45	284.09	C-C
O 1s	100	532.42	OH groups of Cellulose
BCS	**Peak %**	**B.E (eV)**	**Attributed to**
C 1s	49.94	285.58	C-OH
C 1s	29.49	284.06	C-C
C 1s	20.57	286.98	C=O
O 1s	100	532.27	OH groups of cellulose
N 1s	100	399.09	Organic matrix
S 2p	69.93	166.51	Na_2SO_3 bonds
S 2p	22.36	167.76	Na_2SO_3 bonds
S 2p	7.71	165.05	Na_2SO_3 bonds

Table 2: XPS attribution for of BC and BCS

of elements present in BC and BCS samples. The presence of Sulfur is shown by the results of atomic percentage composition of BC and BCS. Table 2 depicts the different functional groups present in BC and BCS.

Figure 3 illustrates the cellulose I XRD profile of BC spectra, where the peaks at 14.3°, 16.8°, 22.5° are attributed to the crystalline character of bacterial cellulose. [23] The 2θ angle values depict that -110 and 110 reflections are close to each other. In the case of BCS sample, the peak is limited to a small broad one related to the quasi-homogenous reaction of cellulose. This reaction causes the destruction of intra-molecular hydrogen bonds within cellulose leading to a decrease in the crystalline regions or loss of cellulose I polymorph. Post precipitation, BCS with an amorphous structure was obtained. [24]

The chemical structure of purified BC and BCS were investigated by FTIR. The broad band in the 3400-3200 cm^{-1} regions in BC and BCS was due to the characteristic O-H stretch as shown in Figure 5. The absorption peaks at 2896, 1649 and 1428 cm^{-1} was due to the C-H stretching of $–CH_2$, O-H bending and $–CH_2$ symmetric bending respectively. The absorption band at 900 cm^{-1} in

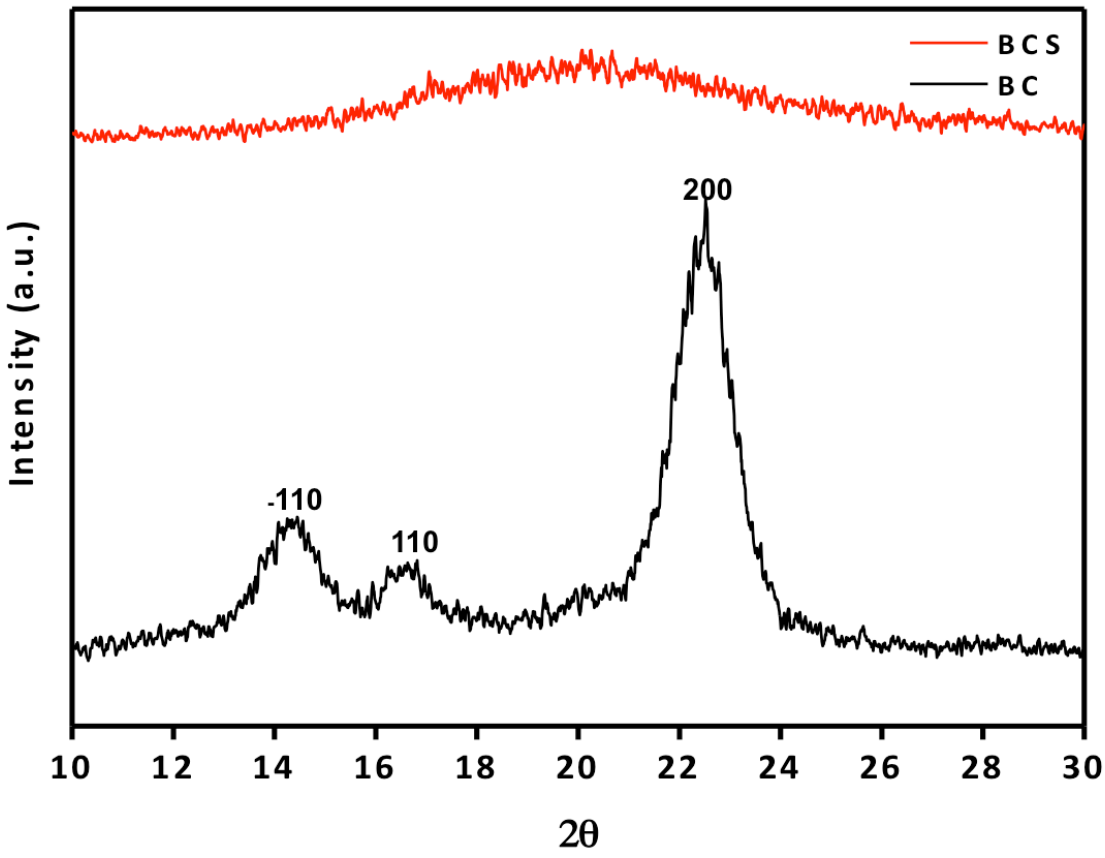

Fig 4: XRD spectra of BC and BCS

BCS sample is attributed to C–O–C stretching of β-(1,4)-glycosidic linkages and the increased peak intensity in this region is attributed to the amorphous nature of sample. [25,26] This result is in agreement to the XRD results of BCS sample. The peaks at 1109, 1057 and 1033 cm^{-1} in BC spectra indicated C_2O_2, C_3O_3 and C_6O_6 stretching respectively, which are assigned to ν(C–O) and ν(C–C). The peaks at 752 and 713 cm^{-1} in BC spectra are attributed to the contribution by cellulose Iα and Iβ respectively. [17,27] Using the equation 1, we found that the mass fraction of BC Iα was 0.865 and this infers the existence of almost pure BC Iα allomorph in the sample. The presence of two new peaks in BCS sample at 1217 and 810 cm^{-1} indicate the successful sulfation of BC hydroxyl groups and are attributed to the asymmetric vibration ν_{as}(O=S=O) and C–O–S stretching vibration ν(C–O–S) respectively. [4,6]

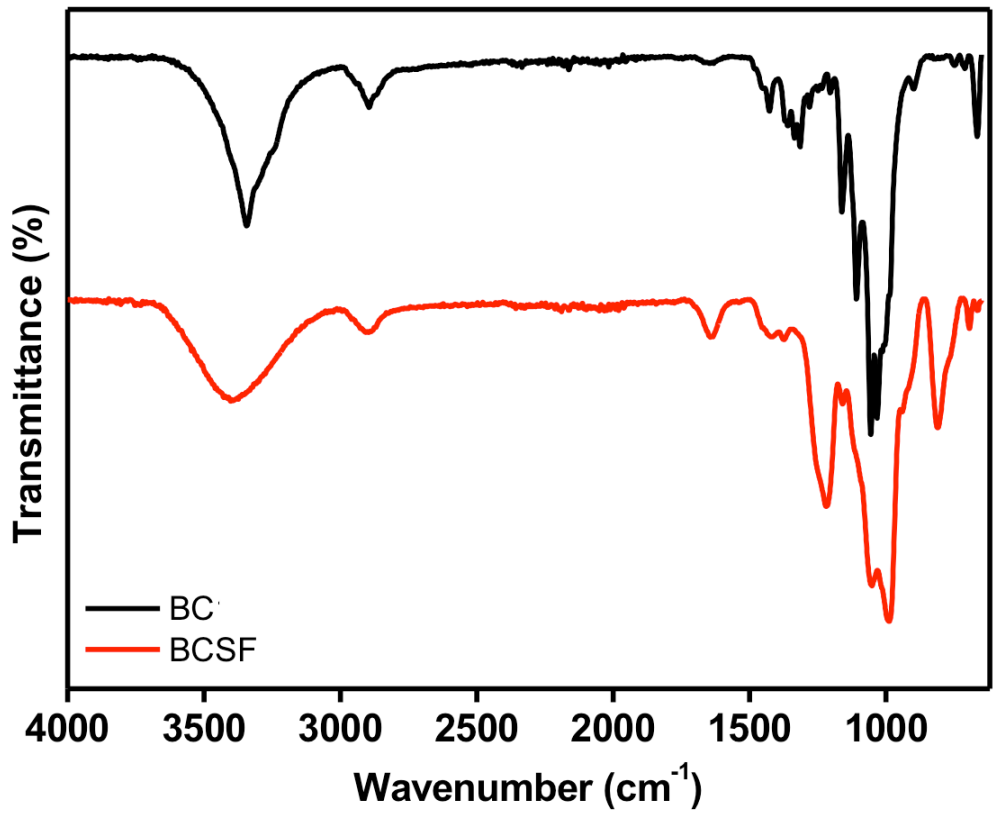

Fig 5: FTIR spectra of BC and BCS samples

Topology of BCS film was unveiled by AFM (Asylum MFP-3D) analysis obtained through non-contact mode (Resonance frequency of 70 kHz, spring constant of 2 N/m). AFM scan size of 5 x 5 µm revealed a mean surface roughness of 1.366 ± 0.348 nm as shown in figure 6, which is better than recombinant protein polymer transparent films and large flat cellulose paper. In the case of optically transparent recombinant protein polymer films, the mean surface roughness of non-treated films was 1.485 ± 0.245 nm, [28] which is higher than BCS film. Similarly, large flat cellulose paper produced through rapid-kothen hybrid method and rapid-kothen method showed surface roughness of 47.5 ± 6.6 nm and 21.9 ± 0.8 nm respectively, [29] which are considerably higher than BCS film.

Using DU 730 Beckman coulter spectrophotometer the optical transparency of 25% BCS film was found to be 90-92% in the visible region of 400-800 nm. This was achieved without incorporating any type of resin matrix or involvement of hot pressing. Figure 7 shows the absorbance and percentage of light transmittance of BCS film.

The BCS average film thickness (2.85 µm) and refractive index (1.43) was determined using Photol FE-3000 instrument at 600nm. The tensile strength of BCS samples (20mm X 20mm) was evaluated with Instron 5566 at a crosshead speed of 10 mm/min. The average tensile strength of BCS film was 125 MPa and young's modulus of 1.038 GPa,

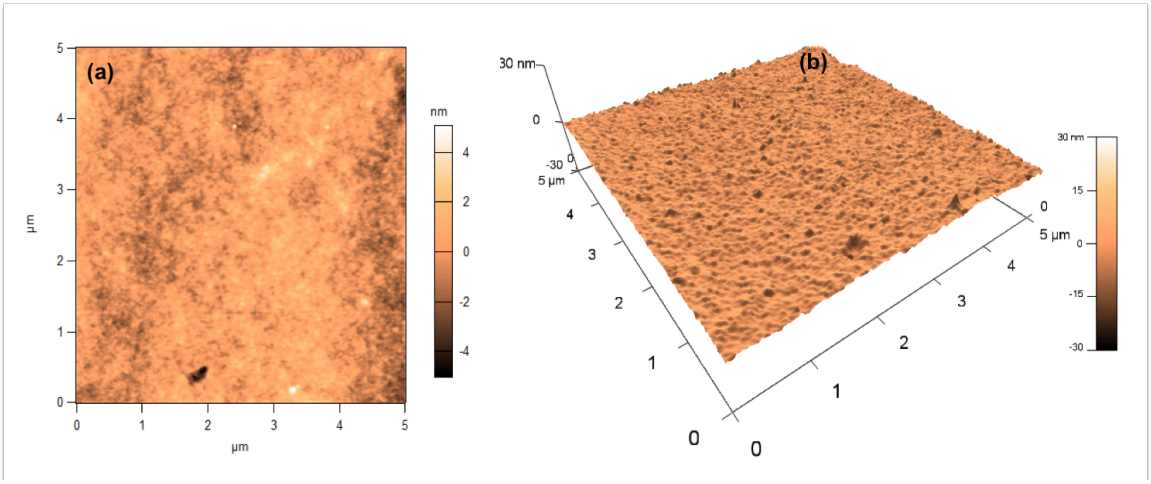

Fig 6: AFM images of BCS film (a) 2-D and (b) 3-D

which infers that BCS films have good mechanical properties, which could be improved through further studies. Figure 8 (a) shows the stress-strain graph of BCS film. Zeta potential of BCS solution with varying concentrations were recorded with Malvern Zetasizer nanoZS. An increasing trend in zeta potential was observed with the increase in concentration of BCS as shown in Figure 8 (b).

The integrity of the BCS film was deemed to be good since it could be easily peeled off from the substrate without any deformity. The BCS film was folded ~100 times to check the flexibility of film, but resulted without any cracks on the film. Noted property of BCS film is that its readily solubility in water (~ 8 seconds). However, when the film is held in oil or alcohol for >48 hours it remained insoluble, but maintained its integrity when recovered.

Water retention and thermal decomposition behavior of BC and BCS samples were determined through TGA. Figure 9 depicts the TGA spectra of BC and BCS respectively, which shows that the BCS is thermally less stable than its precursor BC. TG curve of BC had two main decomposition steps. The first step at 80°C corresponds to the

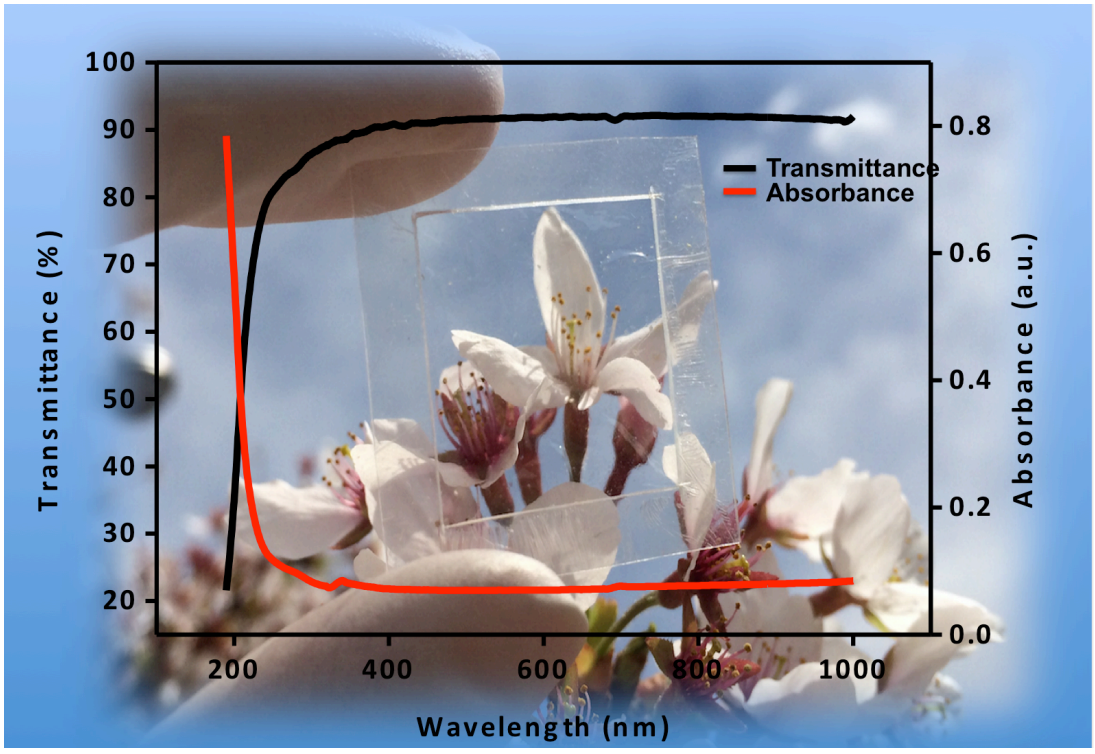

Fig 7: Transmittance and absorbance of BCS film

dehydration of BC and the mass was almost unchanged from 80 – 300°C. The second step from 300 – 363°C has a relatively swift weight loss of 78 %, which was attributed to the decomposition of cellulose backbone. Finally, there was a gradual complete weight loss observed from 363 – 600°C. In the case of BCS, three steps of weight loss at different temperatures were observed. The first step of weight loss was due to the water loss from the sample. The loss from 226 – 262°C was attributed to the decomposition due to the release of volatile compounds and the final step of weight loss from 450 – 525°C was due to the degradation of the remaining residue. However from 525 – 600°C, the weight loss of BCS sample was comparatively lesser. Alamar blue assay was carried out to evaluate the biocompatibility of varying concentrations of BCS samples in mouse fibroblast cells (L929) and mouse mesenchymal stem cells (Kusa) for 24 hours as mentioned elsewhere. [21] The percentage of cell viability was above 88% for both L929 and Kusa cells indicating good biocompatibility and non-toxic nature BCS samples as depicted in Figure 10.

Conclusion

To summarize, the present study involves acetosulfation of BC to obtain cellulose sulfate that has remained untouched till now. The lack of impurities in the form of hemicellulose and lignin prompted us to use BC for our study. BC was synthesized through batch fermentation process using *Komagataeibacter sucrofermentans* strain and was purified via

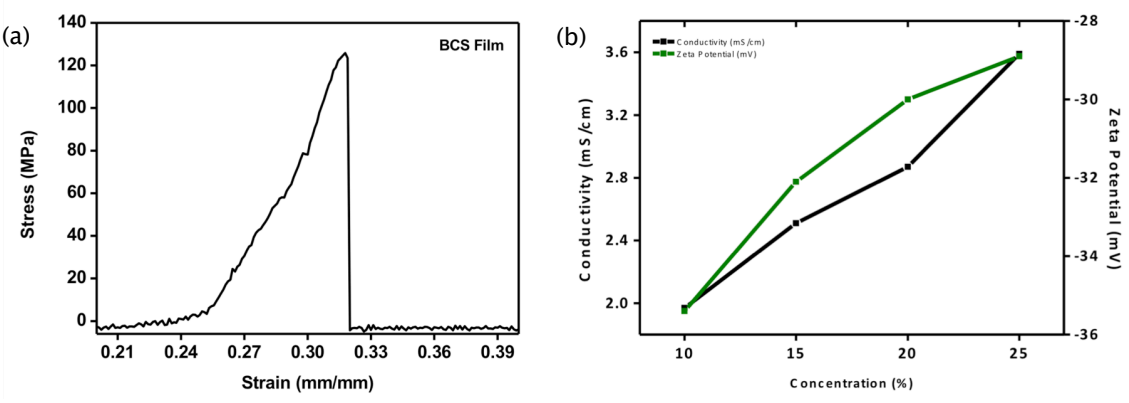

Figure 8 (a): Stress-strain graph of BCS film; (b) Zeta potential and conductivity of BCS solution

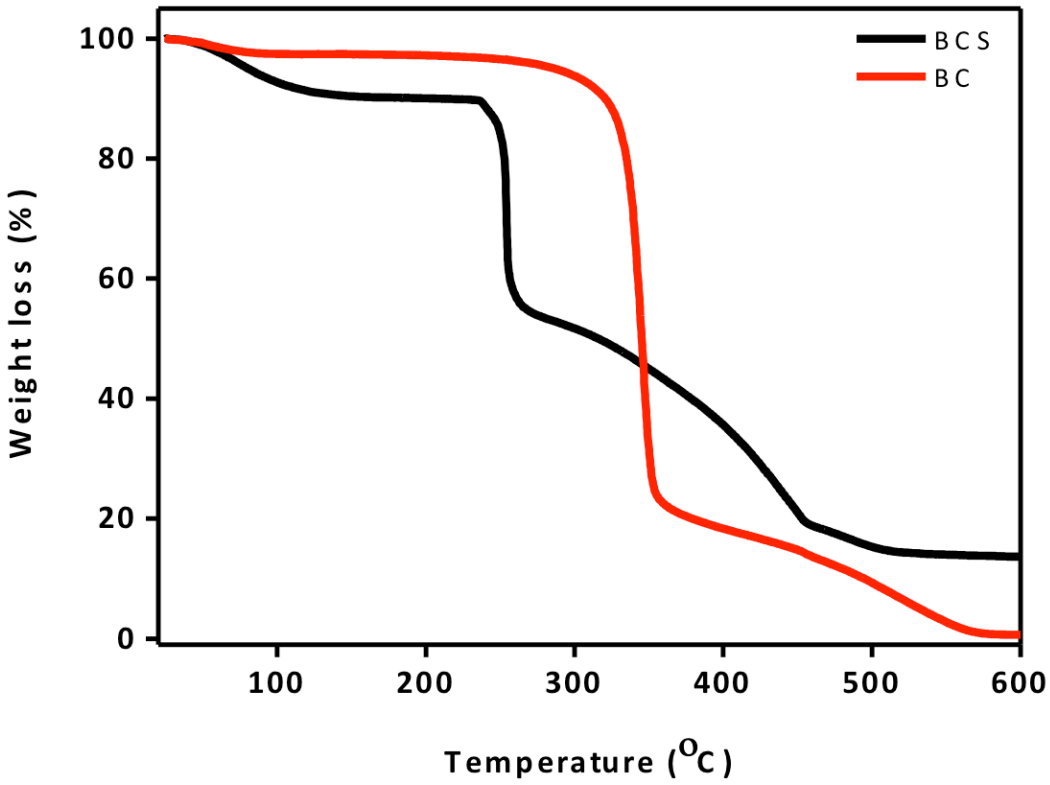

Fig 9: TGA plot of BC and BCS samples

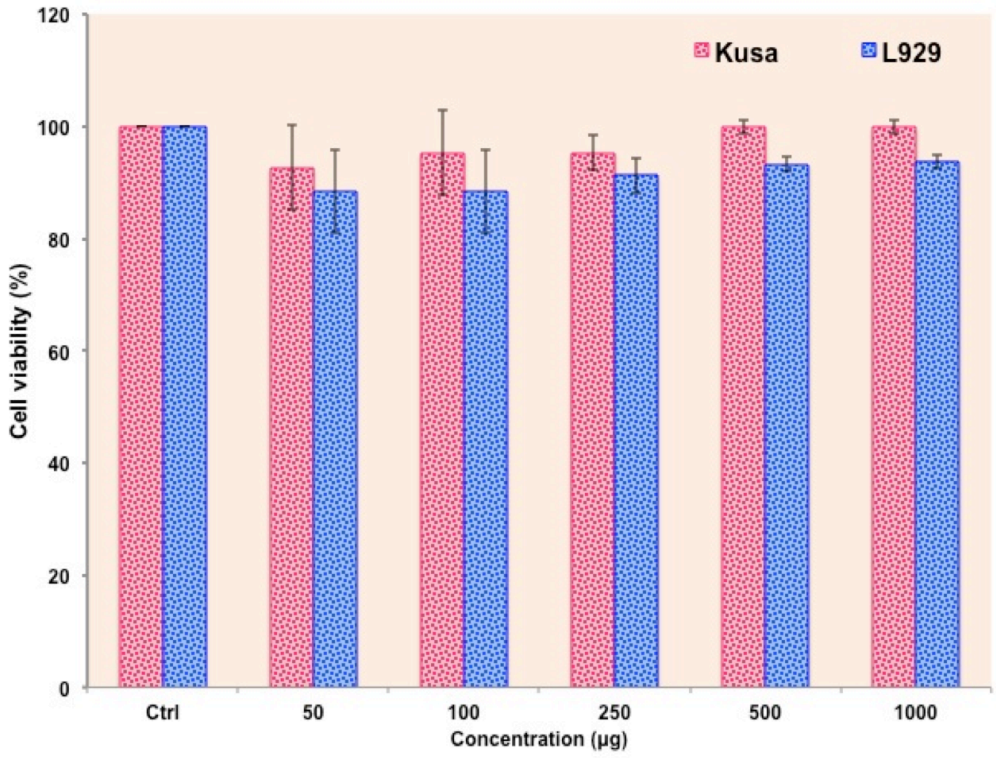

Fig 10: Cell viability studies of L929 and KUSA cells with BCS sample

It was functionalized with sulfate groups through acetosulfation process. We have obtained a highly transparent film through drop casting BCS solution on a glass plate and freeze-drying the same. The film was highly water-soluble but insoluble in oil and alcohol. BCS film exhibits superior mechanical properties like high tensile strength of 125 MPa and young's modulus of 1.038 GPa. The film showed very high transparency (90 – 92 %) in the visible wavelength without the use of any toxic resins and the surface roughness of film was 1.366 ± 0.348 nm. XRD and FTIR results depict the change in nature of BC from crystalline to amorphous and the TGA results show the reduced thermal stability of BCS compared to its precursor BC. Our results reveal that BCS is highly biocompatible and non-toxic to cells. Growth of the cells has been positively correlated with concentration of BCS, which infers the growth enhancing property of BCS. From this we can conclude that BCS film opens up new avenues for optically functional materials and holds great potential for electronic devices, biomedical sciences (wound healing, facial packs etc.). The initial results encouraged us to strongly propose the immediate use of our BCS biocompatible film in food and packaging industries (as edible films) in near future. Application oriented research works in these aspects are in progress in our laboratory.

References

1. A. Svensson, E. Nicklasson, T. Harrah, B. Panilaitis, D. L. Kaplan, M. Brittberg, and P. Gatenholm. Bacterial cellulose as a potential scaffold for tissue engineering of cartilage; *Biomaterials* 26, 419 (**2005)**.
2. D. Klemm, D. Schumann, U. Udhardt, and S. Marsch. Bacterial synthesized cellulose – Artificial blood vessels for microsurgery; *Prog. Polym. Sci.* 26, 1561 (**2001**).
3. S. P. Lin, I. L. Calvar, J. M. Catchmark, J. R. Liu, A. Demirci, and K. C. Cheng. Biosynthesis, production and applications of bacterial cellulose; *Cellulose* 20, 2191 (**2013)**.
4. Z. Qin, L. Ji, X. Yin, L. Zhu, Q. Lin, and J. Qin. Synthesis and

characterization of bacterial cellulose sulfates using a SO_3/Pyridine complex in DMAc/LiCl; *Carbohyd. Polym.* 101, 947 (**2013**).

5. K. Hettrich, W. Wagenknecht, B. Volkert, and S. Fischer. New possibilities of the acetosulfation of cellulose; *Macromol. Symp.* 262, 162 (**2008**).
6. L. Zhu, J. Qin, X. Yin, L. Ji, Q. Lin, and Z. Qin. Direct sulfation of bacterial cellulose with a $ClSO_3H$/DMF complex and structure characterization of the sulfates; *Polym. Adv. Technol.* 25, 168 (**2013**).
7. G. Chen, B. Zhang, J. Zhao, and H. Chen. Development and characterization of food packaging film from cellulose sulfate; *Food Hydrocolloids* 35, 476 (**2014**).
8. W. K. Czaja, D. J. Young, M. Kawecki, and R. M. Brown Jr. The future prospects of microbial cellulose in biomedical applications; *Biomacromolecules* 8, 1 (**2007**).
9. A. G. Figueiredo, A. R. Figueiredo, A. Alonso-Varona, S. C. Fernandes, T. Palomares, E. Rubio-Azpeitia, A. Barros-Timmons, A. J. Silvestre, C. Pascoal Neto and C. S. Freire. Biocompatible Bacterial Cellulose-Poly(2-hydroxyethyl methacrylate) Nanocomposite Films; *Biomed. Res. Int.* 2013: 698141 **(2013).**
10. M. Nogi and H. Yano. Transparent Nanocomposites Based on Cellulose Produced by Bacteria Offer Potential Innovation in the Electronics Device Industry; *Adv. Mater.* 20, 1849 (**2008**).
11. H. S. Barud, S. J. L. Ribeiro, C. L. P. Carone, R. Ligabue, S. Einloft, P. V. S. Queiroz, A. P. B. Borges, and V. D. Jahno. Optically transparent membrane based on bacterial cellulose/polycaprolactone; *Polimeros* 23, 135 (**2013**).
12. S. H. Yoon, S. H. J. Jin, M. C. Kook, and Y. R. Pyun. Electrically conductive bacterial cellulose by incorporation of carbon nanotubes; *Biomacromolecules* 7, 1280 (**2006**).
13. H. Yano, J. Sugiyama, A. N. Nakagaito, M. Nogi, T. Matsuura, M. Hikita, and K. Handa. Optically transparent composites reinforced

with networks of bacterial nanofibers; *Adv. Mater.* 17, 153 (2005).

14. A. Hestrin and M. Schramm. Synthesis of cellulose by *Acetobacter xylinum* II. Preparation of freeze-dried cells capable of polymerizing glucose to cellulose; *Biochem. J.* 58, 345 (**1954**).
15. M. E. Embuscado, J. N. BeMiller, and J. S. Marks. Isolation and partial characterization of cellulose produced by *Acetobacter xylinum*; *Food Hydrocolliod* 10, 75 (**1996**).
16. K. Zhang, E. Brendler, and S. Fischer. FT Raman investigation of sodium cellulose sulfate; *Cellulose* 17, 427 (**2010**).
17. T. Imai, J. Sugiyama, T. Itoh and F. Horii. Almost Pure I_{α} cellulose in the cell wall of *Glaucocystis*; *J. Struct. Biol.* 127, 248 **(1999).**
18. Y. Feng, X. Zhang, Y. Shen, K. Yoshino, and W. Feng. A mechanically strong, flexible and conductive film based on bacterial cellulose/graphene nanocomposite; *Carbohyd. Polym.* 87, 644 (**2012**).
19. D. Klemm, B. Philipp, T. Heinze, U. Heinze, and W. Wagenknecht. Comprehensive Cellulose Chemistry. Volume 1: Fundamentals and analytical methods; *Wiley VCH* p. 115ff (**1998).**
20. K. Zhang, E. Brendler, A. Geissler, and S. Fischer. Synthesis and spectroscopic analysis of cellulose sulfates with regulable total degrees of substitution and sulfation patterns via ^{13}C NMR and FT Raman spectroscopy; *Polymer* 52, 26-(**2011**).
21. S. Raveendran, B. Dhandayuthapani, Y. Nagoka, Y. Yoshida, T. Maekawa, and D. S. Kumar. Biocompatible nanofibers based on extremophilic bacterial polysaccharide, mauran from *Halomonas maura*; *Carbohyd. Polym.* 92, 1225 (**2013**).
22. J. F. Moulder, W. F. Stickle, P. E. Sobol, K. D. Bomben. Handbook of X-ray photoelectron spectroscopy; Physical electronics, Inc. USA, (**1995**).
23. W. Czaja, D. Romanovicz, and D. Brown. Structural investigations of microbial cellulose produced in stationary and agitated culture; *Cellulose* 11, 403 (**2004**).

24. K. Zhang, D. Peschel, E. Bäucker, T. Groth, and S. Fischer. Synthesis and characterisation of cellulose sulfates regarding the degrees of substitution, degrees of polymerisation and morphology; *Carbohyd. Polym*. 83, 1659 (**2011)**.
25. D. Ciolacu, F. Ciolacu, V. I. Popa. Amorphous cellulose – structure and characterization; *Cellulose Chem.Technol.* 45, 13 (**2011**).
26. M. C. I. M. Amin, A. G. Abadi, and H. Katas. Purification, characterization and comparative studies of spray-dried bacterial cellulose microparticles; *Carbohyd Polym.* 99, 180 (**2014**).
27. Y. Zhiyong, S. Chen, H. Wang, B. Wang, and J. Jiang. Biosynthesis of bacterial cellulose/multi-walled carbon nanotubes in agitated culture; *Carbohyd. Polym.* 74, 659 (**2008)**.
28. W. Teng, Y. Huang, J. Cappello, and X. J. Wu. Optically transparent recombinant silk-elastinlike protein polymer films; *Phys. Chem. B* 115, 1608 (**2011**).
29. H. Sehaqui, A. Liu, Q. Zhou, and L. A. Berglund. Fast preparation procedure for large, flat cellulose and cellulose/inorganic nanopaper structure. *Biomacromolecules* 11, 2195 (**2010)**.

6

Synthesis of Bacterial Cellulose Sulfate/Ag Nanoparticles Composite film

"Anyone who has never made a mistake has never tried anything new"

- Albert Einstein

Recent progress of modern healthcare and food packaging technologies initiates searching novel materials with superior safety properties for their applications. Antimicrobial polymer composites with highly active antimicrobial agents are a class of materials that are in demand for such applications. With the advent of nanotechnology, the ability to manipulate a material at nanoscale has imparted huge merit that directly affects the material of choice. This chapter discusses the application of functionalized bacterial nanocellulose in food packaging and biomedical applications. Through acetosulfation, BC has been functionalized to BCS and thereafter, BCS film is incorporated with AgNPs to get the broad-spectrum antimicrobial properties. Various characterizations like FTIR, Zeta potential, UV-vis spectroscopy, TEM and SEM analysis have been performed to assess the physical and chemical features. This film holds tremendous potential in food packaging and modern healthcare owing to the broad-spectrum applications it has to offer.

Introduction

Currently the world is witnessing the resurrection of biopolymers for a wide range of applications to which synthetic polymers were preferred earlier. This drastic revival could be attributed to the increasing industrial demand for biocompatible and biodegradable materials. Also, the intensifying awareness about the environment friendly materials across the globe is helping the cause of biopolymer-based materials resurgence. Prominent family of natural polymers include plant based polysaccharides, cellulose and starch. [1] Along with plants, microorganisms are also capable of producing polysaccharides that have slight advantage over plant cellulose in terms of higher purity, incredible mechanical properties and crystallinity. [2, 3] Owing to their remarkable properties, microbial polysaccharides have found potential applications in bionanotechnology and biomedical fields. Cosmetics and food industries have employed them as bioadhesives, thickeners, stabilizers, gelling agents and probiotics. [4-6]

The need for superior quality and longer shelf life has encouraged the use and development of edible films. [7-8] A packaging material composed of an edible component, forms an edible film and is used to directly coat the food or wrap it, without compromising the original ingredients or process. The primary objective of an edible film is to intercept the exchange of gas, moisture, lipid, solute or aroma between the food and its immediate environment. [9] Major biopolymers used widely as constituents of edible film are polysaccharides, proteins and lipids. [10] Among these specifically cellulose derivatives, such as chitosan, alginate, carrageenan, pectin and starch have good film forming capacities. [11] Carboxymethyl cellulose (CMC), methyl cellulose (MC), hydroxypropyl methyl cellulose (HPMC), hydroxypropyl cellulose (HPC) have also been applied as edible coatings to some fruits and vegetables for acquiring barrier properties to oil, air or moisture. [12, 13]

Apart from food industries, polymer thin films hold immense potential for biomedical applications as well. Antimicrobial coatings with silver (Ag) have been used to make bactericidal thin films owing to the

antimicrobial ability of Ag. [14] Modified chitosan-based thin films were found to have remarkable antithrombogenic and protein repellent properties. [15] Constant evolution of nanotechnological applications in agriculture and food sectors, food quality and safety levels have elevated. [16, 17] Silver nanoparticles (AgNPs) has been utilized in wide range of products that include clothing, sprays, cleaning solutions, deodorants and antimicrobial agents. [18] Though the nanoparticles have found a lot of applications, their mode of action as an antimicrobial agent still remains a matter of active research. Present notion about the bactericidal mechanism of nanoparticle is oxidative stress or disruption of DNA replication or interference with vital cellular processes. [19]

While significant interest has been shown on cellulose derivatives, bacterial cellulose has not received much attention until recently. Since, bacterial cellulose is already available in edible form (nata de coco), famous desert that originated from Philippines, it can find a safe application in the field of edible films. In the present study, we have used an incipient material bacterial cellulose sulfate BCS film incorporated with AgNPs to evaluate its potential in food packaging and biomedical applications.

Most of the human pathogens have developed resistance towards available drugs through their mutations, which is rising to be a global threat. [20, 21] Recently, it has been realized that inorganic nanomaterials have potential to be used as antimicrobial agents as they demonstrate composition, size, shape, chemical functionality and surface charge-dependent antimicrobial profile towards controlling pathogenic microorganisms. In this context, predominantly silver nanoparticles (AgNPs) are found to exhibit significantly higher level of toxicity. [22-24]

This chapter deals with the synthesis of novel BCS/AgNP composite films. There are negligible reports about BCS application or characterization with respect to food packaging films incorporated with AgNPs and biomedical applications. BCS film can surpass the conventional packaging with their biocompatible and biodegradable properties, thereby reducing toxic waste generation.

Materials and Methods

Dialysis membrane was purchased from Spectrum Laboratories Inc. (Rancho Dominquez, USA) that has an approximate molecular weight cut off of 500 Da. All other chemicals used were of analytical grade and were used as received.

BC Production and Modification

BC was synthesized in our lab by using *Komagataeibacter sucrofermentans* JCM 9730^T bacterial strain in Hestrin-Schramm (HS) medium as mentioned elsewhere. [25] BC was purified through alkali treatment and functionalized through acetosulfation process to produce BCS. [26] Briefly, Acetosulfation of BC was carried out as described elsewhere. [27] Briefly, 2.5g of BC were suspended in 125 ml of anhydrous DMF in room temperature for over 14 h. Reaction agent consisting cholorosulphuric acid and acetic anhydride in DMF was dropped in cellulose suspension under vigorous stirring. The resulting solution was maintained at 50°C for 5 h and then cooled to room temperature. This reaction agent was then poured into saturated ethanolic solution of anhydrous sodium acetate. Through centrifugation the precipitate was collected and washed with 4% sodium acetate solution in ethanol. Deacetylation was carried out using 1M ethanolic solution of NaOH for 15 h and pH was adjusted to 8 with acetic acid/ethanol (50/50, w/w). The final product was dissolved in water, filtered, dialyzed and freeze dried.

Synthesis of Tyrosine mediated AgNP

Synthesis of AgNPs^{Tyr} methodology was mentioned elsewhere. [28] Briefly, 300 mL aqueous solution consisting of 0.1 mM L-tyrosine and 1 mM KOH were allowed to boil. Under alkaline boiling conditions, $AgNO_3$ was added to the above solution, resulting in 0.2 mM equivalent of Ag ion concentration. The above solution was further boiled for 5 min, which resulted in a yellow color solution consisting of tyrosine-reduced AgNPs^{Tyr}. To increase the metal concentration by a factor of three, this AgNPs^{Tyr} solution was further boiled to reduce the volume to 100 mL.

This colloidal solution was found highly stable even after concentration, signifying that $AgNPs^{Tyr}$ were strongly capped by tyrosine amino acid. Further, concentrated $AgNPs^{Tyr}$ solution was dialyzed three times against deionized water using cellulose dialysis membrane to remove the excess KOH, potentially unreduced metal ions and unbound amino acid, if any.

Particle Size Distribution

Both particle size distribution and zeta potential were evaluated using a Zetasizer Nano ZS (Malvern Instruments Inc., USA) that uses laser diffraction to measure the parameters. All analyzes were performed in triplicate.

Preparation of BCS/AgNP Composite Films

25 % of BCS – Ag solution was prepared and left in stirring for 12 hours. After 12 hours of stirring at room temperature, with the so-called drop casting method, the sample was transferred to a plastic plate and subjected to vacuum drying. The film samples were stored in desiccator until further analysis.

Electron Microscopy and FTIR Analysis

BCS film were sputter coated with osmium and scanning electron microscopy (SEM) images were obtained on a JEOL, JSM-7400F scanning electron microscope at room temperature. Transmission Electron Microscopy (TEM) images of AgNPs were obtained on a JEOL, JEM-2200FS transmission electron microscope.

The chemical structure characterization was analyzed through Fourier Transform Infrared (FTIR) (Perkin Elmer) with a resolution of 4 cm^{-1} in the region of 4000 to 400 cm^{-1}.

Thickness Measurement and Integrity

5 random positions on the film were chosen for thickness measurement on BCS-chitosan film using a model Photol FE-3000 instrument, Otsuka, Electronics, Japan).

UV-VIS Spectroscopy

UV-vis spectroscopy was carried out through Beckman coulter-730 spectrophotometer over a wavelength range of 200-1000 nm.

Antimicrobial activity assay

To investigate the antibacterial activity of films, 1 cm diameter disks were cut from different composite bioactive films and placed on inoculated nutrient medium. The method was previously standardized by adjusting the microbial inoculation rate and the volume of the agar medium layer. Dishes were incubated at 37 °C for 24 h. Data was expressed as growth inhibitory zone diameter (cm) for three replicates. [18]

Results and Discussions

AgNPs were successfully synthesized through the tyrosine-mediated method. The formation of typical yellow color solution at the end of reaction confirmed the formation of $AgNPs^{Tyr}$. After the formation of $AgNPs^{Tyr}$, the nanoparticles were subjected to several characterizations.

SEM images of the of BC, BCS freeze dried and film samples were recorded after coating with osmium. The SEM images revealed that the morphology of BC completely changed after the functionalized with sulfate groups. Post functionalization, the fibrous structure of BC was completely lost. Figure 1 shows the SEM images of BC and right pure BC and figure 2 depicts the SEM images of BCS free-dried and BCS film respectively.

After the morphology was confirmed, BCS was subjected to solubility tests. BCS was highly soluble compared to the BC as such, which was insoluble in most solvents. Through drop casting technique, BCS films were made as described in previous chapter. The film was highly soluble in water as it took just 8 seconds for it dissolve. However, the film was not soluble in ethanol or methanol even when kept submerged for >48 hours. Solubility of BCS film in oil was also tested

and the films were kept submerged in olive oil for >48 hours and a similar trend were observed as that of alcohol, it was insoluble in oil as well. The insolubility of BCS film in alcohol or oil gives a lot of hope for food packaging owing to the high biocompatibility and mechanical strength of BCS films as discussed in earlier chapters.

UV-Vis spectroscopy is performed to determine the structural, especially the morphological particularities of $AgNPs^{Tyr}$ from the dispersed phase perspective. The absorption results as displayed in Figure 3 indicate the presence of AgNPs. The UV-Vis absorption was measured in the range of 190 – 1000 nm in Beckman coulter D 730 instrument. $AgNPs^{Tyr}$ was the treated with 25% BCS and then UV-Vis was recorded again. Figure 4 shows UV-Vis absorption of AgNP/BCS sample.

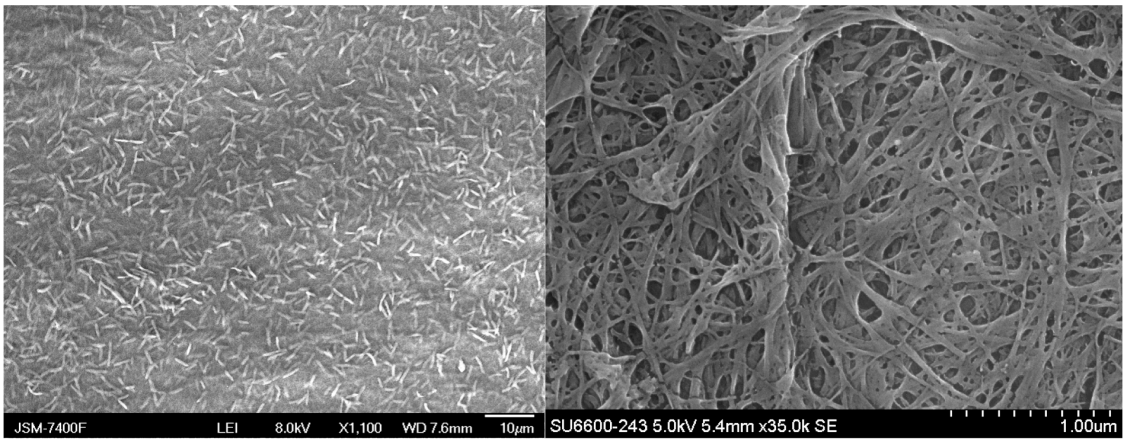

Fig 1: BC with bacterial cells (left) and Pure BC (right)

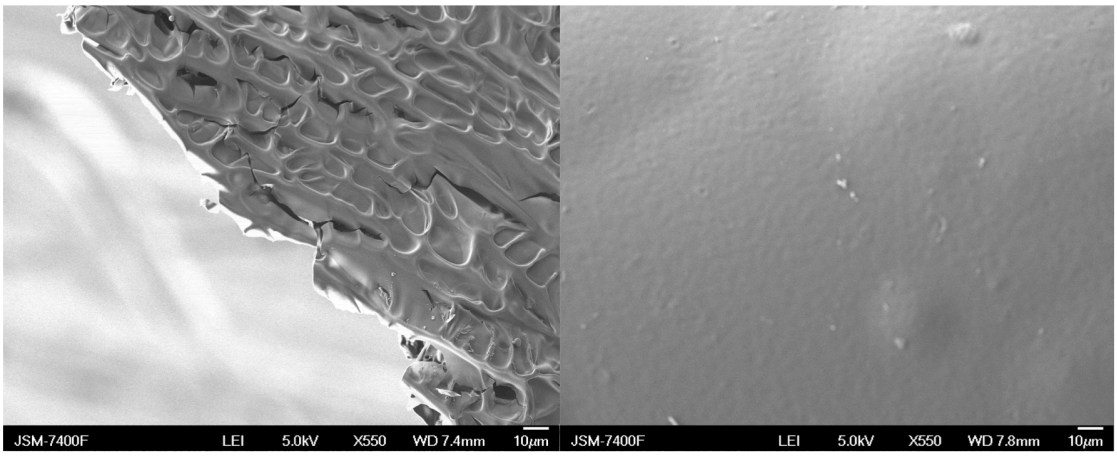

Fig 2: Freeze dried BCS (left) and BCS Film (right)

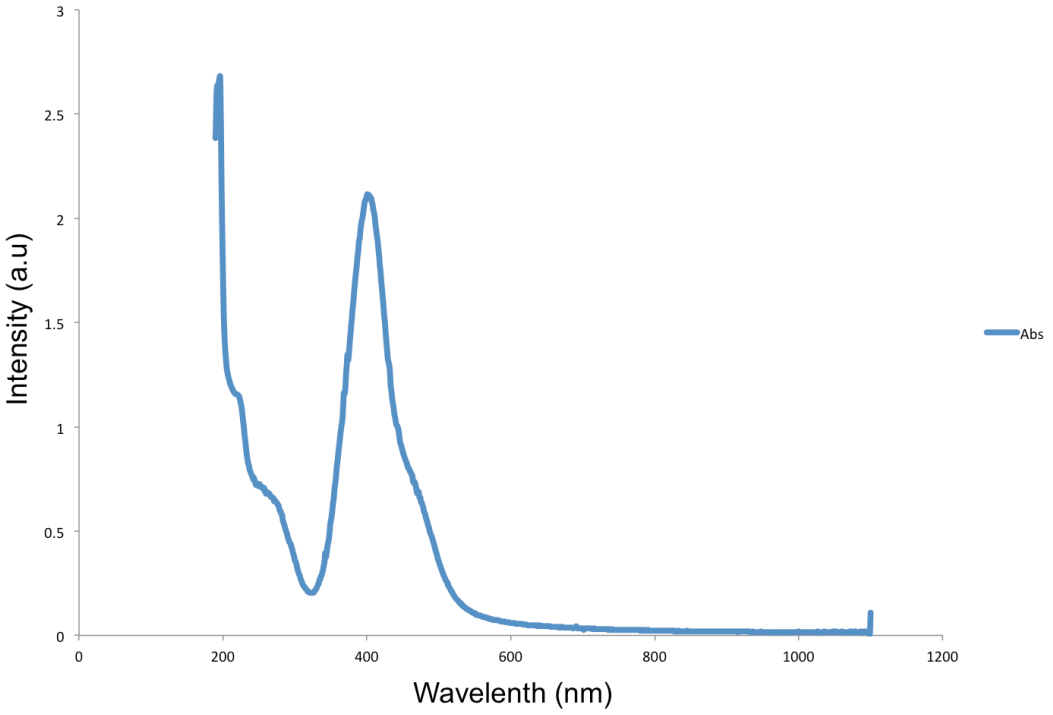

Fig 3: UV-VIS absorbance of AgNP

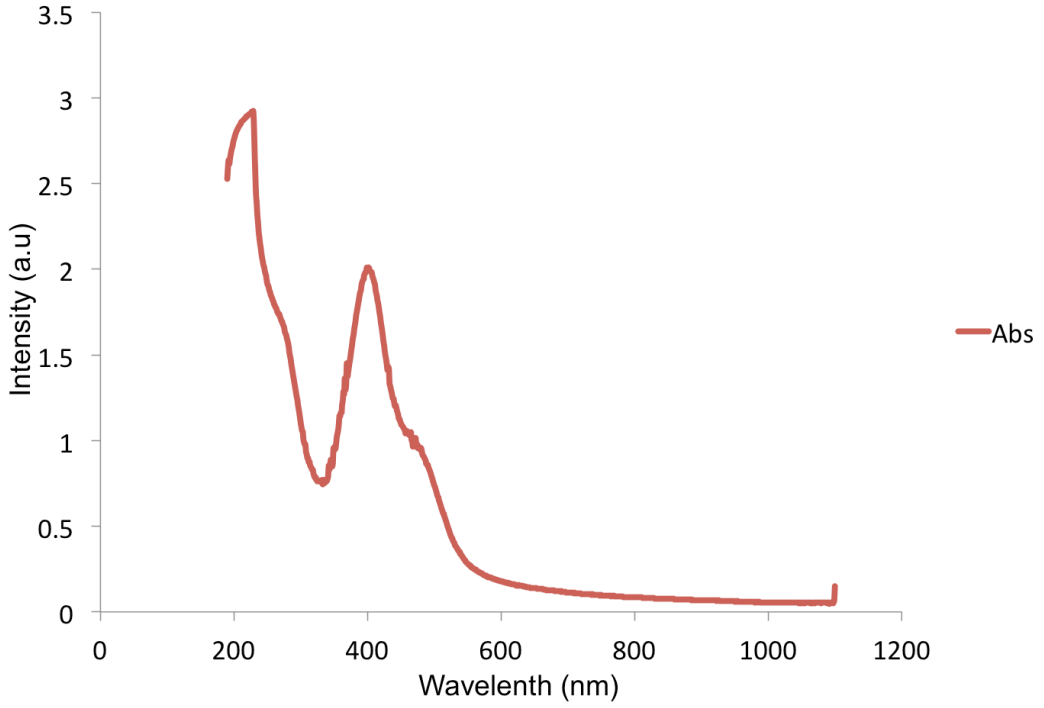

Fig 4: UV-VIS absorbance of AgNP/BCS

The UV-Vis results suggest the successful formation of AgNPs and AgNP/BCS complex, which was confirmed with TEM analysis. AgNO3 ions shows a distinct absorption at around 434 nm, which corresponds to surface plasmon resonance (SPR) of silver nanoparticles established at 420 nm in previous studies [29]. It is observed that the silver SPR band occurs initially at 430 nm; after completion of the reaction, the wavelength of the SPR band stabilizes at 434 nm.

Morphology and successful formation of AgNPs were observed with the aid of TEM. Generally, spherical morphology was observed throughout the sample, when random sampling was performed at different locations. The AgNPs were well dispersed in the solution but in some places, aggregates were also observed as seen in the TEM images. Figure 5 illustrates the TEM results of AgNP.

Particle size of the AgNPs were noted with the aid of Zetasizer ZS. The average particle size was observed to be ~70 nm as depicted in figure 6.

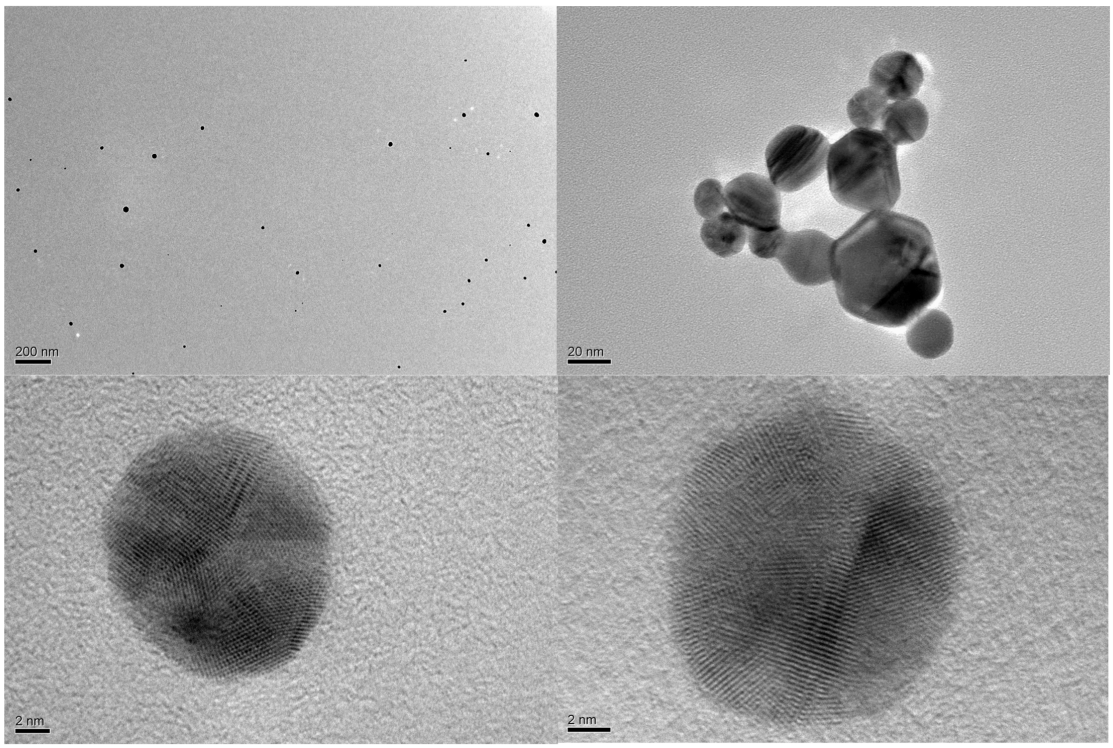

Fig 5: TEM images of AgNP's

The chemical structure of BCS was investigated by FTIR. The broad band in the 3400-3200 cm^{-1} regions in BC and BCS was due to the characteristic O-H stretch as shown in Fig. 4. The absorption peaks at 2896, 1649 and 1428 cm^{-1} was due to the C-H stretching of $-CH_2$, O-H bending and $-CH_2$ symmetric bending respectively. The absorption band at 900 cm^{-1} is attributed to C-O-C stretching of β-(1,4)-glycosidic linkages and the increased peak intensity in this region is attributed to the amorphous nature of sample. BCS shows a high intensity peak in this region, which infers the amorphous nature of the sample. [30, 31, 27] This result corresponds to the XRD results of BCS sample. The peaks at 1109, 1057 and 1033 cm^{-1} indicated C2O2, C3O3 and C6O6 stretching respectively. The peaks at 752 and 713 cm^{-1} are attributed to the contribution by cellulose Iα and Iβ respectively. The presence of two new peaks in BCS sample at 1217 and 810 cm^{-1} indicate the successful sulfation of BC hydroxyl groups and are attributed to the asymmetric vibration $\nu_{as}(O=S=O)$ and C-O-S stretching vibration ν(C-O-S) respectively. [32] Figure 7 illustrates the FTIR results of BCS samples that confirm the successful sulfation of BC samples.

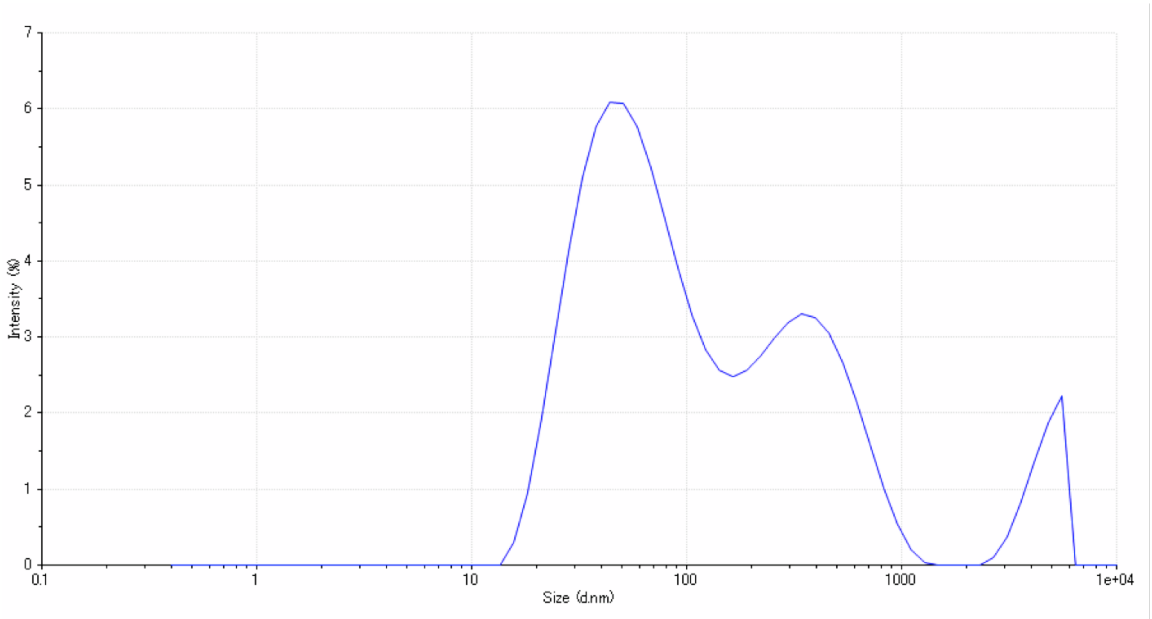

Fig 6: AgNPs size evaluation using Zetasizer

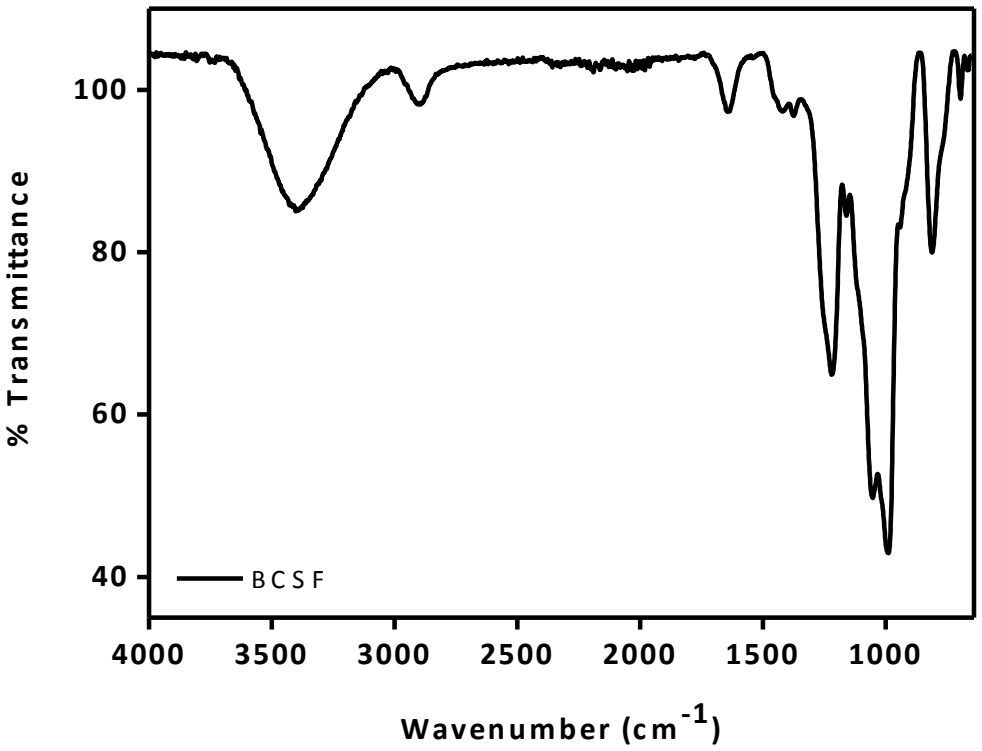

Fig 7: FTIR spectra of BCS Film

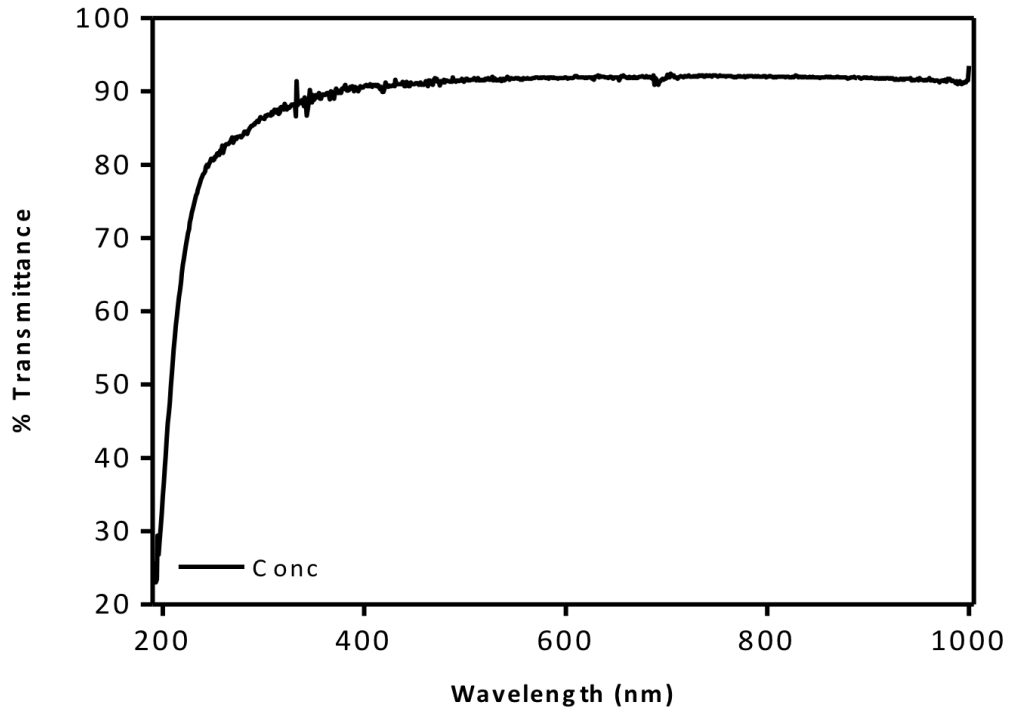

Fig 8: Optical transmittance spectra of BCS Film

The BCS/AgNP composite films were synthesized using 25% BCS sample, which was dissolved in AgNP solution (w/v) and left for stirring for 12 hours. After 12 hours of stirring the AgNP-BCs solution were cast in a plastic plate through drop-casting method for film formation and was vacuum dried. The transparency of the film was observed and evaluated through Beckman coulter spectrophotometer. Figure 8 shows the transmittance results of BCS film.

The antibacterial efficacy of AgNP's was tested with two model bacteria, *Escherichia coli* and *Staphylococcus epidermidis*. Figure 9 shows the antibacterial study results. The results indicated that AgNPs formed were effective on *Staphylococcus epidermidis*, but were found to be a little ineffective in the case of *Escherichia coli*. This could be attributed to the size dependent factor as reported earlier, [33] wherein metal nanoparticles of 1-10 nm diameter are considered to exhibit a direct interaction with biological systems and do not show much variation in their biological profile within this size range. [34] Moreover, AgNPs are known to undergo a shape-dependent interaction with the gram-negative bacterium *E. coli*, and therefore AgNPs shape also contributes to their antimicrobial profile. [35]

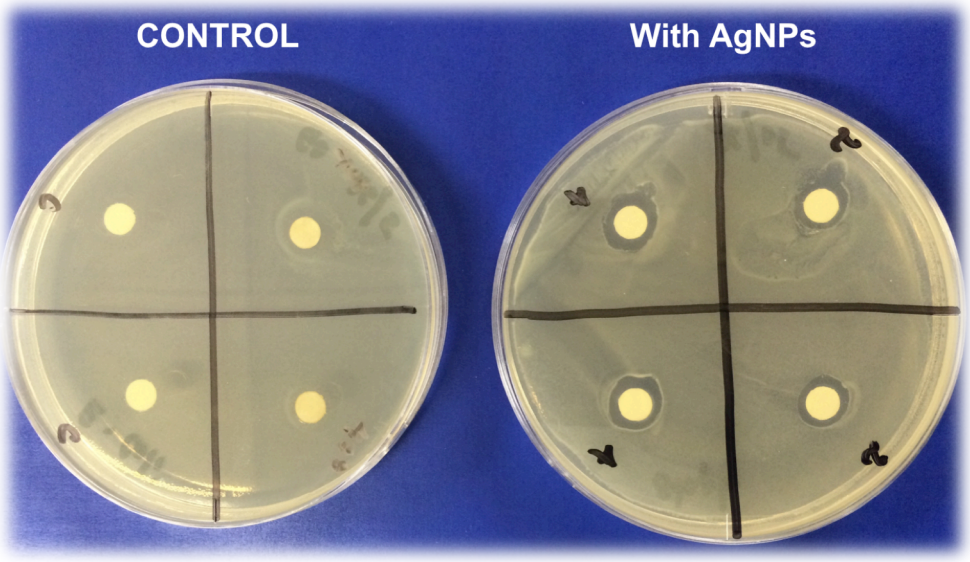

Fig 9: Antimicrobial assay for BCS sample

Conclusion

This chapter establishes the significance of size of AgNPs for on antibacterial studies. In a typical nanoparticle synthesis route, tyrosine capping agent are employed during synthesis and when these materials are tested for biological applications, the observed effect is generally assigned either to nanoparticle composition, size or shape. This study strongly indicates that as such, great care must be taken while assigning biological mode of action to the physico-chemical properties of different nanoparticle systems. Further investigation is to be done on the interaction of BCS and AgNP with the cell lines and bacterial cells. This preliminary study explains the immense potential of the BCS/AgNP composite films for various applications in healthcare and active food packaging. Further studies are in progress, which would certainly enhance the properties of this film.

References

1. Vroman and L.Tighzert, "Biodegradablepolymer,"*Materials*, 2, 307-344, (**2009**).
2. P. Ross, R. Mayer, and M. Benziman. Cellulose biosynthesis and function in bacteria; *Microbiol. Rev.* 55, 35-38 **(1991)**.
3. S. Bielecki, A. Krystynowicz, M. Turkiewicz, and H. Kali- nowska, "Bacterial cellulose," in *Biopolymers: Polysaccharides I. Munster*, A. Steinbuchel, Wiley-VCH, GmbH, Weinheim, Gremany, 5, 37-90 (**2002**).
4. F. Donot, A. Fontana, J. C. Baccou, and S. S. Galindo. Microbial exopolysaccharides: main examples of synthesis, excretion, genetics and extraction; *Carbohyd. Polym.*, 87, 951-962 **(2012)**.
5. F. Freitas, V. D. Alves, and M. A. M. Reis. Advances in bacterial exopolysaccharides: from production to biotechnological applications; *Trends Biotechnol*. 29, 388-398 (**2011**).
6. E.T. Onur. Microbial production of extracellular polysaccharides from biomass. *Pretreatment techniques for biofuels and biorefineries green energy and technology*, 35-56 **(2013)**.

7. M. A. Garcia, A. Pinotti, and N. E. Zaritzk. Physicochemical, water vapor barrier and mechanical properties of corn starch and chitosan composite films; Starch- Starke 58 (9), 453-463 **(2006)**.
8. F. Debeaufort, J. A. Q. Gallo, and A. Voilley. Edible films and coatings: tomorrow's packagings: a review; *Critical Reviews in Food Science and Nutrition* 38(4), 299-313 **(1998)**.
9. G. Chen, B. Zhang, B. Zhao, and H. Chen. Development and characterization of food packaging film from cellulose sulfate; *Food Hydrocolliods* 35, 476-483 **(2014)**.
10. A. Jimenez, M. J. Fabra, P. Talens, and A. Chiralt. Edible and biodegradable starch films: a review; *Food and Bioprocess Technology* 5(6), 2058-2076 **(2012)**.
11. G. Chen, B. Liu, and B. Zhang. Characterization of composite hydrocolloid film based on sodium cellulose sulfate and cassava starch; *J Food eng.*, 125:105-111 **(2014)**.
12. M. Vargas, C. Pastor, A. Chiralt, D. J. M. Clements, and M. C. Gonzalez. Recent advances in edible coatings for fresh and minimally processed fruits; *Crit. Rev. Food Sci. Nutr.* 48, 496-511 (**2008)**.
13. C. Johansson, J. Bras, I. Mondragon, P. Nechita, D. Plackett, P. Simon, D. G. Svetec, S. Virtanen, M. G. Baschetti, C. Breen, F. Clegg, and S. Aucejo. Renewable fibers and bio-based materials for packaging applications – a review of recent developments; *Bioresources* 7 (2), 2506-2552 **(2012)**.
14. C. Aymonier, U. Schlotterbeck, L. Antonietti, P. Zacharias, R. Thomann, J.C. Tiller, and S. Mecking. Hybrids of silver nanoparticles with amphiphilic hyperbranched macromolecules exhibiting antimicrobial properties; *Chemical Communications* 24, 3018-19 **(2002)**.
15. V.K. Vendra, L. Wu, and S. Krishnan. Polymer thin films for biomedical applications. *Nanotechnologies for the life sciences*. Wiley & sons. **(2011).**
16. Y. Li, Y. Jiang, F. Liu, F. Ren, G. Zhao, X. Leng. Fabrication and characterization of TiO_2/whey protein isolate nanocomposite film;

Food Hydrocolloids 25, 1098–1104 **(2011)**.

17. T. V. Duncan. Applications of nanotechnology in food packaging and food safety: barrier materials, antimicrobials and sensors; *J Colloid Interface Sci.* 36, 1–24 **(2011)**.
18. M. R. D. Moura, L. H.C. Mattoso, V. Zucolotto. Development of cellulose-based bactericidal nanocomposites containing silver nanoparticles and their use as active food packaging; *J Food Engineering*, 109, 520–524 **(2012)**.
19. M. K. Morsy, K. H. Hassan., A. M. Sharoba, H. H. E. Tanahi, and C. N. Cutter. Incorporation of essential oils and nanoparticles in pullulan films to control food borne pathogens on meat and poultry products; *J Food Sci.*, 79; M675–684 **(2014)**.
20. M. Leeb. Antibiotics: A shot in the arm. Nature 431: 892–893. Doi:10.1038/431892a **(2004)**.
21. S.R. Norrby, C.E. Nord, and R. Finch. Lack of development of new antimicrobial drugs: a potential serious threat to public health. *Lancet Infect Dis* 5, 115–119 **(2005)**.
22. R. M. Amin, M. B. Mohamed, M. B. Ramadan, T. Verwanger, B. Krammer. Rapid and sensitive microplate assay for screening the effect of silver and gold nanoparticles on bacteria; *Nanomedicine* 4, 637–643 **(2009)**.
23. C. N. Lok, C. M. Ho, R. Chen, Q. Y. He, W. Yu, H. Sun, P. K. Tam, J. F. Chiu and C. M. Che. Silver nanoparticles: Partial oxidation and antibacterial activities; *J Biol Inorg Chem JBIC Publ Society of Bio. Inorganic Chem.*12, 527–534 **(2007)**.
24. W. R. Li, X. B. Xie, Q. S. Shi, H. Y. Zeng, Y. S. Ou-Yang and Y. B. Chen. Antibacterial activity and mechanism of silver nanoparticles on Escherichia coli. *Appl. Microbiol. Biotechnol.* 85, 1115–1122 **(2010)**.
25. S. Hestrin, and M. Schramm. Synthesis of cellulose by *Acetobacter xylimum II*. Preparation of freeze-dried cells capable of polymerizing glucose to cellulose; *Biochem. J* 58(2), 345–352 **(1954)**.

26. K. Zhang, E. Brendler, A. Geissler and S. Fischer. Synthesis and spectroscopic analysis of cellulose sulfates with regulable total degrees of substitution and sulfation patterns via ^{13}C NMR and FT Raman spectroscopy. *Polymer* 52, 26-32 **(2010)**.
27. Y. Yang, J. Jia, J. Xing, J. Chen, S. Lu. Isolation and characteristics analysis of a novel high bacterial cellulose producing strain Gluconacetobacter intermedius CIs26; *Carbohyd. Polym.* 92; 2012, **(2013).**
28. H. K. Daima, P.R. Selvakannan, R. Shukla, S.K. Bhargava, and V. Bansal. Fine-tuning the antimicrobial profile of biocompatible gold nanoparticles by sequential surface functionalization using polyoxometalates and lysine. PLoS One, DOI: 10.1371/journal.pone.0079676 **(2013)**.
29. P. Devaraj, P. Kumari, C. Aarti, and A. Renganathan. Synthesis and characterization of silver nanoparticles using cannonball leaves and their cytotoxic activity against mcf-7 cell line; *J Nanotechnol.*, Article ID 598328 **(2013)**.
30. M. C. I. M. Amin, A. G. Abadi and H. Katas. Purification, characterization and comparative studies of spray-dried bacterial cellulose microparticles; *Carbohyd. Polym.* 99, 180 (2014).
31. Z. Yan, S. Chen, H. Wang, B. Wang, and J. Jiang; Biosynthesis of bacterial cellulose/multi-walled carbon nanotubes in agitated culture; *Carbohyd. Polym.* 74(3), 659 **(2008)**.
32. L. Zhu, J. Qin, X. Yin, L. Ji, and Q. L. Z. Qin. Direct sulfation of bacterial cellulose with $ClSO_3H$/DMF complex and structure characterization of the sulfates; *Polym. Adv. Technol.* 25, 168-172. **(2013)**.
33. G. A. M. Castanon, N. N. Martinez, M. F. Gutierrez, J. R. M. Mendoza, and F. Ruiz. Synthesis and antibacterial activity of silver nanoparticles with different sizes; *J Nanopart Res* 10, 1343-1348. **(2008)**.

34. J. R. Morones, J. L. Elechiguerra, A. Camacho, K. Holt, J. B. Kouri, J. T. Ramirez, and M. J. Yacaman. The bactericidal effect of silver nanoparticles; *Nanotechnology* 16: 2346-2353. **(2005).**

35. S. Pal, Y. K. Tak, and J. M. Song. Does the antibacterial activity of silver nanoparticles depend on the shape of the nanoparticle? A study of the gram-negative bacterium *Escherichia coli*. *Appl. Environ. Microbiol*. 73, 1712-1720 **(2007)**.